BioMed Research International

Microbial Enzymes and Their Applications in Industries and Medicine 2016

Guest Editors: Periasamy Anbu, Subash C. B. Gopinath, Bidur P. Chaulagain, and Thangavel Lakshmipriya

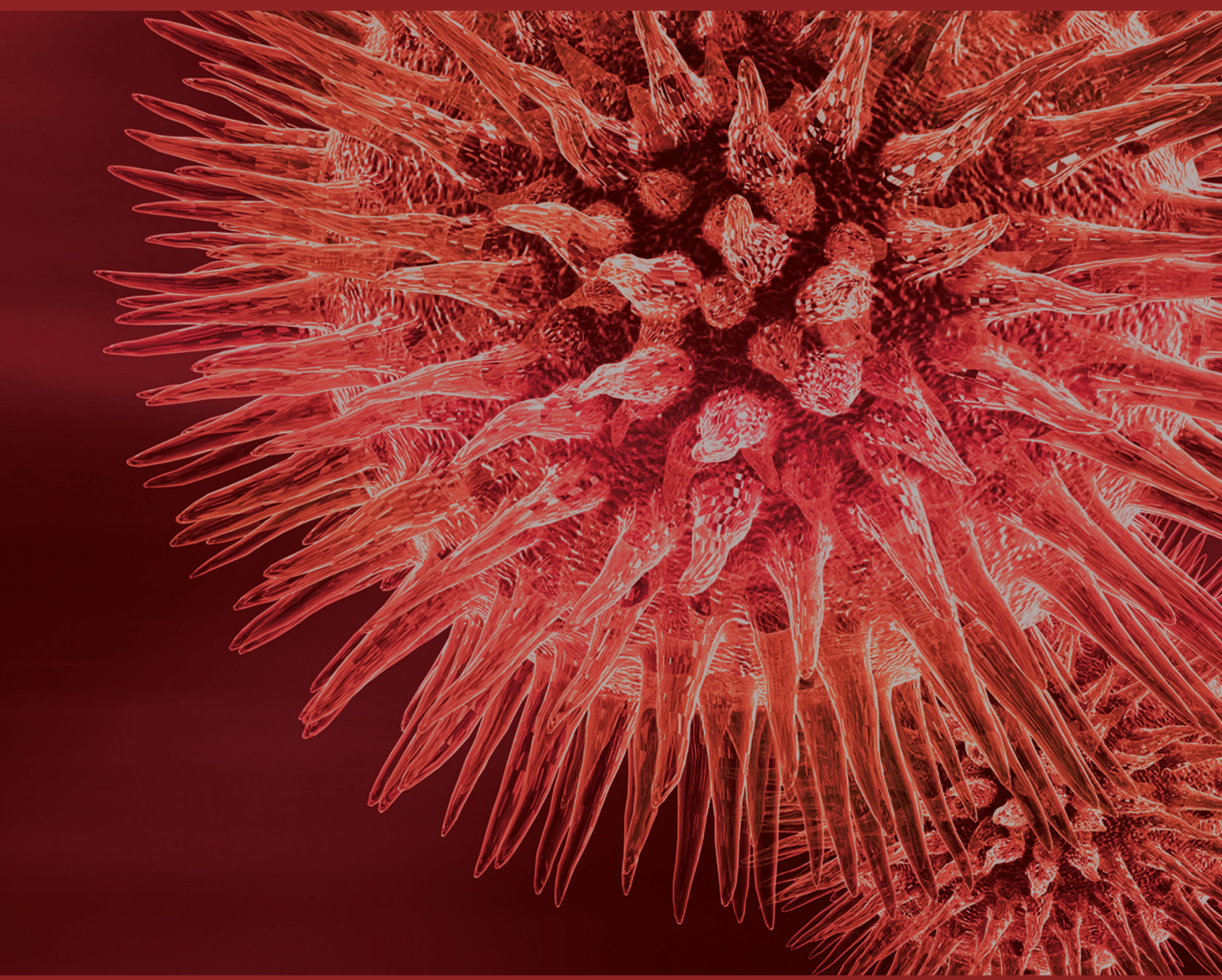

Microbial Enzymes and Their Applications in Industries and Medicine 2016

BioMed Research International

Microbial Enzymes and Their Applications in Industries and Medicine 2016

Guest Editors: Periasamy Anbu, Subash C. B. Gopinath, Bidur P. Chaulagain, and Thangavel Lakshmipriya

Contents

Hindawi
BioMed Research International
Volume 2017, Article ID 2195808, 3 pages
http://dx.doi.org/10.1155/2017/2195808

Editorial

Microbial Enzymes and Their Applications in Industries and Medicine 2016

Periasamy Anbu,[1] Subash C. B. Gopinath,[2,3] Bidur Prasad Chaulagain,[4] and Thangavel Lakshmipriya[1,2]

[1] *Department of Biological Engineering, College of Engineering, Inha University, Incheon 402-751, Republic of Korea*
[2] *Institute of Nano Electronic Engineering (INEE), Universiti Malaysia Perlis, 01000 Kangar, Perlis, Malaysia*
[3] *School of Bioprocess Engineering, Universiti Malaysia Perlis, 02600 Arau, Perlis, Malaysia*
[4] *Directorate of Research and Training, Himalayan College of Agricultural Sciences and Technology (HICAST), P.O. Box 25535, Kalanki, Kathmandu, Nepal*

Correspondence should be addressed to Periasamy Anbu; anbu25@yahoo.com and Subash C. B. Gopinath; subash@unimap.edu.my

Received 14 December 2016; Accepted 4 January 2017; Published 28 March 2017

Enzymes are biocatalysts that play an important role in metabolic and biochemical reactions [1]. Microorganisms are the primary source of enzymes, because they are cultured in large quantities in short span of time and genetic manipulations can be done on bacterial cells to enhance the enzyme production [2–4]. In addition, the microbial enzymes have been paid more attention due to their active and stable nature than enzymes from plant and animal [2–4]. Most of the microorganisms are unable to grow and produce enzyme under harsh environments that cause toxicity to microorganisms. However, some microorganisms have undergone various adaptations enabling them to grow and produce enzymes under harsh conditions [5, 6]. Recently several lines of study have been initiated to isolate new bacterial and fungal strains from harsh environments such as extreme pH, temperature, salinity, heavy metal, and organic solvent for the production of different enzymes having the properties to yield higher [6–9]. This special issue covers six articles including one review article, highlighting the importance and applications of biotechnologically and industrially valuable microbial enzymes.

There are redundancies in genetic code that amino acid might be encoded by multiple synonymous codons. This scenario gives an opportunity to choose a codon other than the naturally occurring one in the genome to optimize the production with heterologous expression system. Codon optimization in another sense is a guided mutagenesis in the gene expression system which can be utilized for the benefits of human kind, ranging from industrial agriculture to medicine. J. Wang et al. have applied a series of strategies to improve the expression level of recombinant endo-β-1,4-xylanase from *Aspergillus usamii* in *Pichia pastoris*. The endo-β-1,4-xylanase gene (xynB) from *A. usamii* was optimized for expression in *P. pastoris*. Their analysis showed the codon for amino acid residues in *P. pastoris* is different from the original codon of *A. usamii*. Thus they replaced the codons in endo-β-1,4-xylanase gene to fit to the cellular environment of *P. pastoris*. Similarly they optimized the codons of *Vitreoscilla hemoglobin gene* (vhb) to fit to heterologous expression system in *P. pastoris* cell system. While optimizing codons they replaced the AT-rich stretches with GC-rich stretches, because G+C content affects the secondary structure of mRNA and influences the expression level of heterologous gene. Totally, 105 and 57 amino acids were optimized in native xynB and vhb, respectively. Besides optimizing the genetic system, J. Wang et al. have also optimized the environment to express those recombinant genes. The codon optimized *vhb* gene has significantly improved the oxygen availability for host *P. pastoris* since oxygen supply is one of most critical factors for the cell growth and heterologous protein expression in recombinant *P. pastoris*. By optimizing the temperature effect on the system they increased the xylanase production combined with higher cell viability. Overall, this work has supported the notion of

genetic engineering in code optimization and a piece of novel work for the recombinant biotechnology.

X. Jia and his colleagues have produced the recombinant catalase in *Escherichia coli* from *Geobacillus* sp. gene *(Kat)*. This *Kat* gene has 1,467 bases and encoded a catalase with 488 amino acid residuals with 81% similarity to the previously studied *Bacillus* sp. catalase. Fermentation broth of the recombinant *E. coli* showed a high catalase activity level up to 35,831 U/mL. The purified recombinant catalase had a specific activity of 40,526 U/mg and a *Km* of 51.1 mM. The optimal reaction temperature of this recombinant enzyme is 60 to 70°C, and it exhibits a high activity over a wide range of reaction temperatures. The enzyme retained 94.7% of its residual activity after incubation at 60°C for 1 hour. The high yield and excellent thermophilic properties of this recombinant catalase have valuable features for industrial applications.

In the work performed by M. Karkovska et al., a laboratory column-type bioreactor for removing a toxic D-lactate on permeabilized thermotolerant methylotrophic yeast (*Hansenula polymorpha* "tr6") cells and alginate gel was constructed and tested. Using recombinant *H. polymorpha* "tr6" overproduced the D-lactate: cytochrome c-oxidoreductase. At about 6-fold overexpression of D-lactate, cytochrome c-oxidoreductase under a strong constitutive promoter *(prAOX)* was demonstrated. Overexpression of D-lactate dehydrogenase coupled with the deletion of L-lactate-cytochrome *c* oxidoreductase activity opens the possibility for usage of the strain as a base for construction of bioreactor for removing D-lactate from fermented products due to the oxidation to nontoxic pyruvate.

RNases are regarded as alternative to classical chemotherapeutic agents due to their selective cytotoxicity towards tumor cells. In the work demonstrated by Y. Sokurenko et al., extracellular ribonuclease from *Bacillus licheniformis* (balifase), a new member of the N1/T1 RNase superfamily, is shown to have antitumor effects. The new RNase produced is with a high degree of structural similarity with binase (73%) and barnase (74%) having a molecular weight of 12422 Daltons and pI 8.9. The physicochemical properties of balifase are similar to those of barnase. The gene organization and promoter activity of balifase are closer to binase. In this study, similar to the biosynthesis of binase, balifase synthesis was induced under phosphate starvation; however, in contrast to binase, balifase does not form dimers under natural conditions. This study also proposed that the highest stability of balifase allows retaining its structure without oligomerization.

In their review, S. Gopinath et al. focused on importance of microbial amylase in the field of biotechnology. In this article, the authors have discussed isolation and screening of amylase from bacterial strains. They also discussed the improvement of enzyme production by optimization and recombinant DNA technology. The major advantages of microbial enzymes in many industries such as food, detergent, pharmaceutical, paper, and textile industries are discussed. The technologies of high-throughput screening and processing with efficient microbial species, along with the ultimate coupling of genetic engineering of amylase-producing strains, will all help in enhancing amylase production for industrial and medicinal applications.

Efficient delivery of drug to the target cell is very important for treatment. Drugs with brain tissue related treatments are hindered by the blood brain barrier. Flurbiprofen is one of the potent drugs that may help to prevent Alzheimer's disease but it has problem with blood-brain barrier permeability. To overcome this problem J. Xin et al. have worked to design and modify this drug as L-ascorbyl flurbiprofenate with the addition of ascorbic acid as a specific carrier system for brain delivery. In the process they have tried to optimize lipase-catalyzed esterification and transesterification. They found that synthesis of L-ascorbyl flurbiprofenate was influenced by the specific reaction conditions and the most important step was the efficient removal of byproducts during the reaction. While comparing those esterification and transesterification methods, although the rate of esterification was found slower than that of transesterification, from the standpoint of productivity and the amount of steps required, lipase-catalyzed esterification was found superior for the synthesis of L-ascorbyl flurbiprofenate.

Periasamy Anbu
Subash C. B. Gopinath
Bidur Prasad Chaulagain
Thangavel Lakshmipriya

References

[1] P. Nigam, "Microbial enzymes with special characteristics for biotechnological applications," *Biomolecules*, vol. 3, no. 3, pp. 597–611, 2013.

[2] P. Anbu, S. C. B. Gopinath, A. C. Cihan, and B. P. Chaulagain, "Microbial enzymes and their applications in industries and medicine," *BioMed Research International*, vol. 2013, Article ID 204014, 2 pages, 2013.

[3] P. Anbu, S. C. B. Gopinath, B. P. Chaulagain, T.-H. Tang, and M. Citartan, "Microbial enzymes and their applications in industries and medicine 2014," *BioMed Research International*, vol. 2015, Article ID 816419, 3 pages, 2015.

[4] S. C. B. Gopinath, P. Anbu, T. Lakshmipriya, and A. Hilda, "Strategies to characterize fungal lipases for applications in medicine and dairy industry," *BioMed Research International*, vol. 2013, Article ID 154549, 10 pages, 2013.

[5] Y. N. Sardessai and S. Bhosle, "Industrial potential of organic solvent tolerant bacteria," *Biotechnology Progress*, vol. 20, no. 3, pp. 655–660, 2004.

[6] P. Anbu, "Enhanced production and organic solvent stability of a protease from *Brevibacillus laterosporus* strain PAP04," *Brazilian Journal of Medical and Biological Research*, vol. 49, no. 4, Article ID e5178, 2016.

[7] P. Anbu, S. C. B. Gopinath, A. Hilda, T. Lakshmipriya, and G. Annadurai, "Optimization of extracellular keratinase production by poultry farm isolate *Scopulariopsis brevicaulis*," *Bioresource Technology*, vol. 98, no. 6, pp. 1298–1303, 2007.

[8] S. C. B. Gopinath, A. Hilda, T. Lakshmi Priya, G. Annadurai, and P. Anbu, "Purification of lipase from *Geotrichum candidum*: conditions optimized for enzyme production using Box-Behnken design," *World Journal of Microbiology and Biotechnology*, vol. 19, no. 7, pp. 681–689, 2003.

[9] S. C. B. Gopinath, P. Anbu, and A. Hilda, "Extracellular enzymatic activity profiles in fungi isolated from oil-rich environments," *Mycoscience*, vol. 46, no. 2, pp. 119–126, 2005.

Hindawi
BioMed Research International
Volume 2017, Article ID 5751262, 6 pages
http://dx.doi.org/10.1155/2017/5751262

Research Article

Synthesis of L-Ascorbyl Flurbiprofenate by Lipase-Catalyzed Esterification and Transesterification Reactions

Jia-ying Xin,[1,2] Li-rui Sun,[1] Shu-ming Chen,[3] Yan Wang,[1] and Chun-gu Xia[2]

[1]*Key Laboratory for Food Science & Engineering, Harbin University of Commerce, Harbin 150076, China*
[2]*State Key Laboratory for Oxo Synthesis & Selective Oxidation, Lanzhou Institute of Chemical Physics, Chinese Academy of Sciences, Lanzhou 730000, China*
[3]*College of Animal Science and Veterinary Medicine, Shanxi Agricultural University, Taigu 030801, China*

Correspondence should be addressed to Jia-ying Xin; xinjiayingvip@163.com

Received 17 May 2016; Accepted 31 July 2016; Published 21 March 2017

Academic Editor: Bidur P. Chaulagain

The synthesis of L-ascorbyl flurbiprofenate was achieved by esterification and transesterification in nonaqueous organic medium with Novozym 435 lipase as biocatalyst. The conversion was greatly influenced by the kinds of organic solvents, speed of agitation, catalyst loading amount, reaction time, and molar ratio of acyl donor to L-ascorbic acid. A series of solvents were investigated, and tert-butanol was found to be the most suitable from the standpoint of the substrate solubility and the conversion for both the esterification and transesterification. When flurbiprofen was used as acyl donor, 61.0% of L-ascorbic acid was converted against 46.4% in the presence of flurbiprofen methyl ester. The optimal conversion of L-ascorbic acid was obtained when the initial molar ratio of acyl donor to ascorbic acid was 5 : 1. kinetics parameters were solved by Lineweaver-Burk equation under nonsubstrate inhibition condition. Since transesterification has lower conversion, from the standpoint of productivity and the amount of steps required, esterification is a better method compared to transesterification.

1. Introduction

The treatment of Alzheimer's disease is still a major challenge for the medical field. The clinical failure of efficient Alzheimer's disease drug delivery may be largely attributed to the low permeability of drugs due to the blood-brain barrier and a lack of appropriate drug delivery systems [1]. Flurbiprofen is one of the most potent nonsteroidal anti-inflammatory drugs (NSAIDs) and may help to prevent Alzheimer's disease [2, 3]. However, poor brain delivery of flurbiprofen and its serious gastrointestinal side effects have hampered the application of flurbiprofen as neuroprotective agents [4].

Localized and controlled delivery of drugs at their desired site of action can reduce toxicity and increase treatment efficiency. L-Ascorbic acid is essential for many enzymatic reactions, which is transported directly across the blood-brain barrier via Naþ-dependent vitamin C transporter SVCT2 and particularly prevalent in the brain [1]. It has been reported that L-ascorbic acid could be used as a carrier to promote brain drug delivery [5–7]. To overcome the problems of the low blood-brain barrier permeability of flurbiprofen and to increase its delivery to the brain for the treatment of Alzheimer's disease, one attractive approach is to design and synthesize flurbiprofen ester prodrug named L-ascorbyl flurbiprofenate containing ascorbate as a specific carrier system for brain delivery.

So far, there are very few reports on the lipase-catalyzed synthesis of L-ascorbyl flurbiprofenate. Wang and Tang studied the synthesis of L-ascorbyl flurbiprofenate by lipase-catalyzed esterification of L-ascorbic acid with flurbiprofen in tertiary amyl alcohol but no optimum operating parameters were provided [8]. Liu and Tang investigated the kinetics and thermodynamics of the lipase-catalyzed esterification of L-ascorbic acid with flurbiprofen in 2-methy-l,2-butanol [9]. Only limited information on the lipase-catalyzed esterification was available. There were no reports on the lipase-catalyzed synthesis of L-ascorbyl flurbiprofenate by transesterification. However, solvent properties, quantity of enzyme, and molar ratio of L-ascorbic acid to flurbiprofen may influence the biocatalytic reaction. So far, the influence

of these factors for the synthesis of L-ascorbyl flurbiprofenate has not been investigated in detail. To obtain high conversion, it is important to determine the optimal reaction conditions and understand the kinetics parameters.

The present study focused on lipase-catalyzed synthesis of L-ascorbyl flurbiprofenate. The lipase-catalyzed esterification and transesterification approaches have been compared. It was worthwhile to compare the merits and demerits of the two processes and optimize process conditions.

2. Experimental

2.1. Materials. Novozym 435 lipase (Lipase B from *Candida antarctica* immobilized on macroporous acrylic resin; specific activity: 10,000 U/g) was purchased from Novozymes, Denmark. Porcine pancreas lipase Type II (powder, 30–90 U/mg) and *Candida rugosa* lipase (Type VII, powder, 706 U/mg) were purchased from Sigma.

(*R*, *S*)-flurbiprofen (purity > 99%) was purchased from Shanghai Mei Lan Chemical Co. Ltd. (Shanghai, China). The purity of substrates is over 99.7% for L-ascorbic acid. All solvents were dehydrated before use with activated 3 Å molecular sieves. Thin-layer chromatography (TLC) plates were purchased from Merck (KGaA, Darmstadt, Germany).

2.2. Synthesis of Ester. The methyl ester of (*R*, *S*)-flurbiprofen was prepared by the classical methodology using thionyl chloride and methanol. Thionyl chloride, 15 mL (0.20 mol), was added dropwise to cooled, stirred suspension of (*R*, *S*)-flurbiprofen (0.12 mol) in methanol (250 mL). The reaction mixture was refluxed for 2.5 h, and then the solvent was evaporated and the residue purified by column chromatography using SiO_2 as adsorbent and petroleum ether purified as eluant and its purity was > 98% using the HPLC methods described in a later section.

2.3. Reaction Conditions. Unless otherwise stated, the esterification and transesterification reactions were performed in 50 mL closed, screw-capped glass vials containing 25 mL of organic solvent, flurbiprofen or flurbiprofen methyl ester (26–260 mmol/L), L-ascorbic acid (26 mmol/L), and 800 mg of molecular sieve 3 Å. The reaction had been started by adding 40 mg of lipase. The headspace in the vials was filled with nitrogen gas and refilled after each sampling. The reaction mixture was stirred with a magnetic stirrer at different temperature. In both cases, samples were withdrawn at specified time intervals for measurement of the conversion. Control experiments without enzymes were carried out in parallel.

2.4. Analytical Methods. In order to monitor the reaction progress, samples of 100 μL were withdrawn at intervals and analyzed by thin-layer chromatography (TLC) on silica gel 60 F_{254} plates with fluorescent indicators. The TLC migration was carried out with a solvent mixture of chloroform/methanol/glacial acetic acid/water (80 : 10 : 8 : 2, V/V/V/V). The TLC plates were visualized under UV. Results were estimated from intensity of spots on TLC.

Quantitative analysis was done by HPLC (Thermo U3000), on a XDB C18 reversed phase column (5 μm, 4.6 × 150 mm) with acetonitrile/water/formic acid (80/20/0.2, V/V/V) as mobile phase at 1 mL/min flow rate. Detection was achieved using UV detection at 294 nm. Samples were filtered to remove the enzyme and molecular sieves and 100 μL of the solution was diluted with acetonitrile/water/formic acid (80/20/0.2, V/V/V). L-Ascorbic acid was a limiting substrate throughout this study; therefore, the conversion was calculated as the ratio in moles of the product to initial L-ascorbic acid. All experiments were performed in triplicate and standard deviations were calculated.

The enantiomeric excess values of flurbiprofen and flurbiprofen methyl ester (ee) were determined by HPLC (Agilent 1200) by using a chiral column (Chiralcel OD-H, 5 μm, 250 mm × 4.6 mm) capable of separating the *R*- and *S*-isomers of flurbiprofen and flurbiprofen methyl ester, and the mobile phase was hexane/isopropanol/trifluoroacetic acid solution (98 : 2 : 0.1, V/V/V), at a flow rate of 1.0 mL/min. UV detection at 294 nm was used for quantification at the 25°C. The enantiomeric excess (ee) was obtained from peak areas of the *R*- and *S*-isomers of flurbiprofen or flurbiprofen methyl ester by the following equation: $ee = (A_S - A_R)/(A_S + A_R)$, where A_S is peak areas of the *S*-isomer and A_R is peak areas of the *R*-isomer.

2.5. Kinetic Study. Reactions were carried out no more than 5% conversion and the initial rate was determined as the slope of the reaction curve tangent to the initial stage of the reaction and expressed as mol of products $h^{-1}\,L^{-1}$. Because all experiments were performed in triplicate, reaction curves were constructed using average values of the reaction rate for each experimental point. A linear portion of the reaction curve at various substrate concentrations consisted of 5 experimental points, where the number of experimental points included was determined by the condition that correlation coefficients of the initial straight line must be above 0.95.

3. Results and Discussion

3.1. Esterification and Transesterification. It was previously reported that esterification of flurbiprofen with L-ascorbic acid by lipase in tert-amyl alcohol produced L-ascorbyl flurbiprofenate regioselectively, which was only the product identified in the HPLC analysis [9]. In this paper, lipase-catalyzed acylation of L-ascorbic acid was performed in presence of racemic flurbiprofen (esterification) or racemic flurbiprofen methyl ester (transesterification). Both kinds of reaction led to only one product identified as L-ascorbyl flurbiprofenate in the HPLC analysis. Furthermore, the chiral HPLC analysis indicated that the lipases also display stereospecificity in the esterification and transesterification. The *R*-isomer reacted with the Novozym 435 lipase; the *S*-isomer reacted with the *Candida rugosa* lipase and porcine pancreas lipase cannot catalyze the reaction. It has been reported that *S*-flurbiprofen and *R*-flurbiprofen have the same physiological activity in prevention of the development of Alzheimer's disease but *R*-flurbiprofen has reduced side effects related to inhibition of

Table 1: The effect of solvent on the conversion of esterification and transesterification.

Solvent	log *P*	Conversion of L-ascorbic acid (%)	
		Esterification	Transesterification
Acetone	−0.23	4.6	30.0
Tert-butanol(2-methyl-2-propanol)	0.60	36.0	38.5
Ethyl acetate	0.68	11.1	9.8
Tert-amyl alcohol; 2-methyl-butanol	0.89	35.3	36.5
Benzene	2.00	—	—
Chloroform	2.00	3.5	—
Toluene	2.50	—	—

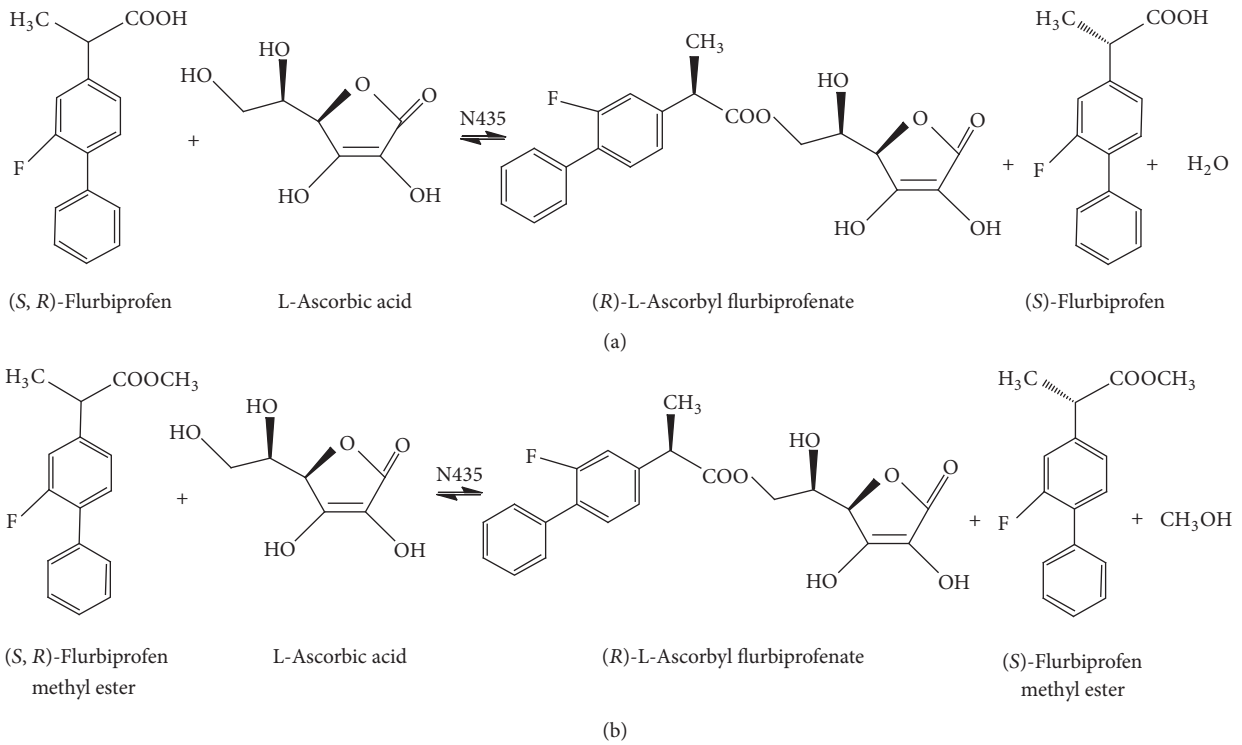

Figure 1: Novozym 435 lipase-catalyzed esterification (a) and transesterification (b).

cyclooxygenase (COX) [10–12]. Thus, Novozym 435 lipase, identified as a *R*-stereospecific catalyst, has been employed in further experiments. The two reactions for the preparation of L-ascorbyl flurbiprofenate are shown in Figure 1.

3.2. Effect of Solvent. Different organic solvents had different ability to distort the essential water layer around lipase and could greatly influence the activity of lipase. Moreover, organic solvent relatively influenced the solubility of the substrates, and thus it would affect the synthesis of the L-ascorbyl flurbiprofenate. The polarity of L-ascorbic acid is very different from those of flurbiprofen and flurbiprofen methyl ester. Because of this significant difference in polarity, such a solvent with relatively high solubility of flurbiprofen, flurbiprofen methyl ester, and L-ascorbic acid needs to be found.

Therefore, esterification and transesterification strategies for the lipase-catalyzed synthesis of L-ascorbyl flurbiprofenate were compared using different organic solvents. The effect of various organic solvents on conversion of L-ascorbic acid was studied under similar conditions using 50 mg Novozym 435 lipase, 800 mg of molecular sieve 3 Å, 2.3 mmoles of flurbiprofen or flurbiprofen methyl ester, 0.57 mmoles of ascorbic acid, and 25 mL organic solvent at 160 rpm, at 50°C for 72 h. It was clear from Table 1 that the type of organic solvent strongly influenced the synthesis of L-ascorbyl flurbiprofenate. In the case of esterification and transesterification, tert-butanol was the best solvent with tert-amyl alcohol as the next best. However, the reaction product was not inspected in benzene and toluene.

log *P* is widely used to represent the characteristics of the organic solvent system where *P* is the partition coefficient of

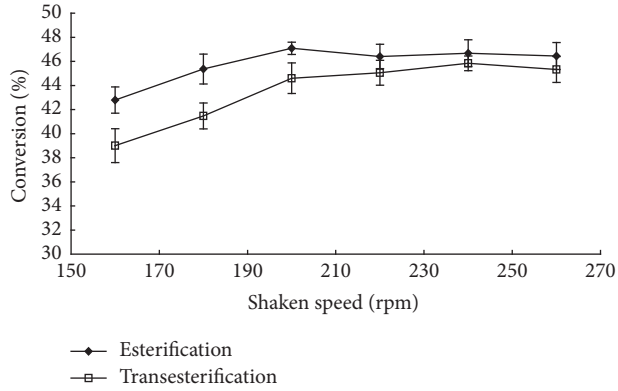

Figure 2: The effect of speed of agitation on the conversion of esterification and transesterification.

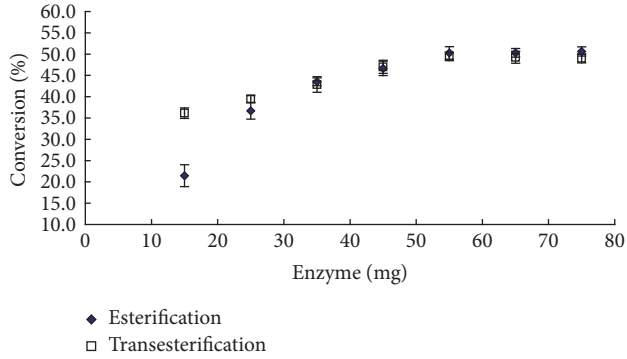

Figure 3: The effect of catalyst loading amount on the conversion of esterification and transesterification.

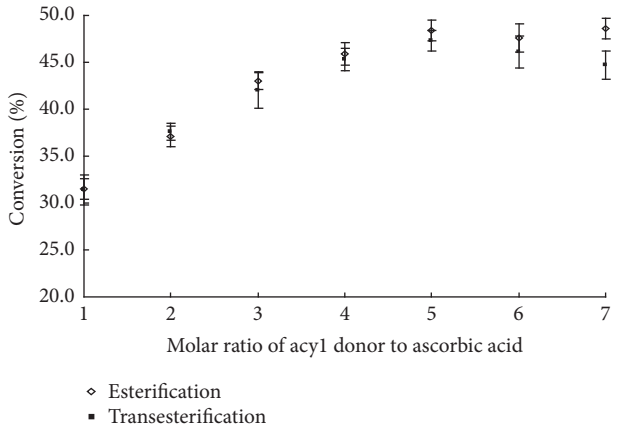

Figure 4: The effect of the molar ratio of acyl donor to ascorbic acid on the conversion of esterification and transesterification.

the solvent between water and octanol [13]. It is generally reported that solvents with $\log P < 2$ are high polarity that may strip water from enzyme molecules easily and are less suitable for biocatalytic purpose [14]. In this case, no correlation of the lipase activity with $\log P$ of the solvents could be established. This could be attributed that L-ascorbic acid had very low concentration in solvents with high $\log P$. Since tert-butanol was the optimum solvent for esterification and transesterification, it was used as the solvent for transesterification and esterification in further experiments.

3.3. Effect of Speed of Agitation. In the case of immobilized enzyme, external mass transfer limitations may be important. The reactants have to diffuse from the bulk liquid to the external surface of the catalyst. External mass transfer can be minimized by carrying out the reaction at an optimum speed of agitation. The effect of speed of agitation was studied both for esterification and transesterification over the range of 160–260 rpm by taking 50 mg Novozym 435 lipase, 800 mg of molecular sieve 3 Å, 2.3 mmoles of flurbiprofen or flurbiprofen methyl ester, 0.57 mmoles of ascorbic, and 25 mL tert-butanol at 50°C for 72 h. The conversions in both the cases were independent of the speed of agitation at and beyond 180 rpm for esterification and transesterification (Figure 2). This indicated that the influence of external mass transfer limitation was negligible and a speed of agitation of 180 rpm did not limit reaction rate. So all subsequent experiments were carried out at 180 rpm.

3.4. Effect of Catalyst Loading Amount. Internal diffusion problems could happen when the substrate could not reach the inner parts of the support. L-Ascorbyl flurbiprofenate synthesis as a function of catalyst loading amount was studied at 50°C and 180 rpm for 72 h. The conversion of the reaction increased with increasing immobilized lipase loading ranging from 15 mg to 55 mg in both the cases; a linear relationship between the conversion and enzyme load demonstrated that the internal diffusion limitations could be minimized. Maximal conversion was achieved with 55 mg lipase for esterification and transesterification after conversion became constant and no further increases (Figure 3).

Also, in the case of esterification reaction, the conversion was lower than the transesterification reaction under 15 mg and 25 mg lipase addition and the asymptotes were seen in the conversion for transesterification and esterification when the amount of enzyme added was beyond 35 mg. Since there was no significant increase in the conversion with increased catalyst loading from 55 mg to 75 mg, further parameters were studied using 55 mg catalyst loading.

3.5. Effect of the Molar Ratio of Acyl Donor to Ascorbic Acid. The molar ratio of one substrate to another is an important parameter affecting the conversion. The solubility of L-ascorbic acid in tert-butanol at 50°C was 26 mmol/L, which is saturated in tert-butanol that would be limiting as substrate. Therefore, the effect of the molar ratio of the reactants was studied by keeping the concentration of L-ascorbic acid and the catalyst quantity constant and varying the concentration of acyl donor in both esterification and transesterification. Figure 4 showed the effect of the molar ratio on the conversion for the synthesis of L-ascorbyl flurbiprofenate. Molar ratio of acyl donor to ascorbic acid was varied from 1 : 1 to 7 : 1, and the L-ascorbic acid was kept constant. The conversion at a reaction time of 72 h for

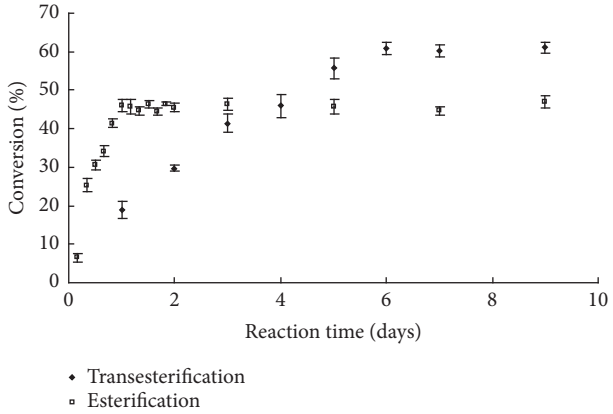

Figure 5: Time course of the synthesis of L-ascorbyl flurbiprofenate.

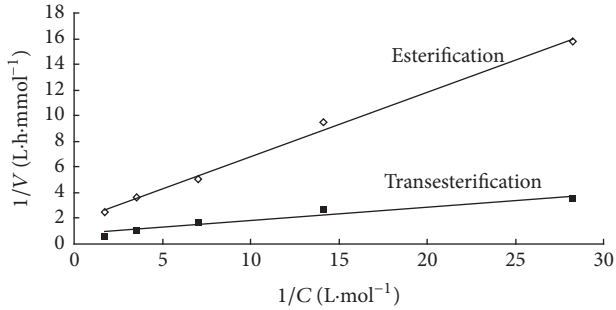

Figure 6: The Lineweaver-Burk plot of $1/V_0$ versus $1/[S]$.

esterification and transesterification was compared. Indeed, within experimental error, at a fixed concentration of L-ascorbic acid and loading amount of Novozym 435 lipase, the conversion increased with increasing acyl donor concentrations up to a critical value. For esterification and transesterification, when using higher ratios of flurbiprofen or flurbiprofen methyl ester over L-ascorbic acid, conversion increased and highest conversion (61.0% for esterification and 46.4% for transesterification) occurred at 5 : 1 molar ratio of flurbiprofen or flurbiprofen methyl ester to L-ascorbic acid. At molar ratios greater than 5 : 1, a constant conversion was observed.

3.6. Effect of Reaction Time. Figure 5 showed the changes in the conversion with time for the direct esterification and transesterification in tert-butanol at 50°C with molar ratio of acyl donor to ascorbic acid of 5 : 1. Direct esterification and transesterification reaction had a different initial rate and maximal conversion. In the case of transesterification reaction, the rate was faster than that of the esterification reaction under otherwise similar conditions within the reaction time of 24 h. This could be attributed that lipase had higher activity for flurbiprofen methyl ester and lower activity with flurbiprofen. Also the difference consisted in the maximal conversion of L-ascorbic acid, which was 61.0% occurring after 144 h of incubation for esterification, against 46.4% occurring after 72 h of incubation for transesterification. This difference might be due to methanol production during the transesterification reaction which was not eliminated by the 3 Å molecular sieve and disadvantageous reaction equilibrium for L-ascorbyl flurbiprofenate production. Even if water was also produced as a coproduct during the esterification reaction, the 3 Å molecular sieve favors its elimination by adsorption and then contributes to shift the reaction equilibrium towards the synthesis of L-ascorbyl flurbiprofenate.

3.7. Kinetic Study. The effects of several parameters including organic solvent, speed of agitation, enzyme amount, substrate molar ratio, and reaction time on conversion of L-ascorbic acid were investigated to optimize the conditions. Since L-ascorbic acid was dissolved in tert-butanol with a saturated concentration of 26 mmol/L, the effect of concentration of flurbiprofen or flurbiprofen methyl ester on the rate of reaction was investigated systematically over a wide range with a constant L-ascorbic acid concentration. For the determination of initial rates, esterification and transesterification were conducted by using 55 mg Novozym 435 lipase with appropriate quantities of acyl donor (flurbiprofen or flurbiprofen methyl ester) and L-ascorbic acid. In esterification and transesterification experiments, the amount of flurbiprofen was varied from 35 to 568 mmol/L at a fixed quantity of L-ascorbic acid (26 mmol/L). The initial rates were determined for each experiment. From the initial rate determined, it showed that when the concentration of acyl donor (flurbiprofen or flurbiprofen methyl ester) was increased, by keeping the concentration of L-ascorbic acid constant, the initial rate of reaction increased proportionally. This presumed that there was no evidence of inhibition by acyl donor (flurbiprofen or flurbiprofen methyl ester) at all the concentrations tested. According to the rate equation for the ping-pong bi-bi mechanism without substrate inhibition [15], the Lineweaver-Burk plot of $1/V_0$ versus $1/[S]$ in Figure 6 showed the kinetic parameter values. The apparent Michaelis-Menten kinetics are K_{rn} = 0.29 mol/L and apparent V_{max} = 0.563 mmol/L·h for flurbiprofen. Apparent Michaelis-Menten kinetics are K_{rn} = 0.14 mol/L and apparent V_{max} = 1.34 mmol/L·h for flurbiprofen methyl ester. This indicated that Novozym 435 lipase has higher affinity for flurbiprofen methyl ester and lower affinity with flurbiprofen. Transesterification has higher reaction rate than esterification.

4. Conclusion

The L-ascorbyl flurbiprofenate has been synthesized successfully by lipase-catalyzed transesterification and esterification in tert-butanol. The goal of this work was to compare lipase-catalyzed esterification and transesterification approaches. Both approaches were studied in a systematic way including the effect of various parameters. We have tried to optimize lipase-catalyzed esterification and transesterification to ensure meaningful and objective comparison among different approaches. Synthesis of L-ascorbyl flurbiprofenate was influenced by reaction conditions. The equilibrium shift

towards the L-ascorbyl flurbiprofenate synthesis was limited in spite of the presence of an excess of acyl donor. The most important strategy seemed to be the efficient removal of by-products, such as water or methanol. Addition of molecular sieves 3 Å during reaction could control water activity of the system. However, addition of molecular sieves 3 Å during reaction could not control methanol content. It was observed that the rate of the transesterification was much higher than that of esterification within 24 h. If the experiments were conducted for a long time, the conversion would reach asymptotic values and then the conversion of esterification was higher than that of the transesterification. This reflected a greater reactivity of flurbiprofen methyl ester in the lipase-catalyzed transesterification reaction as compared with esterification. However, the inherent drawback associated with lipase-catalyzed transesterification was the production of methanol and the equilibrium was usually not in favor of transesterification. Also, in the transesterification, flurbiprofen had to be chemically converted to its methyl ester and then subjected to the transesterification catalyzed by lipase. Although the rate of esterification is slower than that of transesterification, if a choice is at all available, from the standpoint of productivity and the amount of steps required, lipase-catalyzed esterification has been judged to be superior for the synthesis of L-ascorbyl flurbiprofenate.

Competing Interests

The authors declare that they have no competing interests.

Acknowledgments

The authors thank the National Natural Science Foundation of China (21573055), the Scientific Research Fund of Heilongjiang Province (GC13C111), the Open Project Program of the State Key Laboratory for Oxo Synthesis and Selective Oxidation, and the State Key Laboratory of Chemical Resource Engineering for support.

References

[1] Y. Zhao, B. Y. Qu, X. Y. Wu et al., "Design, synthesis and biological evaluation of brain targeting L-ascorbic acid prodrugs of ibuprofen with 'lock-in' function," *European Journal of Medicinal Chemistry*, vol. 82, pp. 314–323, 2014.

[2] B. P. Imbimbo, "The potential role of non-steroidal anti-inflammatory drugs in treating Alzheimer's disease," *Expert Opinion on Investigational Drugs*, vol. 13, no. 11, pp. 1469–1481, 2004.

[3] L. Gasparini, E. Ongini, D. Wilcock, and D. Morgan, "Activity of flurbiprofen and chemically related anti-inflammatory drugs in models of Alzheimer's disease," *Brain Research Reviews*, vol. 48, no. 2, pp. 400–408, 2005.

[4] S. Côté, P.-H. Carmichael, R. Verreault, J. Lindsay, J. Lefebvre, and D. Laurin, "Nonsteroidal anti-inflammatory drug use and the risk of cognitive impairment and Alzheimer's disease," *Alzheimer's & Dementia*, vol. 8, no. 3, pp. 219–226, 2012.

[5] X.-Y. Wu, X.-C. Li, J. Mi, J. You, and L. Hai, "Design, synthesis and preliminary biological evaluation of brain targeting L-ascorbic acid prodrugs of ibuprofen," *Chinese Chemical Letters*, vol. 24, no. 2, pp. 117–119, 2013.

[6] S. Manfredini, B. Pavan, S. Vertuani et al., "Design, synthesis and activity of ascorbic acid prodrugs of nipecotic, kynurenic and diclophenamic acids, liable to increase neurotropic activity," *Journal of Medicinal Chemistry*, vol. 45, no. 3, pp. 559–562, 2002.

[7] Y. Laras, M. Sheha, N. Pietrancosta, and J.-L. Kraus, "Thiazolamide-ascorbic acid conjugate: a γ-secretase inhibitor with enhanced blood-brain barrier permeation," *Australian Journal of Chemistry*, vol. 60, no. 2, pp. 128–132, 2007.

[8] Z. Wang and L. H. Tang, "Design, synthesis and characterization of ascorbic acid pro-drugs of flurbiprofen," *Strait Pharmaceutical Journal*, vol. 22, no. 110, pp. 213–217, 2010.

[9] X. N. Liu and L. H. Tang, "Kinetics and thermodynamics of L-ascorbyl profen esters synthesis catalyzed by lipase in 2-methyl-2-butanol," *Chinese Journal of Bioprocess Engineering*, vol. 8, no. 6, pp. 33–39, 2010.

[10] J. L. Eriksen, S. A. Sagi, T. E. Smith et al., "NSAIDs and enantiomers of flurbiprofen target γ-secretase and lower Aβ42 in vivo," *Journal of Clinical Investigation*, vol. 112, no. 3, pp. 440–449, 2003.

[11] H. Geerts, "Drug evaluation: (R)-flurbiprofen–an enantiomer of flurbiprofen for the treatment of Alzheimer's disease," *The Investigational Drugs Journal*, vol. 10, no. 2, pp. 121–133, 2007.

[12] C. Hansch, A. Leo, and D. Hoekman, *Exploring QSAR: Hydrophobic, Electronic, and Steric Constants*, American Chemical Society, 1995.

[13] C. Hansch, A. Leo, and D. Hoekman, *Exploring QSAR—Hydrophobic, Electronic, and Steric Constants*, American Chemical Society, Washington, DC, USA, 1995.

[14] Q.-X. Song and D.-Z. Wei, "Study of Vitamin C ester synthesis by immobilized lipase from *Candida* sp.," *Journal of Molecular Catalysis B: Enzymatic*, vol. 18, no. 4–6, pp. 261–266, 2002.

[15] G. D. Yadav and P. S. Lathi, "Intensification of enzymatic synthesis of propylene glycol monolaurate from 1,2-propanediol and lauric acid under microwave irradiation: kinetics of forward and reverse reactions," *Enzyme and Microbial Technology*, vol. 38, no. 6, pp. 814–820, 2006.

Hindawi
BioMed Research International
Volume 2017, Article ID 1272193, 9 pages
http://dx.doi.org/10.1155/2017/1272193

Review Article

Biotechnological Processes in Microbial Amylase Production

Subash C. B. Gopinath,[1,2] Periasamy Anbu,[3] M. K. Md Arshad,[1] Thangavel Lakshmipriya,[1] Chun Hong Voon,[1] Uda Hashim,[1] and Suresh V. Chinni[4]

[1] *Institute of Nano Electronic Engineering, Universiti Malaysia Perlis, 01000 Kangar, Perlis, Malaysia*
[2] *School of Bioprocess Engineering, Universiti Malaysia Perlis, 02600 Arau, Perlis, Malaysia*
[3] *Department of Biological Engineering, College of Engineering, Inha University, Incheon 402-751, Republic of Korea*
[4] *Department of Biotechnology, Faculty of Applied Sciences, AIMST University, 08100 Bedong, Malaysia*

Correspondence should be addressed to Subash C. B. Gopinath; subash@unimap.edu.my

Received 29 October 2016; Accepted 27 November 2016; Published 9 February 2017

Academic Editor: Nikolai V. Ravin

Amylase is an important and indispensable enzyme that plays a pivotal role in the field of biotechnology. It is produced mainly from microbial sources and is used in many industries. Industrial sectors with top-down and bottom-up approaches are currently focusing on improving microbial amylase production levels by implementing bioengineering technologies. The further support of energy consumption studies, such as those on thermodynamics, pinch technology, and environment-friendly technologies, has hastened the large-scale production of the enzyme. Herein, the importance of microbial (bacteria and fungi) amylase is discussed along with its production methods from the laboratory to industrial scales.

1. Introduction

The International Enzyme Commission has categorized six distinct classes of enzymes according to the reactions they catalyze: EC1 Oxidoreductases; EC2 Transferases; EC3 Hydrolases; EC4 Lyases; EC5 Isomerases; and EC6 Ligases [1]. In general, biologically active enzymes can be obtained from plants, animals, and microorganisms. Microbial enzymes have been generally favored for their easier isolation in high amounts, low-cost production in a short time, and stability at various extreme conditions, and their cocompounds are also more controllable and less harmful. Microbially produced enzymes that are secreted into the media are highly reliable for industrial processes and applications. Furthermore, the production and expression of recombinant enzymes are also easier with microbes as the host cell. Applications of these enzymes include chemical production, bioconversion (biocatalyst), and bioremediation. In this aspect, the potential uses of different microbial enzymes have been demonstrated [2–5]. With regard to industrial applications, enzyme purification studies have predominantly focused on proteases, lipases, and amylases [4–12]. Furthermore, several microbes have been isolated from different sources for the production of extracellular hydrolases [5, 13, 14], which are either endohydrolases or exohydrolases. In this overview, we focus on the microbial hydrolase enzyme amylase for its downstream applications in industries and medicines.

2. Amylase and Its Substrates

Amylases are broadly classified into α, β, and γ subtypes, of which the first two have been the most widely studied (Figures 1(a) and 1(b)). α-Amylase is a faster-acting enzyme than β-amylase. The amylases act on α-1-4 glycosidic bonds and are therefore also called glycoside hydrolases. The first amylase was isolated by Anselme Payen in 1833. Amylases are distributed widely in living systems and have specific substrates [15, 16]. Amylase substrates are widely available from cheap plant sources, rendering the potential applications of the enzyme more plentiful in terms of costs. Amylases can be divided into endoamylases and exoamylases. The endoamylases catalyze hydrolysis in a random manner within the starch molecule. This action causes the formation of linear and branched oligosaccharides of various chain lengths. The

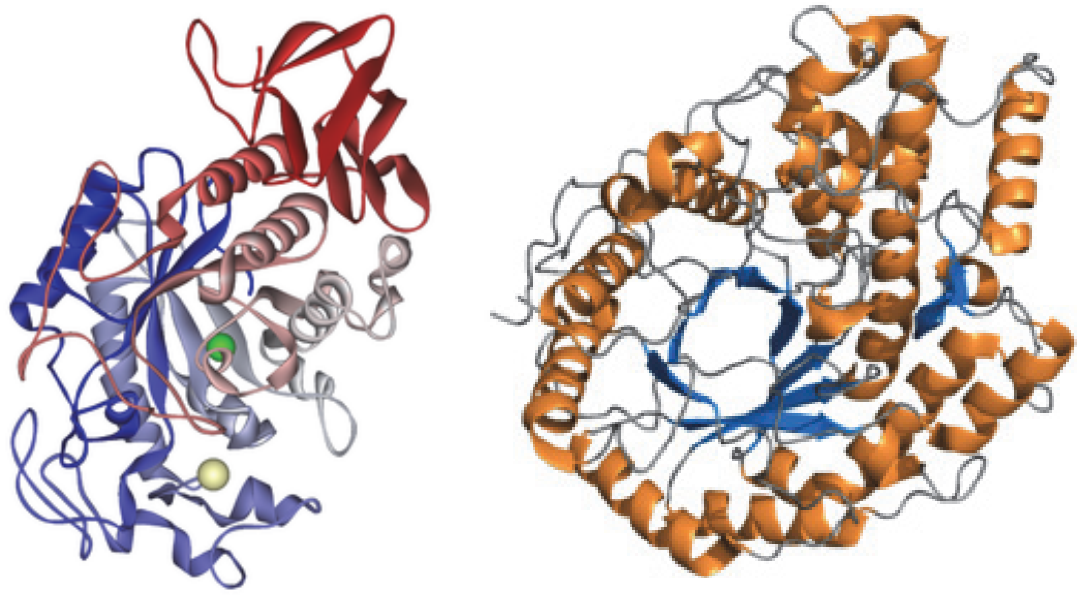

(a) (b)

Figure 1: Three-dimensional structures of amylases. (a) α-Amylase (RCSB PDB accession code 1SMD; the calcium-binding regions are indicated). (b) β-Amylase (RCSB PDB accession code PDB 2xfr).

exoamylases hydrolyze the substrate from the nonreducing end, resulting in successively shorter end products [16]. All α-amylases (EC 3.2.1.1) act on starch (polysaccharide) as the main substrate and yield small units of glucose (monosaccharide) and maltose (disaccharide) (Figure 2). Starch is made up of two glycose polymers, amylose and amylopectin, which comprise glucose molecules that are connected by glyosidic bonds. Both polymers have different structures and properties. A linear polymer of amylose has a maximum of 6000 glucose units linked by α-1,4 glycosidic bonds, whereas amylopectin is composed of α-1,4-linked chains of 10–60 glucose units with α-1,6-linked side chains of 15–45 glucose units. Saboury [17] revealed the α-amylases to be metalloenzymes that require metal (calcium) ions to maintain their stability, activity, and structural confirmation. Based on sequence alignments of α-amylases, Nielsen and Borchert [18] revealed that these enzymes have four conserved arrangements (I–IV), which are found as β-strands 3, 4, and 5 in the loop connecting β-strand 7 to α-helix 7 (Figure 3). Despite the fact that amylases are broadly available from different sources, past focus has been on only microbial amylases, owing to their advantages over plant and animal amylases, as discussed above. Microbial amylases have been isolated from several stains and explored for amylase production by the methods described below.

3. Isolation Methods

The isolation of potential and efficient bacterial or fungal strains is important before being screened for their production of enzymes of interest. As stated elsewhere, microbes are ubiquitous and can be obtained from any source. However, the most efficient strains are usually obtained from substrate-rich environments, from which the microbes can be adopted to use a particular substrate [5, 13]. The common method of strain isolation is through serial dilution, whereupon the number of colonies is minimized and thus easy to select [13]. Another method is through substrate selection, where efficient strains are isolated according to their affinity for a particular substrate [14]. Through these methods, several bacteria and fungi have been isolated and studied for amylase production.

4. Microbial Amylase

Microbial amylases obtained from bacteria, fungi, and yeast have been used predominantly in industrial sectors and scientific research. The level of amylase production varies from one microbe to another, even among the same genus, species, and strain. Furthermore, the level of amylase production also differs depending on the microbe's origin, where strains isolated from starch- or amylose-rich environments naturally produce higher amounts of enzyme. Factors such as pH, temperature, and carbon and nitrogen sources also play vital roles in the rate of amylase production, particularly in fermentation processes. Because microorganisms are amenable to genetic engineering, strains can be improved for obtaining higher amylase yields. Microbes can also be fine-tuned to produce efficient amylases that are thermostable and stable at stringent conditions. Such improvements can also reduce contamination by background proteins and minimize the reaction time and lead to less energy expenditure in the amylase reaction [20]. The selection of halophilic strains is also beneficial to the production of amylase under extreme conditions (Figure 4).

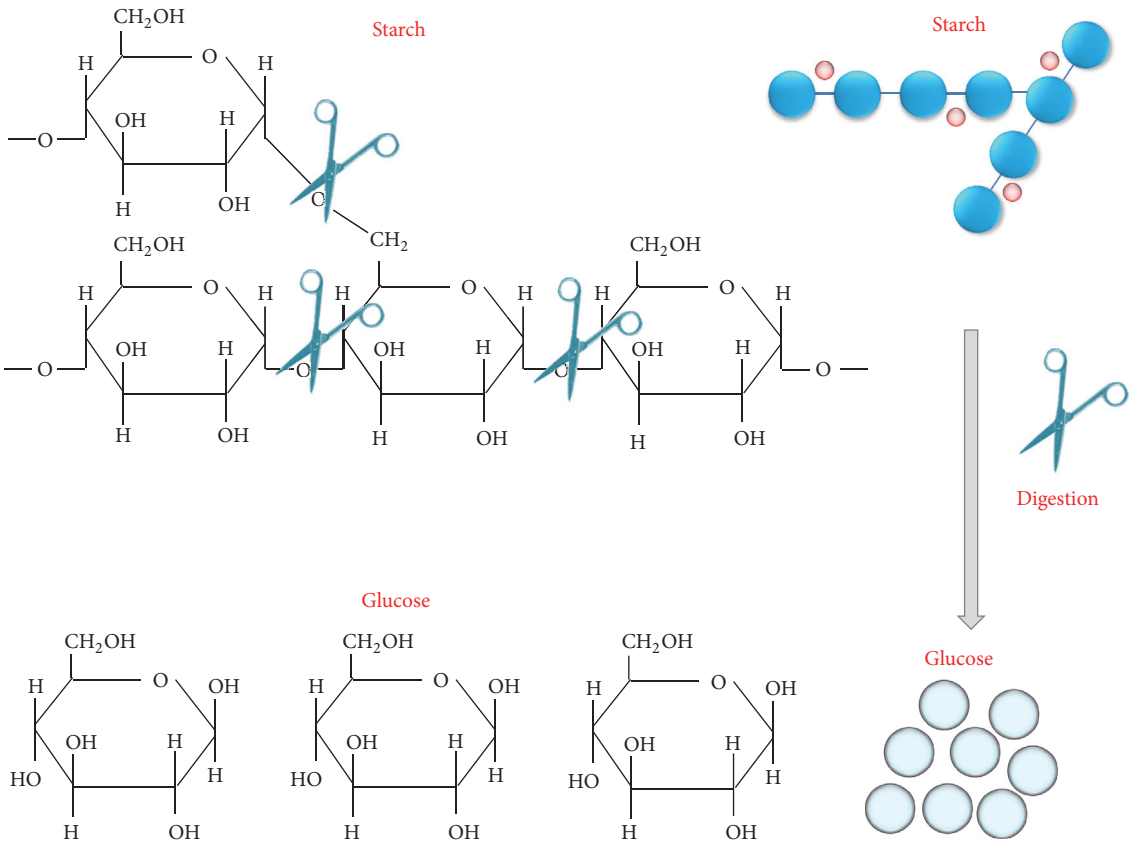

FIGURE 2: Scheme for the hydrolysis of starch by amylase. Starch is a polysaccharide made up of simple sugars (glucose). Upon the action of amylase, either glucose (a monosaccharide) or maltose (a disaccharide with two glucose molecules) is released.

4.1. Bacterial Amylases. Among the wide range of microbial species that secrete amylase, its production from bacteria is cheaper and faster than from other microorganisms. Furthermore, as mentioned above, genetic engineering studies are easier to perform with bacteria and they are also highly amenable for the production of recombinant enzymes. A wide range of bacterial species has been isolated for amylase secretion. Most are *Bacillus* species (*B. subtilis*, *B. stearothermophilus*, *B. amyloliquefaciens*, *B. licheniformis*, *B. coagulans*, *B. polymyxa*, *B. mesentericus*, *B. vulgaris*, *B. megaterium*, *B. cereus*, *B. halodurans*, and *Bacillus* sp. Ferdowsicous), but amylases from *Rhodothermus marinus*, *Corynebacterium gigantea*, *Chromohalobacter* sp., *Caldimonas taiwanensis*, *Geobacillus thermoleovorans*, *Lactobacillus fermentum*, *Lactobacillus manihotivorans*, and *Pseudomonas stutzeri* have also been isolated [1, 12, 16, 20, 21]. Halophilic strains that produce amylases include *Haloarcula hispanica*, *Halobacillus* sp., *Chromohalobacter* sp., *Bacillus dipsosauri*, and *Halomonas meridiana* [22]. More studies involving the isolation and improvement of novel strains will pave the way to creating important strains. For example, Dash et al. [23] identified a new *B. subtilis* BI19 strain that produces amylase efficiently and, upon optimizing the conditions, enhanced the enzyme production about 3.06 folds. Three-dimensional structural analysis of such amylases helps in improving their efficiency. For example, the crystal structure of α-amylase from *Anoxybacillus* has provided insight into this enzyme subclass [19]. Studies on the three-dimensional structure also aid in the alteration or mutation of particular amino acids to improve the efficiency and functions of the enzyme or protein [24–26].

4.2. Fungal Amylases. Fungal enzymes have the advantage of being secreted extracellularly. In addition, the ability of fungi to penetrate hard substrates facilitates the hydrolysis process. In addition, fungal species are highly suitable for solid-based fermentation. The first fungal-produced amylase for industrial application was described several decades ago [27]. Efficient amylase-producing species include those of genus *Aspergillus* (*A. oryzae*, *A. niger*, *A. awamori*, *A. fumigatus*, *A. kawachii*, and *A. flavus*), as well as *Penicillium* species (*P. brunneum*, *P. fellutanum*, *P. expansum*, *P. chrysogenum*, *P. roqueforti*, *P. janthinellum*, *P. camemberti*, and *P. olsonii*), *Streptomyces rimosus*, *Thermomyces lanuginosus*, *Pycnoporus sanguineus*, *Cryptococcus flavus*, *Thermomonospora curvata*, and *Mucor* sp. [12, 16, 20, 21].

5. Recombinant Amylase

Genetic engineering and recombinant DNA technology are the current molecular techniques used to promote efficient

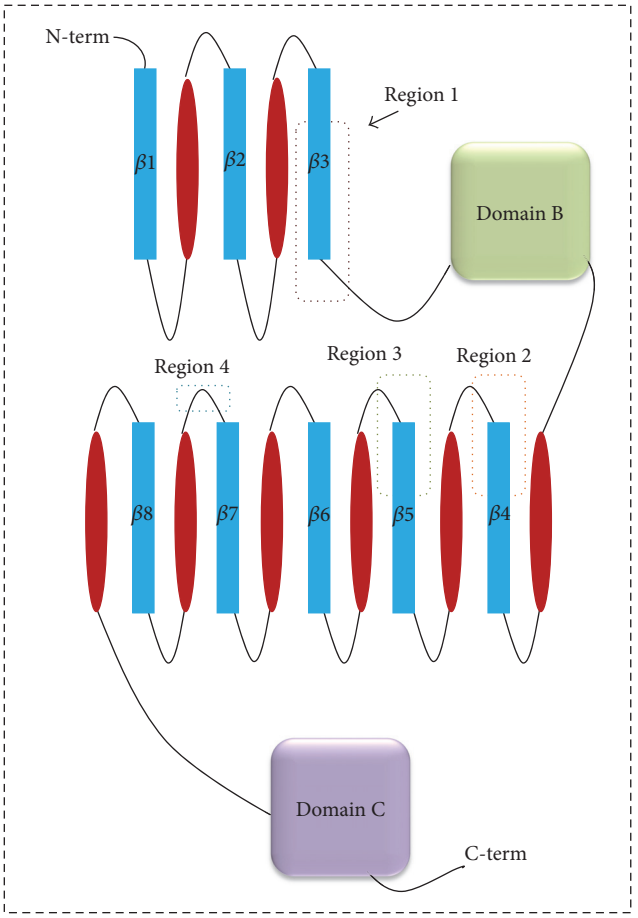

Figure 3: Topology of α-amylases. The positions of four conserved sequence patterns are indicated with dashed boxes [18].

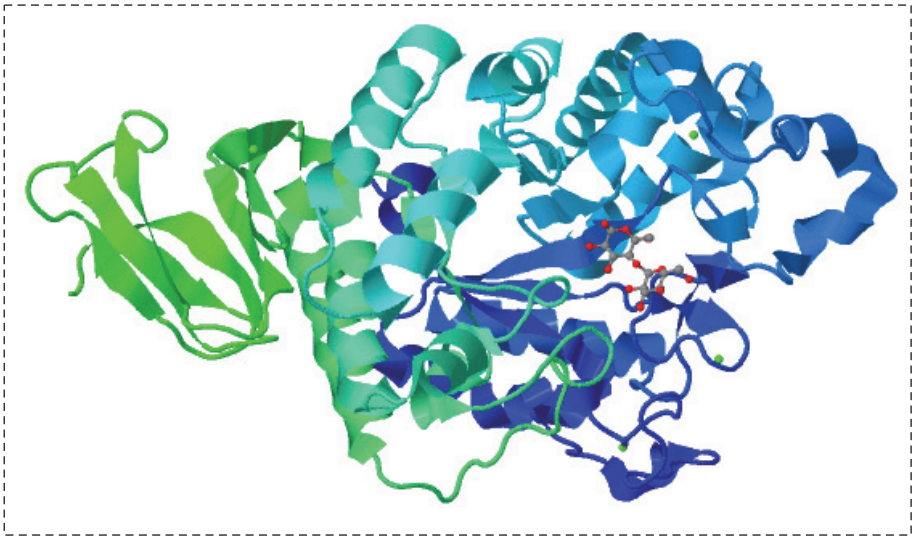

Figure 4: A flowchart for microbial amylase. Three-dimensional structure of the α-amylase from *Anoxybacillus* (RCSB PDB accession code 5A2C) [19] is shown.

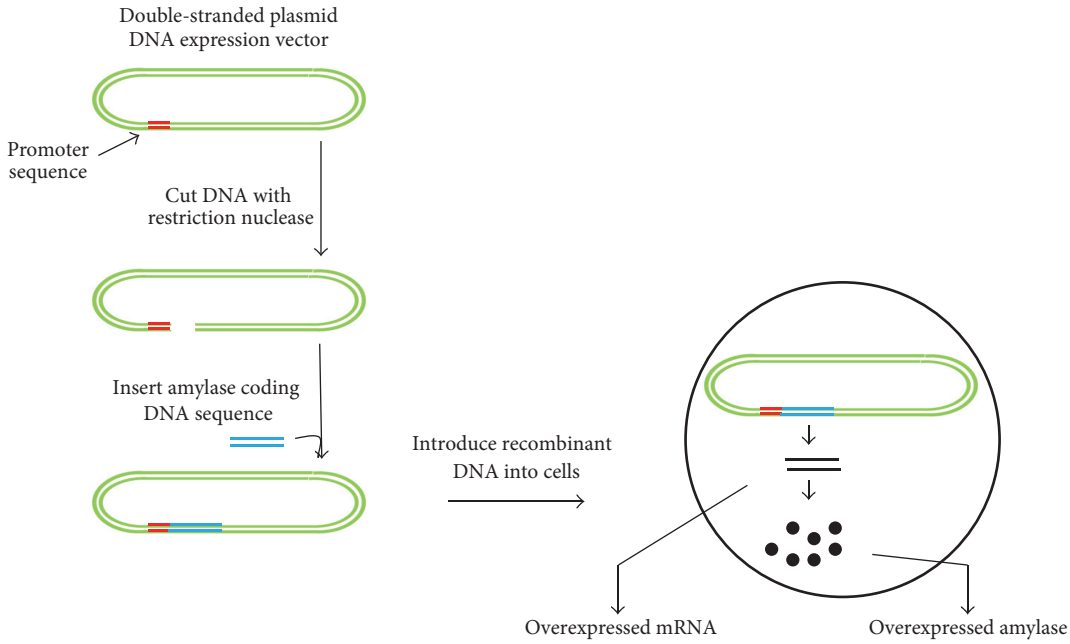

Figure 5: Recombinant DNA technology for amylase production. The steps involve selection of an efficient amylase gene, insertion of the gene into an appropriate vector system, transformation into an efficient bacterial system to produce a higher amount of recombinant mRNA, and overproduction of amylase from the bacterial system.

enzyme production [18, 28–30]. Recombinant DNA technology for amylase production involves the selection of an efficient amylase gene, gene insertion into an appropriate vector system, transformation in an efficient bacterial system to produce a high amount of recombinant protein (in the presence of an expression-vector promoter-inducing agent), and purification of the protein for downstream applications (Figure 5). In this technology, high-copy numbers of the gene promote higher yields of amylase [30]. On the other hand, screening mutant libraries for selection of the best mutant variants for recombinant amylase production has been more successful (Figure 6). Zhang et al. [31] deleted *amyR* (encoding a transcription factor) from *A. niger* CICC2462, which led to the production of enzyme/protein specifically with lower background protein secretion. Wang et al. [32] generated a new strategy to express the α-amylase from *Pyrococcus furiosus* in *B. amyloliquefaciens*. This extracellular thermostable enzyme is produced in low amount in *P. furiosus*, but its expression in *B. amyloliquefaciens* was significantly increased and had good stability at higher temperature (optimum 100°C) and lower pH (optimum pH 5). By mimicking the *P. furiosus* system, they obtained a novel amylase with yields ~3000- and 14-fold higher amylase units/milliliter than that produced in *B. subtilis* and *Escherichia coli*, respectively.

6. Screening Microbial Amylase Production

Production or secretion of amylase can be screened by different common methods, including solid-based or solution-based techniques. The solid-based method is carried out on nutrient agar plates containing starch as the substrate, whereas solution-based methods include the dinitro salicylic acid (DNS) and Nelson-Somogyi (NS) techniques. In the solid-agar method, the appropriate strain (fungi or bacteria) is pinpoint-inoculated onto the starch-containing agar at the center of the Petri plate. After an appropriate incubation period, the plate is flooded with iodine solution, which reveals a dark bluish color on the substrate region and a clear region (due to hydrolysis) around the inoculum, indicating the utilization of starch by the microbial amylase. Gopinath et al. [7] applied this method to determine the amylase activity of *Aspergillus versicolor*, as well as that of *Penicillium* sp., in their preliminary study (Figure 7).

In the solution-based DNS method, the appropriate substrate and enzyme are mixed in the right proportion and reacted for 5 min at 50°C. After cooling to room temperature, the absorbance of the solution is read at 540 nm. Gusakov et al. [33] applied this method to detect the release of reducing sugars from substrate hydrolysis by *Bacillus* sp. amylase. They found that the amylase activity could reach up to 0.75 U mL^{-1} after 24 h of incubation. Similarly, in the NS method, amylase and starch are mixed and incubated for 5 min at 50°C. Then, a Somogyi copper reagent is added to stop the reaction, followed by boiling for 40 min and a subsequent cool-down period. A Nelson arsenomolybdate reagent is then added and the mixture is incubated at room temperature for 10 min. Then, after diluting with water, the solution is centrifuged at high speed and the supernatant is measured at 610 nm [34]. Apart from these, several other methods are available for amylase screening, but all use the same substrate (starch).

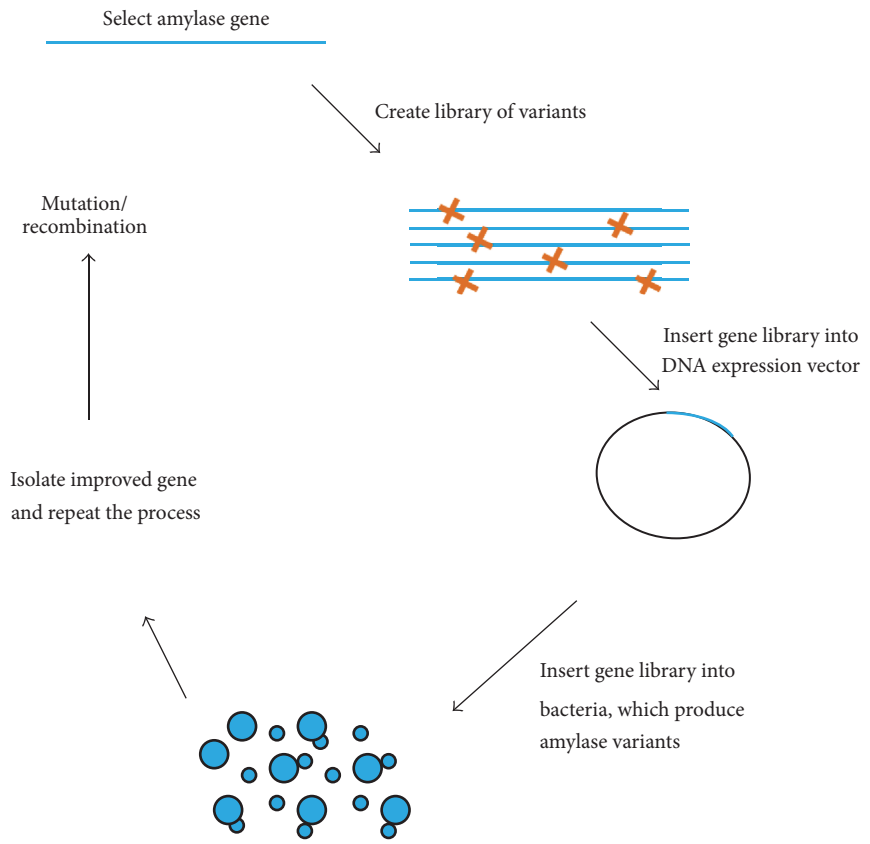

Figure 6: Mutant library screening. Selection of the best variants is a more successful technique for the ultimate application in recombinant amylase production.

7. Enhancing Microbial Amylase Production

The primary objective in amylase production enhancement is to perform basic optimization studies. This can be done either experimentally or by applying design of experiments (DOE) with further confirmation by the suggested experiments from the DOE [35, 36]. Several DOE methods have been proposed and, with the advancement of software, are capable of better predictions [35–38]. Gopinath et al. [8] performed an optimization study by using a Box-Behnken design, involving three variables (incubation time, pH, and starch as the substrate), for higher amylase production by the fungus *A. versicolor*. The laboratory experiments were in good agreement with the values predicted from DOE, with a correlation coefficient of 0.9798 confirming the higher production. Srivastava et al. [37] optimized the conditions for immobilizing amylase covalently, using glutaraldehyde as the crosslinker on graphene sheets. In this study, Box-Behnken-designed response surface methodology was used, with the efficiency of immobilization shown as 84%. This kind of study is important when molecules such as glutaraldehyde are used, owing to two aldehyde groups being available at both ends of the molecule. By optimization study, the chances of immobilizing a higher number of glutaraldehyde molecules can be predicted. In another study, the enzyme-assisted extraction and identification of antioxidative and α-amylase inhibitory peptides from Pinto beans were performed, using a factorial design with different variables (extraction time, temperature, and pH) [38]. Another way to enhance the action of amylase is by its encapsulation or entrapment on alginate or other beads (Figure 8). This method facilitates the slow and constant release of enzyme and increases its stability.

8. Industrial Applications of Microbial Amylase

Amylase makes up approximately 25% of the world enzyme market [1]. It is used in foods, detergents, pharmaceuticals, and the paper and textile industries [12, 21]. Its applications in the food industry include the production of corn syrups, maltose syrups, glucose syrups, and juices and alcohol fermentation and baking [1]. It has been used as a food additive and for making detergents. Amylases also play an important role in beer and liquor brewing from sugars (based on starch). In this fermentation process, yeast is used to ingest sugars, and alcohol is produced. Fermentation is suitable for microbial amylase production under moisture and proper growth conditions. Two kinds of fermentation processes have been followed: submerged fermentation and solid-state

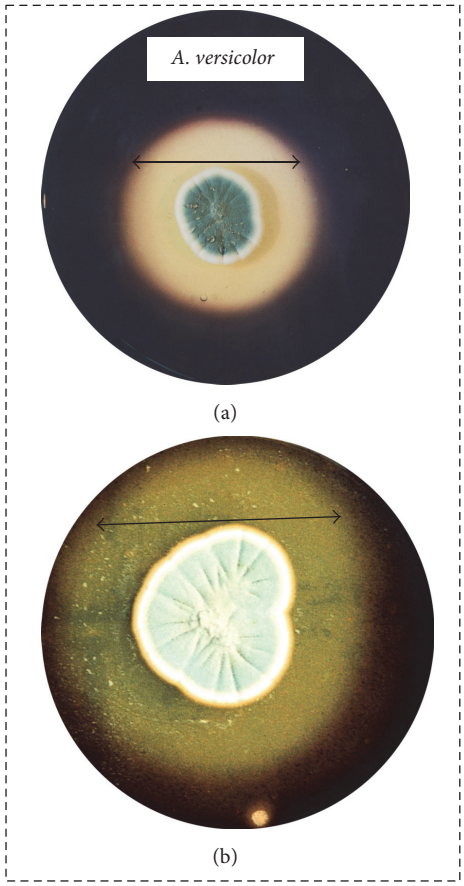

Figure 7: Amylase production on agar plate. In this solid-based method, the starch-containing agar plate is pinpoint-inoculated with the microorganism at the center of the Petri plate. After an appropriate incubation period, flooding the plate with iodine solution reveals a dark bluish color on the substrate region. The clear region around the inoculum indicates the zone of hydrolysis. (a) Amylolytic activity by *Aspergillus versicolor*; (b) amylolytic activity by *Penicillium* sp.

fermentation. The former is the one traditionally used and the latter has been more recently developed. In traditional beer brewing, malted barley is mashed and its starch is hydrolyzed into sugars by amylase at an appropriate temperature. By varying the temperatures and conditions for α- or β-amylase activities, the unfermentable and fermentable sugars are determined. With these changes, the alcohol content and flavor and mouthfeel of the end product can be varied.

The potential industrial applications of enzymes are determined by the ability to screen new and improved enzymes, their fermentation and purification in large scale, and the formulations of enzymes. As stated above, different methods have been established for enzyme production. In the case of amylase, the crude extract can function well in most of the cases, but for specific industrial applications (e.g., pharmaceuticals), purification of the enzyme is required. This can be accomplished by ion-exchange chromatography, hydrophobic interaction chromatography, gel filtration, immunoprecipitation, polyethylene glycol/Sepharose gel separation, and aqueous two-phase and gradient systems [2], where the size and charge of the amylase determine the method chosen. Automated programming system with the above methods has improved the processes greatly.

With these developments, microbial amylase production has successfully replaced its production by chemical processes, especially in industry [39]. Production of amylase has been improved by using genetically modified strains that reduce the polymerization of maltose during amylolytic action [20]. For further improvement in the industrial process, the above-mentioned DOE and encapsulation methods can be implemented.

9. Future Perspectives

Among the different enzymes, amylase possesses the highest potential for use in different industrial and medicinal purposes. The involvement of modern technologies, such as white biotechnology, pinch technology, and green technology, will hasten its industrial production on a large scale. This will be further facilitated by implementation of established fermentation technologies with appropriate microbial species (bacteria or fungi) and complementation

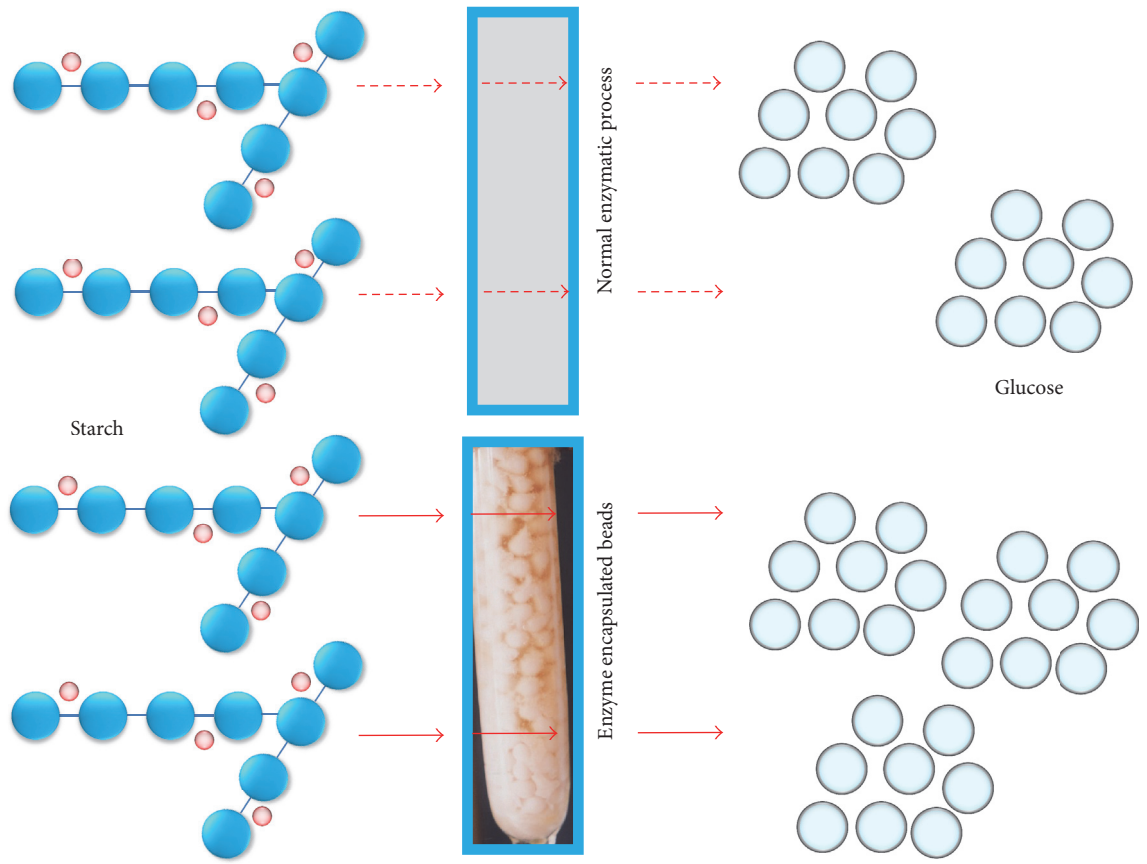

Figure 8: Efficient application of amylase. Differences between the conventional methods of amylase utilization against alginate bead-encapsulated amylase are shown.

of other biotechnological aspects. The technologies of high-throughput screening and processing with efficient microbial species, along with the ultimate coupling of genetic engineering of amylase-producing strains, will all help in enhancing amylase production for industrial and medicinal applications.

Competing Interests

The authors declare that there is no conflict of interests regarding the publication of this paper.

Acknowledgments

This study was supported by an Inha University Research Grant from Inha University, Republic of Korea.

References

[1] K. Mojsov, "Microbial α-amylases and their industrial applications: a review," *International Journal of Management, IT and Engineering*, vol. 2, pp. 583–609, 2012.

[2] S. C. B. Gopinath, P. Anbu, T. Lakshmipriya, and A. Hilda, "Strategies to characterize fungal lipases for applications in medicine and dairy industry," *BioMed Research International*, vol. 2013, Article ID 154549, 10 pages, 2013.

[3] S. C. B. Gopinath, P. Anbu, T. Lakshmipriya et al., "Biotechnological aspects and perspective of microbial Keratinase production," *BioMed Research International*, vol. 2015, Article ID 140726, 10 pages, 2015.

[4] P. Anbu, "Characterization of solvent stable extracellular protease from Bacillus koreensis (BK-P21A)," *International Journal of Biological Macromolecules*, vol. 56, pp. 162–168, 2013.

[5] P. Anbu and B. K. Hur, "Isolation of an organic solvent-tolerant bacterium *Bacillus licheniformis* PAL05 that is able to secrete solvent-stable lipase," *Biotechnology and Applied Biochemistry*, vol. 61, no. 5, pp. 528–534, 2014.

[6] S. C. B. Gopinath, A. Hilda, T. L. Priya, and G. Annadurai, "Purification of lipase from Cunninghamella verticillata and optimization of enzyme activity using response surface methodology," *World Journal of Microbiology and Biotechnology*, vol. 18, no. 5, pp. 449–458, 2002.

[7] S. C. B. Gopinath, A. Hilda, T. Lakshmi Priya, G. Annadurai, and P. Anbu, "Purification of lipase from Geotrichum candidum: conditions optimized for enzyme production using Box-Behnken design," *World Journal of Microbiology and Biotechnology*, vol. 19, no. 7, pp. 681–689, 2003.

[8] S. C. B. Gopinath, A. Hilda, T. Lakshmi Priya, G. Annadurai, and P. Anbu, "Statistical optimization of amylolytic activity by *Aspergillus versicolor*," *Asian Journal of Microbiology, Biotechnology and Environmental Sciences*, vol. 5, no. 3, pp. 327–330, 2003.

[9] T. S. Kumarevel, S. C. B. Gopinath, A. Hilda, N. Gautham, and M. N. Ponnusamy, "Purification of lipase from *Cunninghamella verticillata* by stepwise precipitation and optimized conditions for crystallization," *World Journal of Microbiology and Biotechnology*, vol. 21, no. 1, pp. 23–26, 2005.

[10] P. Anbu, S. C. B. Gopinath, A. Hilda, T. Lakshmi Priya, and G. Annadurai, "Purification of keratinase from poultry farm isolate-*Scopulariopsis brevicaulis* and statistical optimization of enzyme activity," *Enzyme and Microbial Technology*, vol. 36, no. 5-6, pp. 639–647, 2005.

[11] P. Anbu, S. C. B. Gopinath, A. Hilda, N. Mathivanan, and G. Annadurai, "Secretion of keratinolytic enzymes and keratinolysis by *Scopulariopsis brevicaulis* and *Trichophyton mentagrophytes*: regression analysis," *Canadian Journal of Microbiology*, vol. 52, no. 11, pp. 1060–1069, 2006.

[12] I. Hussain, F. Siddique, M. S. Mahmood, and S. I. Ahmed, "A review of the microbiological aspect of α-amylase production," *International Journal of Agriculture and Biology*, vol. 15, no. 5, pp. 1029–1034, 2013.

[13] S. C. B. Gopinath, P. Anbu, and A. Hilda, "Extracellular enzymatic activity profiles in fungi isolated from oil-rich environments," *Mycoscience*, vol. 46, no. 2, pp. 119–126, 2005.

[14] P. Anbu, A. Hilda, and S. C. B. Gopinath, "Keratinophilic fungi of poultry farm and feather dumping soil in Tamil Nadu, India," *Mycopathologia*, vol. 158, no. 3, pp. 303–309, 2004.

[15] H. Guzmàn-Maldonado, O. Paredes-Lòpez, and C. G. Biliaderis, "Amylolytic enzymes and products derived from starch: a review," *Critical Reviews in Food Science and Nutrition*, vol. 35, no. 5, pp. 373–403, 1995.

[16] R. Gupta, P. Gigras, H. Mohapatra, V. K. Goswami, and B. Chauhan, "Microbial α-amylases: a biotechnological perspective," *Process Biochemistry*, vol. 38, no. 11, pp. 1599–1616, 2003.

[17] A. A. Saboury, "Stability, activity and binding properties study of α-amylase upon interaction with Ca^{2+} and Co^{2+}," *Biologia—Section Cellular and Molecular Biology*, vol. 57, no. 11, pp. 221–228, 2002.

[18] J. E. Nielsen and T. V. Borchert, "Protein engineering of bacterial α-amylases," *Biochimica et Biophysica Acta*, vol. 1543, no. 2, pp. 253–274, 2000.

[19] K. P. Chai, N. F. B. Othman, A.-H. Teh et al., "Crystal structure of *Anoxybacillus* α-amylase provides insights into maltose binding of a new glycosyl hydrolase subclass," *Scientific Reports*, vol. 6, Article ID 23126, 2016.

[20] A. Sundarram and T. P. Krishna Murthy, "α-amylase production and applications: a review," *Journal of Applied & Environmental Microbiology*, vol. 2, no. 4, pp. 166–175, 2014.

[21] P. M. de Souza and P. O. E. Magalhaes, "Application of microbial-amylase in industry—a review," *Brazilian Journal of Microbiology*, vol. 41, pp. 850–861, 2010.

[22] K. Kathiresan and S. Manivannan, "α-Amylase production by *Penicillium fellutanum* isolated from mangrove rhizosphere soil," *African Journal of Biotechnology*, vol. 5, no. 10, pp. 829–832, 2006.

[23] B. K. Dash, M. M. Rahman, and P. K. Sarker, "Molecular identification of a newly isolated *Bacillus subtilis* BI19 and optimization of production conditions for enhanced production of extracellular amylase," *BioMed Research International*, vol. 2015, Article ID 859805, 9 pages, 2015.

[24] T. Kumarevel, N. Nakano, K. Ponnuraj et al., "Crystal structure of glutamine receptor protein from *Sulfolobus tokodaii* strain 7 in complex with its effector l-glutamine: implications of effector binding in molecular association and DNA binding," *Nucleic Acids Research*, vol. 36, no. 14, pp. 4808–4820, 2008.

[25] T. Kumarevel, K. Sakamoto, S. C. B. Gopinath, A. Shinkai, P. K. R. Kumar, and S. Yokoyama, "Crystal structure of an archaeal specific DNA-binding protein (Ape10b2) from *Aeropyrum pernix* K1," *Proteins*, vol. 71, no. 3, pp. 1156–1162, 2008.

[26] T. Kumarevel, T. Tanaka, M. Nishio et al., "Crystal structure of the MarR family regulatory protein, ST1710, from *Sulfolobus tokodaii* strain 7," *Journal of Structural Biology*, vol. 161, no. 1, pp. 9–17, 2008.

[27] W. Crueger and A. Crueger, *Industrial Microbiology*, Sinauer Associates, Sunderland, Mass, USA, 1989.

[28] J. M. Corbin, B. I. Hashimoto, K. Karuppanan et al., "Semi-continuous bioreactor production of recombinant butyryl-cholinesterase in transgenic rice cell suspension cultures," *Frontiers in Plant Science*, vol. 7, article 412, 2016.

[29] J.-W. Jung, N.-S. Kim, S.-H. Jang, Y.-J. Shin, and M.-S. Yang, "Production and characterization of recombinant human acid α-glucosidase in transgenic rice cell suspension culture," *Journal of Biotechnology*, vol. 226, pp. 44–53, 2016.

[30] Y. J. Son, A. J. Ryu, L. Li, N. S. Han, and K. J. Jeong, "Development of a high-copy plasmid for enhanced production of recombinant proteins in *Leuconostoc citreum*," *Microbial Cell Factories*, vol. 15, no. 1, article 12, 2016.

[31] H. Zhang, S. Wang, X. X. Zhang et al., "The amyR-deletion strain of *Aspergillus niger* CICC2462 is a suitable host strain to express secreted protein with a low background," *Microbial Cell Factories*, vol. 15, article 68, 2016.

[32] P. Wang, P. Wang, J. Tian et al., "A new strategy to express the extracellular α-amylase from *Pyrococcus furiosus* in *Bacillus amyloliquefaciens*," *Scientific Reports*, vol. 6, Article ID 22229, 2016.

[33] A. V. Gusakov, E. G. Kondratyeva, and A. P. Sinitsyn, "Comparison of two methods for assaying reducing sugars in the determination of carbohydrase activities," *International Journal of Analytical Chemistry*, vol. 2011, Article ID 283658, 4 pages, 2011.

[34] T. Kobayashi, H. Kanai, T. Hayashi, T. Akiba, R. Akaboshi, and K. Horikoshi, "Haloalkaliphilic maltotriose-forming α-amylase from the *Archaebacterium Natronococcus* sp. strain Ah-36," *Journal of Bacteriology*, vol. 174, no. 11, pp. 3439–3444, 1992.

[35] R. García, A. Renedo, M. Martínez, and J. Aracil, "Enzymatic synthesis of n-octyl (+)-2-methylbutanoate ester from racemic (±)-2-methylbutanoic acid by immobilized lipase: optimization by statistical analysis," *Enzyme and Microbial Technology*, vol. 30, no. 1, pp. 110–115, 2002.

[36] Y.-N. Chang, J.-C. Huang, C.-C. Lee, I.-L. Shih, and Y.-M. Tzeng, "Use of response surface methodology to optimize culture medium for production of lovastatin by *Monascus ruber*," *Enzyme and Microbial Technology*, vol. 30, no. 7, pp. 889–894, 2002.

[37] G. Srivastava, K. Singh, M. Talat, O. N. Srivastava, and A. M. Kayastha, "Functionalized graphene sheets as immobilization matrix for fenugreek β-amylase: enzyme kinetics and stability studies," *PLoS ONE*, vol. 9, no. 11, Article ID e113408, 2014.

[38] Y.-Y. Ngoh and C.-Y. Gan, "Enzyme-assisted extraction and identification of antioxidative and α-amylase inhibitory peptides from Pinto beans (*Phaseolus vulgaris* cv. *Pinto*)," *Food Chemistry*, vol. 190, pp. 331–337, 2016.

[39] P. Saranraj and D. Stella, "Fungal amylase—a review," *International Journal of Microbiological Research*, vol. 4, pp. 203–211, 2013.

Hindawi Publishing Corporation
BioMed Research International
Volume 2016, Article ID 4239375, 9 pages
http://dx.doi.org/10.1155/2016/4239375

Research Article

Extracellular Ribonuclease from *Bacillus licheniformis* (Balifase), a New Member of the N1/T1 RNase Superfamily

Yulia Sokurenko, Alsu Nadyrova, Vera Ulyanova, and Olga Ilinskaya

Institute of Fundamental Medicine and Biology, Kazan Federal University, Kremlevskaya Str. 18, Kazan 420008, Russia

Correspondence should be addressed to Yulia Sokurenko; sokurenko.yulia@gmail.com

Received 2 June 2016; Accepted 25 July 2016

Academic Editor: Subash C. B. Gopinath

The N1/T1 RNase superfamily comprises enzymes with well-established antitumor effects, such as ribotoxins secreted by fungi, primarily by *Aspergillus* and *Penicillium* species, and bacterial RNase secreted by *B. pumilus* (binase) and *B. amyloliquefaciens* (barnase). RNase is regarded as an alternative to classical chemotherapeutic agents due to its selective cytotoxicity towards tumor cells. New RNase with a high degree of structural similarity with binase (73%) and barnase (74%) was isolated and purified from *Bacillus licheniformis* (balifase, calculated molecular weight 12421.9 Da, pI 8.91). The protein sample with enzymatic activity of 1.5 $\times 10^6$ units/A_{280} was obtained. The physicochemical properties of balifase are similar to those of barnase. However, in terms of its gene organization and promoter activity, balifase is closer to binase. The unique feature of balifase gene organization consists in the fact that genes of RNase and its inhibitor are located in one operon. Similarly to biosynthesis of binase, balifase synthesis is induced under phosphate starvation; however, in contrast to binase, balifase does not form dimers under natural conditions. We propose that the highest stability of balifase among analyzed RNase types allows the protein to retain its structure without oligomerization.

1. Introduction

Ribonuclease (RNase) is involved in many cellular processes including control of gene expression, angiogenesis, apoptosis, and cell defense from pathogens [1–5]. At present, RNase types possessing antitumor and antiviral activities are at the peak of experimental investigation due to their selective toxicity towards cancer or virus-infected cells [3, 6–11]. Among them are secreted RNase types of bacterial origin which belong to N1/T1 (EC 3.1.27.3) superfamily. Such RNase types are small (~12.5 kDa) extracellular basic proteins. Upon RNA hydrolysis these enzymes cleave the 3′,5′-phosphodiester bond between guanosine 3′-phosphate and the 5′-OH group of the adjacent nucleotide, while generating 2′,3′-cyclic guanosine phosphate in the first stage of a catalytic reaction. This stage is reversible and faster than the second one, wherein the cyclic intermediate is converted into the corresponding 3′-phosphate derivative [12]. This type of RNase was isolated from the cultural fluid of *B. amyloliquefaciens* (termed barnase, P00648), *B. pumilus* (binase, P00649), *B. altitudinis* (balnase, A0A0J1IDI7), *B. circulans* (P35078), and *B. coagulans* (P37203). The catalytic activity, molecular structures, and some biological properties of such RNase were explored and characterized [13–17]. The most studied representatives of bacillary RNase are binase and barnase produced by *B. pumilus* and *B. amyloliquefaciens*, respectively. Consisting of ~110 amino acid residues, these enzymes are highly similar in their structure. They also show similar physicochemical and catalytic properties, namely, stability over a wide pH range (3–10) with an optimum at pH 8.5 and nonrequirement in metal ions for ribonucleolytic activity [2].

Bacillus spp. are known to produce another type of extracellular RNase with high molecular weight (~30 kDa) and low level of catalytic activity, while lacking specificity towards guanyl residues. These enzymes are exemplified by *B. subtilis* Bsn and *B. pumilus* binase II [18, 19].

B. licheniformis, the endospore-forming, nonpathogenic Gram-positive bacteria, is used extensively for industrial production of exoenzymes (proteases, α-amylases) and peptide antibiotics [20]. Despite its widespread industrial application, the extracellular RNase from *B. licheniformis* has not yet

been characterized. The RNase encoding *BLI_RS18290* gene (previously known as *BLi03719*) was found among the most dominant protein spots in the extracellular proteome of the *B. licheniformis* grown under phosphate deficiency [21].

Here, we have isolated, purified, and characterized the *B. licheniformis* secreted RNase (balifase). Furthermore, we have compared molecular properties of balifase with those of binase and barnase. We have shown that the level of balifase catalytic activity, as well as its physicochemical characteristics and structural features, is similar to those of the main representatives of bacillary N1/T1 RNase. The unique features of balifase include the formation of an operon together with a gene of its intracellular inhibitor, as well as high stability and inability to form natural dimers.

2. Materials and Methods

2.1. Strain and Growth Conditions. Wild-type strain of *B. licheniformis* ATCC 14580 was obtained from *Bacillus* Genetic Stock Center (BGSC, USA). *B. licheniformis* was grown on standard LB medium or on LP medium (low phosphate peptone: 2%; glucose: 1%; Na_2HPO_4: 0.04%; $CaCl_2$: 0.01%; $MgSO_4 \times 7H_2O$: 0.03%; $MnSO_4$: 0.01%; NaCl: 0.3%). Bacteria were cultivated at 37°C using a laboratory shaker with oscillation intensity of 200 rpm (INFORS HT, Switzerland). Culture growth was determined spectrophotometrically at $\lambda = 590$ nm and expressed as optical density units (OD_{590}).

2.2. RNase Activity. Determination of RNase activity was performed by the measurement of acid-soluble hydrolysis products of high molecular weight yeast RNA as described earlier [22]. The reaction mixture consisting of enzyme solution, RNA, and 0.25 M Tris-HCl buffer, pH 8.5, was incubated for 15 minutes at 37°C. One unit was defined as the amount of enzyme that increases the extinction of acid-soluble products of RNA hydrolysis at 260 nm per min. Specific activity was calculated as the ratio of the total enzyme activity to the amount of the protein.

2.3. Enzyme Preparation. After 24–26 hours of cultivation on LP medium, *B. licheniformis* cells were acidified with acetic acid to pH 5.0, centrifuged at 9000 ×g for 20 minutes at 4°C. The supernatant was diluted twice with sterile distilled water and was applied onto the DEAE-cellulose (Servacel, Germany) column (≈30 mL), equilibrated with 0.01 M Na-acetate buffer, pH 5.0. Then the solution was applied onto the phosphocellulose P-11 (Whatman, England) column (≈50 mL), equilibrated with the same buffer. After that the column was washed with 0.01 M Na-acetate buffer, pH 5.0, until optical density of eluate at 280 nm decreased below 0.05. Then the column was equilibrated with 0.01 M Na-phosphate buffer, pH 7.0. The elution was carried out with 0.2 M Na-phosphate buffer, pH 7.0. Fractions corresponding to RNase activity peak were combined and desalted using centrifugal filter units Ultracel-3K (Merck Millipore, USA). The additional purification was carried out using Biologic DuoFlow FPLC system (BioRad, USA) on the $UNOS_6$ (BioRad, USA) column, equilibrated with 20 mM Na-acetate buffer, pH 5.0. Proteins were eluted using a linear gradient of 0-1 M NaCl.

2.4. SDS-PAGE and Immunoblotting. Proteins were separated by SDS-PAGE [23] and transferred to a nitrocellulose membrane by Mini Trans-Blot cell (BioRad, USA). For the detection of proteins anti-binase antibodies were used [24]. Visualization of protein bands corresponding to RNase was performed using anti-rabbit IgG-POD secondary antibodies (Sigma-Aldrich, USA) and the LumiLight detection system (Roche Diagnostics, Switzerland).

2.5. Zymography. To estimate in-gel RNase activity of proteins we performed zymography analysis as described in [25]. Proteins were separated in 15% polyacrylamide gel with 0.1% SDS (SDS-PAGE) [23]. The resolving gel contained RNA from Torula yeast (Sigma-Aldrich, USA) as a substrate at final concentration of 7 mg/mL. Then the gel was washed with buffer I (10 mM Tris-HCl, 20% isopropanol, pH 7.5) for 10 min to remove SDS and then proteins were refolded by consequent incubation for 10 min in 10 mM Tris-HCl, pH 7.5, and in 100 mM Tris-HCl, pH 7.5. The gel was stained for 10 min with 0.2% toluidine blue (Sigma-Aldrich, USA).

2.6. Bioinformatic Analysis. The RNase sequences were extracted from the databases of the National Center for Biotechnology Information NCBI (http://www.ncbi.nlm.nih.gov/). Gene neighborhoods were compared at "Microbes Online" server of the Virtual Institute for Microbial Stress and Survival (http://www.microbesonline.org/). Orthologs of intracellular RNase inhibitor (barstar) were identified with the help of "EDGAR" server (https://edgar.computational.bio.uni-giessen.de/). For multiple alignment of amino acid sequences the program "MUSCLE" (http://www.ebi.ac.uk/Tools/muscle/) was applied. Alignment was carried out on the basis of standard criteria. The software package "MEGA 6.0" was used for construction of phylogenetic trees [26]. Leader peptide of the extracellular RNase of *B. licheniformis* ATCC 14580 was determined using PRED-TAT tool (http://www.compgen.org/tools/PRED-TAT/submit/). Virtual Footprint tool was used for analysis of the transcription factor binding sites [27]. Comparison of physicochemical properties of proteins was performed using ProtParam tool [28]. The three-dimensional structure of balifase was modeled with the help of I-TASSER server without specifying the template [29]. A FATCAT web server was used for flexible structure comparison and structure similarity search (http://fatcat.burnham.org/).

3. Results and Discussion

3.1. Balifase Is Similar to Barnase by Molecular Properties. To isolate the *B. licheniformis* extracellular RNase which was found upon studies of bacterial cell response to starvation [21], we first compared its gene and amino acid sequence with those of well-studied barnase and binase. The RNase of *B. licheniformis* is encoded by the *BLI_RS18290* gene; a mature protein consists of 109 amino acids. The analysis of the primary structure of *B. licheniformis* RNase showed that the main differences of the *B. licheniformis* RNase from binase and barnase are primarily concentrated in the region of the signal and propeptides. The signal peptide of balifase

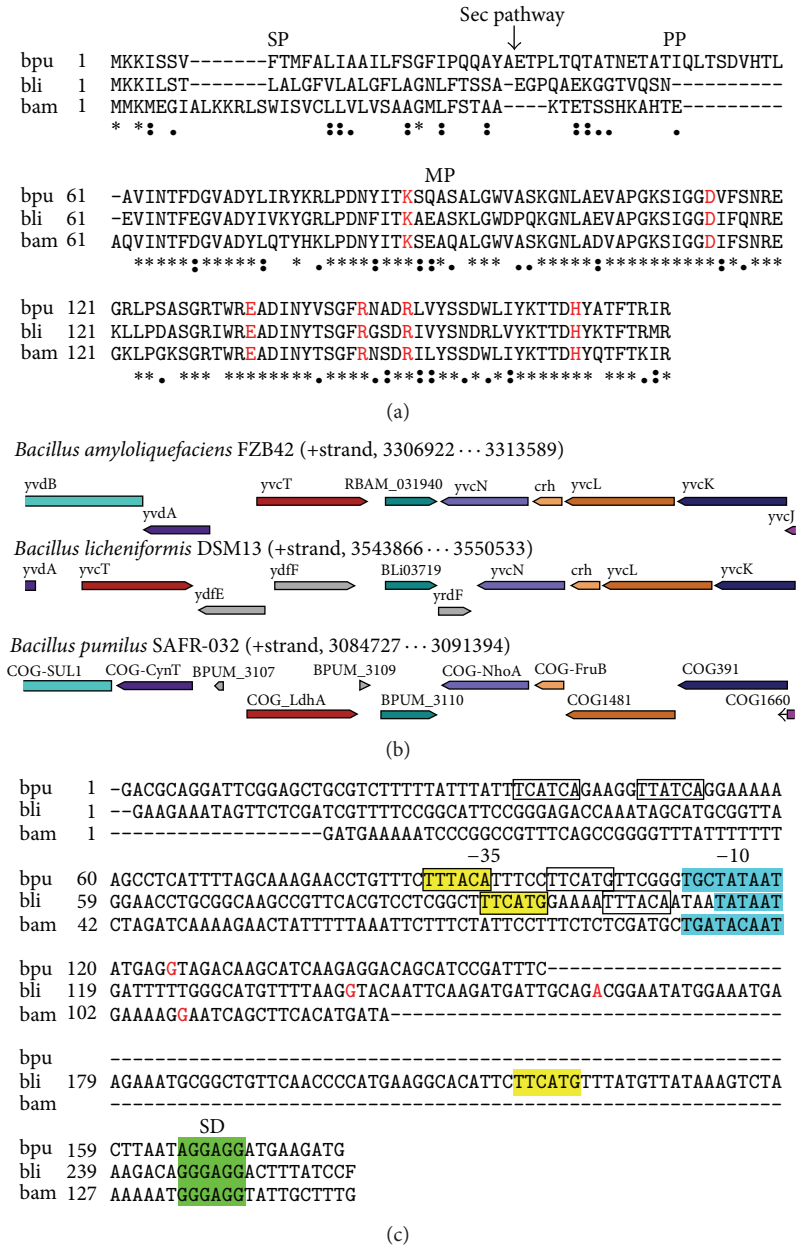

Figure 1: Comparison of *B. licheniformis* RNase with the representatives of N1/T1 RNase family. (a) Sequence alignments of signal peptide (SP), propeptide (PP), and mature peptide (MP) of *B. licheniformis* (bli), *B. amyloliquefaciens* (bam), and *B. pumilus* (bpu) RNase. Identical amino acid residues are marked (∗). Amino acid residues that incorporate to the active site of enzyme are red colored. (b) Gene neighborhood of balifase gene in comparison to barnase and binase genes. The data were adopted from the MicrobesOnline Database (http://www.microbesonline.org/). (c) Promoter regions of guanyl-preferring RNase genes from *B. pumilus* (bpu), *B. licheniformis* (bli), and *B. amyloliquefaciens* (bam). Putative PhoP-binding sites are boxed; (+1) regions are red colored. A colon ":" indicates conservation between groups of strongly similar properties. A period "." indicates conservation between groups of weakly similar properties.

and binase are similar, whereas the propeptide resembles barnase by length. Responsible for transport, maturation, and activation of enzymes, signal peptide may have an effect on spatial organization of proteins. The mature protein is more conserved and differs by 30 and 28 amino acid residues from barnase and binase, respectively (Figure 1(a)). Thus, the RNase of *B. licheniformis* has the 73% and 74% degree of similarity with barnase and binase, respectively. The overall resemblance of the RNase composing the N1/T1 family is reflected in a phylogenetic tree, which was reconstructed based on the primary sequences of the mature RNase (Figure 2(d)). It is shown that the RNase of *B. licheniformis* is equidistant from both *B. amyloliquefaciens* and *B. pumilus* RNase, without forming a single cluster with the latter within the genus.

The three-dimensional structure of balifase was predicted by using the I-TASSER server (Figure 2(a)). The C-score of 1.72 corresponds to a model with high confidence. According

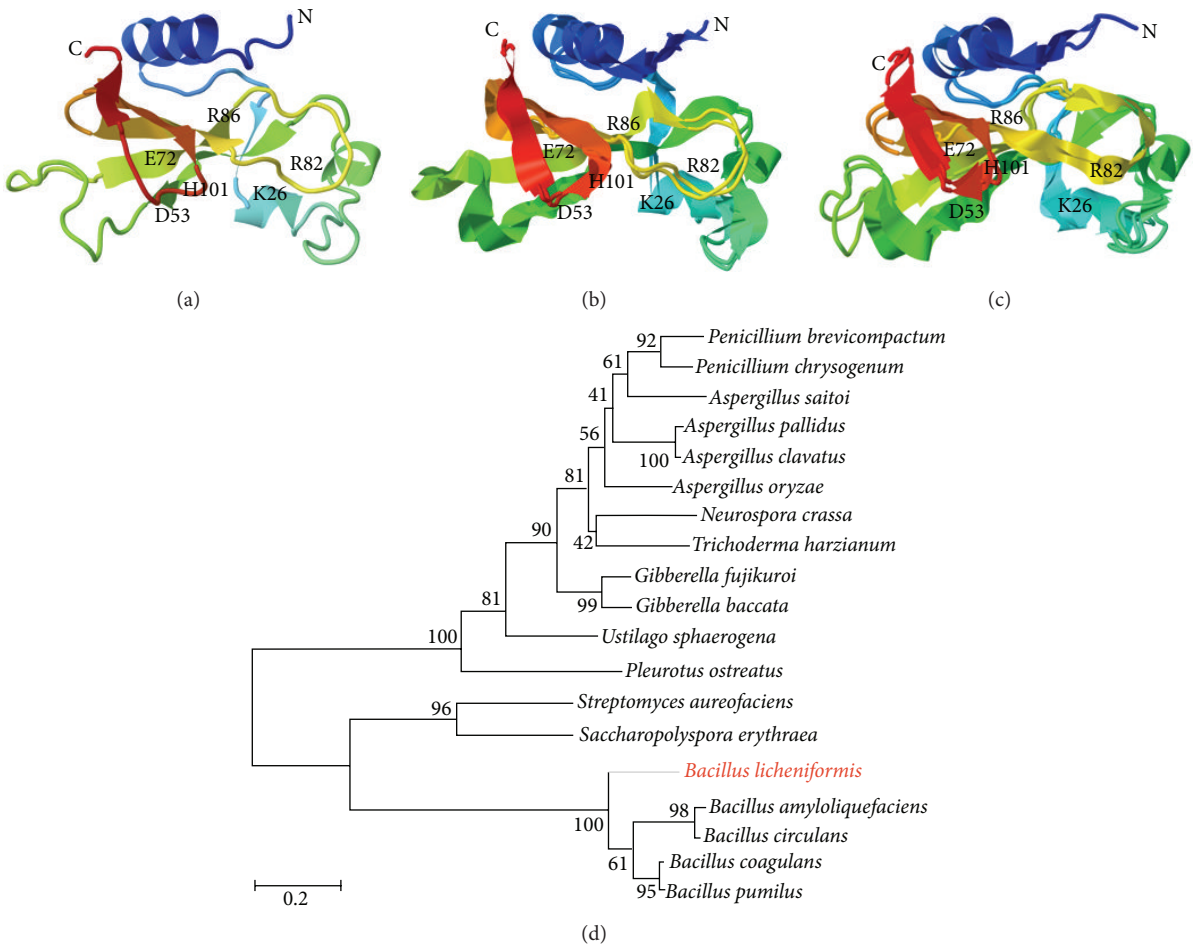

Figure 2: (a) Top model of balifase three-dimensional structure predicted by I-TASSER server without specifying the template. (b) Superimposed three-dimensional structures of binase (PDB ID 1buj) and balifase. (c) Superimposed three-dimensional structures of barnase (PDB ID 1bnr) and balifase. The alignment was performed using the FATCAT server with flexible mode. (d) The phylogenetic tree constructed on the basis of amino acid sequences of RNase from N1/T1 family. The scale bar indicates the average number of amino acid substitutions per site.

to FATCAT pairwise alignment, balifase is very similar to both binase (PDB ID 1buj) and barnase (PDB ID 1bnr) with some minor differences (Figures 2(b) and 2(c)). The P value is <0.05 (with the raw score of 298.54 and 282.20, resp.), which means that the structure pairs are significantly similar. The structure alignment has 109 equivalent positions with an RMSD of 1.30 and 1.53, respectively, without twists.

A set of physicochemical parameters of the *B. licheniformis* RNase, such as molecular weight and pI, was predicted by using the ProtParam tool (Table 1). It is shown that despite some variations in these parameters, balifase, binase, and barnase proteins are found to have similar properties. However, balifase is closer to barnase than binase. It is a more acidic protein compared to barnase. Furthermore, the aliphatic index of balifase and barnase is lower than that of binase, which indicates their lower thermostability. The instability index is significantly higher for balifase than for binase and barnase, which points to the high stability of balifase (Table 1). Generally, a protein with an instability index lower than 40 is predicted as stable [30]. Calculated from the molar extinction coefficient of tyrosine, tryptophan, and cystine [31], the extinction coefficient of balifase allows us to detail the calculation of the protein amount during purification.

Table 1: Physicochemical properties of balifase as compared with binase and barnase.

RNase/characteristics	Balifase	Binase	Barnase
Number of amino acids	109	109	110
Molecular weight	12421.9	12211.6	12382.7
Theoretical pI	8.91	9.52	8.88
Extinction coefficient	19940	26930	26930
Abs 0.1% (=1 g/L)	1.605	2.205	2.175
Grand average of hydropathicity	−0.666	−0.416	−0.643
Instability index	8.92	27.25	24.27
Aliphatic index	72.48	78.81	71.00

Therefore, based on the similarities between barnase and balifase proteins, we have found that the protocol for barnase purification is also suitable for purification of balifase [13].

3.2. Gene Context of B. licheniformis RNase Differs from That of Barnase and Binase. Gene neighborhood information supports a better understanding of putative functions of a protein encoded by a gene of interest. Typically, the neighborhoods combine several genes that are involved in similar process; however, some of these genes can differ. The exploration of the balifase gene *BLI_RS18290* neighborhood showed that it is organized differently from barnase and binase (Figure 1(b)). The RNase gene forms an operon with an intracellular inhibitor gene, downstream of *ydfE* and *ydfF* genes responsible for metal resistance. Yet, these features are not characteristic of binase (*BPUM_3110*) and barnase (*RBAM_031940*). At the 5′-end, they are preceded by the *yvcT* gene encoding gluconate 2-dehydrogenase, as well as the prospective bicistronic operon formed by *yvdA* and *yvdB* genes, which encodes carbonate dehydrogenase and permease of the *SuIP* family. At the 3′-end, the genes for balifase and its inhibitor are followed by *yvcN* (encoding N-acetyltransferase), *crh* (encoding histidine-containing phosphorus-carrying Hpr-like protein), *yvcL* (encoding a DNA-binding protein WhiA, which controls the process of sporulation in spore-forming bacteria), *yvcK* (encoding the factor of gluconeogenesis), and *yvcJ* (encoding a nucleotide-binding protein which hydrolyzes nucleoside triphosphates). The gene context of balifase reflects its participation in phosphorus and carbon metabolism.

The *B. licheniformis* RNase gene context differs from the gene context of other closely related species of bacilli given the fact that balifase gene forms an operon with the gene of intracellular inhibitor YrdF (Figure 1(b)). Our further analysis using the EDGAR server has revealed that the YrdF inhibitor of balifase represents the ortholog of a well-known barnase inhibitor barstar.

The *ydfF* gene encodes a transcriptional regulator, belonging to the family of ArsR-like repressors that activate the transcription of proteins involved in the efflux of metals and/or detoxification by dissociation from operators [32]. The *YdfE* gene product contains flavin reductase domain of various oxidoreductases and monooxygenases. The protein performs an antioxidant function in the oxidation of lipid membrane caused by heavy metals. The expression of the *ydfE* gene is controlled by the *ydfF* gene.

3.3. Regulation of Balifase Gene Expression Is Similar to Binase One. To understand how balifase gene expression is regulated we analyzed its promoter structure. Using computational approach it was impossible to identify (−10) and (−35) regions clearly. Two possible (+1) positions were predicted (Figure 1(c)). Therefore, we compared balifase gene promoter to promoters of binase and barnase. The RNase of *Bacillus* with low molecular weight can be divided into two groups: binase-like and barnase-like RNase [33]. In contrast to barnase, the promoters of binase and balifase genes possess (−10) and (−35) regions.

Besides that, the detection of the transcription factor binding sites was performed (Table 2). It was found that expression of balifase, binase, and barnase could be regulated by AbrB, GerE, and PucR transcription factors. This indicates the involvement of the RNase in scavenge of purines (PucR regulation) as well as in general transition from exponential growth to stationary phase (AbrB regulation). Expression of RNase genes during sporulation could be inhibited by GerE. Binding sites for ComK, which is required for the transcription of late competence genes, were not detected in balifase gene promoter in contrast to binase and barnase ones. Genes for barnase and balifase are potentially controlled by DegU, the regulator of extracellular degradative enzymes biosynthesis in response to nitrogen starvation. Furthermore, we identified the potential binding sites for the PhoP transcription factor, which controls cell response to phosphate deficiency in *Bacillus,* in the *B. licheniformis* RNase gene promoter, and in the binase promoter (Figure 1(c)). Potential binding sites for Hpr, which provides the link between phosphorous and carbon metabolism, and SpoIIID, which regulates gene expression during sporulation, were found in binase and balifase gene promoters as well. Thus, analysis of balifase promoter structure and activity revealed its higher similarity to promoter of binase than of barnase.

3.4. Purification of Balifase. To identify the most suitable media for high-level production of the *B. licheniformis* RNase, we have grown bacteria in LB and low phosphate peptone media (LP) differing by the amount of phosphorus (275 μg/mL and 120 μg/mL, resp.). It was found that the cells produce twice as much amount of RNase when grown on LP medium during 24 h at 37°C. Balifase appears in the culture fluid after 6 h of cultivation and reaches the maximum after 22–24 h corresponding to the early stationary phase (Figure 3(a)).

The purification protocol for barnase [13] was applied for balifase. However, this procedure failed to generate large amounts of pure balifase and, therefore, was modified. For protein purification, samples were collected at 22–24 h and all steps of purification shown in Table 3 were performed. After elution from phosphocellulose, a protein sample with the yield of 75% by activity was obtained. The final purification step was made using the FPLC BioLogic Duo Flow system. Protein was eluted by 0.35 M NaCl (Figure 3(b)). The elution profile was characterized by two additional peaks which had no RNase activity. It was detected via SDS-PAGE that the first fraction contained the protein with the molecular weight of 12 kDa (Figure 4(a)) and RNase activity in the gel (Figure 4(b)). The purity of the sample was shown by mass spectrometry analysis, which also proved the presence of the *B. licheniformis* RNase only (AAU25168.1). Finally, the protein sample with enzymatic activity of 1.5×10^6 units/A_{280} was obtained.

It was observed that the oligomeric forms of balifase with catalytic activity in the gel (Figure 4(c)) appear after concentrating, freezing, and storage. The immunoblot analysis showed that anti-binase antibodies interact with low order oligomers of balifase too (Figure 4(d)). Therefore, we

Table 2: Putative binding sites for transcription factors in barnase, binase, and balifase promoters.

Transcription factors	Barnase	Binase	Balifase
AbrB (controls the expression of genes involved in starvation-induced processes)	TAAAAAAT (125–132)	GAAAAAAG (54–61)	CAAAAATC (119–126 noncoding strand) CATAAACA (219–226 noncoding strand)
ComK (is required for the transcription of the late competence genes)	AAAGAACTATTTT (50–62)	AAAGCCTCATTTT (58–70)	Not detected
DegU (regulates the degradative enzyme expression, genetic competence, biofilm formation, and capsule biosynthesis)	GAAAAATCCCGGCCGTTTCAG (4–24)	Not detected	ATAGTTCTCGATCGTTTTCCG (7–27) ACAATAATATAATGATTTTTG (106–126)
GerE (regulates gene transcription in the terminally differentiated mother-cell compartment during late stages of sporulation)	AAATGGGAGGTA (129–140)	AAATAAATAAAA (25–36 noncoding strand)	AAATAGTTCTCG (5–16) ATATAATGATTT (112–123)
Hpr (provides the link between phosphorous and carbon metabolism)	Not detected	GGTGCTATAATATGAGGTA (109–127)	ATGTTTATGTTATAAAGTC (218–236)
PucR (regulation of purine utilization)	ATACAATGAAA (95–105)	ATTCGGAGCTG (9–19)	TTTCATGGAAA (91–101) GTCCTCGGCTT (82–92)
ResD (regulation of aerobic and anaerobic respiration)	AACTATTTTTAAA (54–66)	TCATTTTAGCAAA (64–76) CTCATTTTAGCAA (63–75)	AAATTTACAATAA (100–112)
SpoIIID (key regulator of transcription during the sporulation process)	Not detected	AGGACAGCAT (141–150) TAGACAAGCA (126–135)	GGCACATTCT (206–215) GGTACAATTC (139–148)

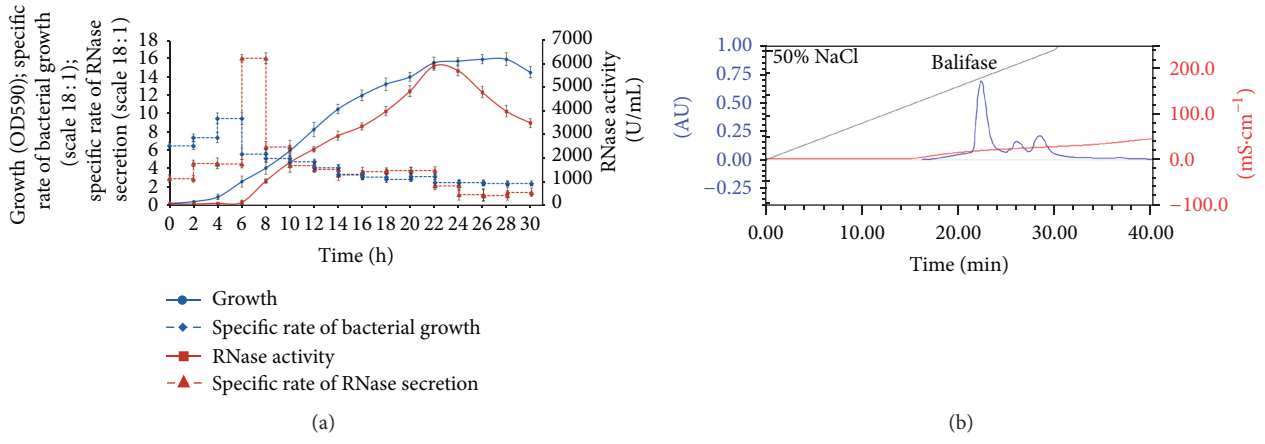

Figure 3: (a) The time-course of *B. licheniformis* ATCC 14580 growth and RNase production on LP medium at 37°C. (b) Elution of balifase fraction in a linear gradient of 0.0–1.0 M NaCl using FPLC Biologic DuoFlow system; AU: absorbance units, mS × cm^{-1}: conductivity.

can conclude that balifase can exist in oligomeric forms in solution but unlike binase, not under natural conditions of biosynthesis [25].

4. Conclusions

The new low molecular weight RNase isolated from *B. licheniformis* (named balifase) has been characterized according to its physicochemical properties, gene context, and promoter organization. Balifase combines physicochemical properties of barnase (pI, grand average of hydropathicity, and aliphatic index) with the regulatory mode of biosynthesis typical for binase. Both balifase gene and gene for its inhibitor are located in one operon which makes the gene organization of balifase unique. Balifase synthesis is induced under phosphate starvation similarly to biosynthesis of binase; however in contrast to binase balifase does not form dimers under natural conditions. We propose that the highest stability of

Table 3: The isolation and purification of *B. licheniformis* RNase.

Stage of purification	Vol (V), mL	A_{280}, units	Specific activity, units/A_{280}	Degree of purification	Yield (by activity), %
Culture fluid after 24 h of cultivation	1200	8	763	1	100
After DEAE-cellulose, pH 5.0	1200	7.8	780	1.02	99.7
After elution from phosphocellulose in 200 mM sodium phosphate buffer, pH 7.0	20	0.7	225000	353	75
After chromatography on $UNOS_6$ column using FPLC system	4	0.45	1.5×10^6	2353	50

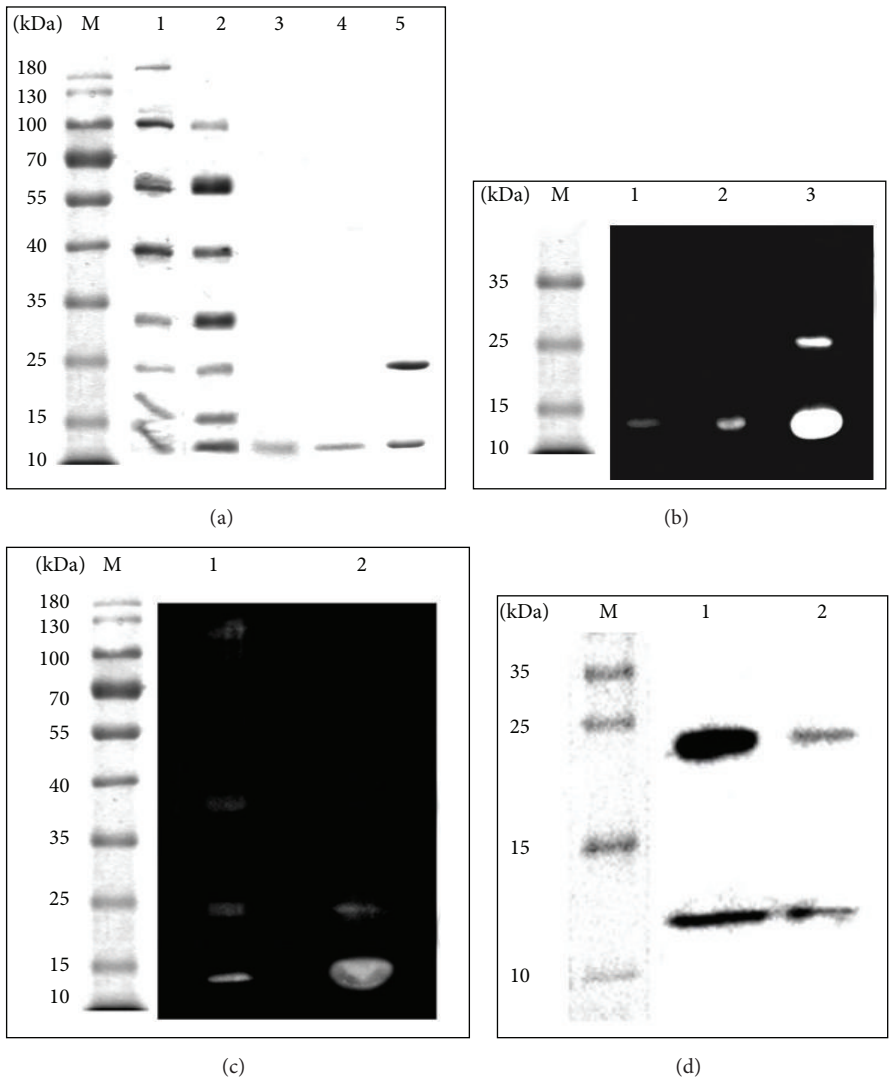

Figure 4: Electrophoretic analysis of purity, enzymatic activity, and antibody specificity of balifase. (a) SDS/PAGE of balifase samples at different stages of purification. 1: before purification in culture fluid, 2: after chromatography on DEAE-cellulose, 3: after chromatography on phosphocellulose P-11, 4: after chromatography on $UNOS_6$ column, 5: binase. (b) Zymography analysis of balifase sample. 1: after chromatography on phosphocellulose P-11; 2: after chromatography on $UNOS_6$ column; 3: binase. (c) Zymography analysis of balifase sample after concentrating, freezing, and storage. 1: balifase; 2: binase. (d) Western Blot analysis of balifase after chromatography on $UNOS_6$ column. 1: binase; 2: balifase.

balifase among analyzed RNase types allows the protein to retain its structure without oligomerization.

Competing Interests

The authors declare that there are no competing interests regarding the publication of this article.

Acknowledgments

The research was performed within the Russian Government Program of Competitive Growth of Kazan Federal University and supported by the Russian Research Foundation Grant no. 14-14-00522. Bioinformatics analysis was done with support of the Russian Foundation for Basic Research Grant no. 15-04-07864; mass spectrometry was performed at Interdisciplinary Center of Kazan Federal University (ID RFMEFI59414X0003).

References

[1] C. M. Arraiano, J. M. Andrade, S. Domingues et al., "The critical role of RNA processing and degradation in the control of gene expression," *FEMS Microbiology Reviews*, vol. 34, no. 5, pp. 883–923, 2010.

[2] K. Takahashi and S. Moore, *The Enzymes, Volume 15, Nucleic Acids, Part B*, Academic Press, New York, NY, USA, 1982.

[3] A. A. Makarov, A. Kolchinsky, and O. N. Ilinskaya, "Binase and other microbial RNases as potential anticancer agents," *BioEssays*, vol. 30, no. 8, pp. 781–790, 2008.

[4] A. Chakrabarti, B. K. Jha, and R. H. Silverman, "New insights into the role of RNase L in innate immunity," *Journal of Interferon & Cytokine Research*, vol. 31, no. 1, pp. 49–57, 2011.

[5] H. F. Rosenberg, "RNase A ribonucleases and host defense: an evolving story," *Journal of Leukocyte Biology*, vol. 83, no. 5, pp. 1079–1087, 2008.

[6] H. A. Cabrera-Fuentes, M. Aslam, M. Saffarzadeh et al., "Internalization of *Bacillus intermedius* ribonuclease (BINASE) induces human alveolar adenocarcinoma cell death," *Toxicon*, vol. 69, pp. 219–226, 2013.

[7] V. A. Mitkevich, I. Y. Petrushanko, P. V. Spirin et al., "Sensitivity of acute myeloid leukemia Kasumi-1 cells to binase toxic action depends on the expression of KIT and AML1-ETO oncogenes," *Cell Cycle*, vol. 10, no. 23, pp. 4090–4097, 2011.

[8] V. A. Mitkevich, O. N. Ilinskaya, and A. A. Makarov, "Antitumor RNases: killer's secrets," *Cell Cycle*, vol. 14, no. 7, pp. 931–932, 2015.

[9] O. N. Ilinskaya, I. Singh, E. Dudkina, V. Ulyanova, A. Kayumov, and G. Barreto, "Direct inhibition of oncogenic KRAS by *Bacillus pumilus* ribonuclease (binase)," *Biochimica et Biophysica Acta (BBA)—Molecular Cell Research*, vol. 1863, no. 7, pp. 1559–1567, 2016.

[10] R. S. Mahmud and O. N. Ilinskaya, "Antiviral activity of binase against the pandemic influenza A (H1N1) virus," *Acta Naturae*, vol. 5, no. 19, pp. 44–51, 2013.

[11] O. N. Ilinskaya and R. S. Mahmud, "Ribonucleases as antiviral agents," *Molecular Biology*, vol. 48, no. 5, pp. 615–623, 2014.

[12] H. Yoshida, "The ribonuclease T1 family," *Methods in Enzymology*, vol. 341, pp. 28–41, 2001.

[13] R. W. Hartley and D. L. Rogerson Jr., "Production and purification of the extracellular ribonuclease of *Bacillus amyloliquefaciens* (barnase) and its intracellular inhibitor (barstar). I. Barnase," *Preparative Biochemistry*, vol. 2, no. 3, pp. 229–242, 1972.

[14] I. A. Golubenko, N. P. Balaban, I. B. Leshchinskaia, T. I. Volkova, and G. I. Kleĭner, "Ribonuclease of *Bacillus intermedius* 7 P: purification by chromatography on phosphocellulose and several characteristics of the homogeneous enzyme," *Biokhimiya*, vol. 44, no. 4, pp. 640–648, 1979.

[15] E. Dudkina, V. Ulyanova, R. Shah Mahmud et al., "Three-step procedure for preparation of pure *Bacillus altitudinis* ribonuclease," *FEBS Open Bio*, vol. 6, no. 1, pp. 24–32, 2016.

[16] A. A. Dementiev, G. P. Moiseyev, and S. V. Shlyapnikov, "Primary structure and catalytic properties of extracellular ribonuclease of *Bacillus circulans*," *FEBS Letters*, vol. 334, no. 2, pp. 247–249, 1993.

[17] S. V. Shliapnikov and A. A. Dement'ev, "Amino acid sequence and catalytic properties of the *Bacillus coagulans* extracellular ribonuclease," *Doklady Akademii Nauk*, vol. 332, no. 3, pp. 382–384, 1993.

[18] A. Nakamura, Y. Koide, H. Miyazaki et al., "Gene cloning and characterization of a novel extracellular ribonuclease of *Bacillus subtilis*," *European Journal of Biochemistry*, vol. 209, no. 1, pp. 121–127, 1992.

[19] M. A. Skvortsova, A. L. Bocharov, G. I. Yakovlev, and L. V. Znamenskaya, "Novel extracellular ribonuclease from *Bacillus intermedius*—Binase II: purification and some properties of the enzyme," *Biochemistry*, vol. 67, no. 7, pp. 802–806, 2002.

[20] M. Schallmey, A. Singh, and O. P. Ward, "Developments in the use of *Bacillus* species for industrial production," *Canadian Journal of Microbiology*, vol. 50, no. 1, pp. 1–17, 2004.

[21] L. T. Hoi, B. Voigt, B. Jürgen et al., "The phosphate-starvation response of *Bacillus licheniformis*," *Proteomics*, vol. 6, no. 12, pp. 3582–3601, 2006.

[22] O. N. Ilinskaya, N. S. Karamova, O. B. Ivanchenko, and L. V. Kipenskaya, "SOS-inducing ability of native and mutant microbial ribonucleases," *Mutation Research—Fundamental and Molecular Mechanisms of Mutagenesis*, vol. 354, no. 2, pp. 203–209, 1996.

[23] U. K. Laemmli, "Cleavage of structural proteins during the assembly of the head of bacteriophage T4," *Nature*, vol. 227, no. 5259, pp. 680–685, 1970.

[24] V. V. Ulyanova, V. S. Khodzhaeva, E. V. Dudkina, A. V. Laikov, V. I. Vershinina, and O. N. Ilinskaya, "Preparations of *Bacillus pumilus* secreted RNase: one enzyme or two?" *Microbiology*, vol. 84, no. 4, pp. 491–497, 2015.

[25] E. Dudkina, A. Kayumov, V. Ulyanova, and O. Ilinskaya, "New insight into secreted ribonuclease structure: binase is a natural dimer," *PLoS ONE*, vol. 9, no. 12, article e115818, 2014.

[26] K. Tamura, G. Stecher, D. Peterson, A. Filipski, and S. Kumar, "MEGA6: molecular evolutionary genetics analysis version 6.0," *Molecular Biology and Evolution*, vol. 30, no. 12, pp. 2725–2729, 2013.

[27] R. Münch, K. Hiller, A. Grote et al., "Virtual footprint and PRODORIC: an integrative framework for regulon prediction in prokaryotes," *Bioinformatics*, vol. 21, no. 22, pp. 4187–4189, 2005.

[28] E. Gasteiger, C. Hoogland, A. Gattiker et al., "Protein identification and analysis tools on the ExPASy server," in *The Proteomics Protocols Handbook*, pp. 571–607, Humana Press, 2005.

[29] J. Yang, R. Yan, A. Roy, D. Xu, J. Poisson, and Y. Zhang, "The I-TASSER suite: protein structure and function prediction," *Nature Methods*, vol. 12, no. 1, pp. 7–8, 2014.

[30] K. Guruprasad, B. V. B. Reddy, and M. W. Pandit, "Correlation between stability of a protein and its dipeptide composition: a novel approach for predicting in vivo stability of a protein from its primary sequence," *Protein Engineering*, vol. 4, no. 2, pp. 155–161, 1990.

[31] S. C. Gill and P. H. von Hippel, "Calculation of protein extinction coefficients from amino acid sequence data," *Analytical Biochemistry*, vol. 182, no. 2, pp. 319–326, 1989.

[32] D. I. Osman and J. S. Cavet, "Bacterial metal-sensing proteins exemplified by *ArsR-SmtB* family repressors," *Natural Product Reports*, vol. 27, no. 5, pp. 668–680, 2010.

[33] V. Ulyanova, V. Vershinina, O. Ilinskaya, and C. R. Harwood, "Binase-like guanyl-preferring ribonucleases are new members of *Bacillus* PhoP regulon," *Microbiological Research*, vol. 170, pp. 131–138, 2015.

Hindawi Publishing Corporation
BioMed Research International
Volume 2016, Article ID 7535604, 8 pages
http://dx.doi.org/10.1155/2016/7535604

Research Article

Cloning, Expression, and Characterization of a Novel Thermophilic Monofunctional Catalase from *Geobacillus* sp. CHB1

Xianbo Jia, Jichen Chen, Chenqiang Lin, and Xinjian Lin

Soil and Fertilizer Institute, Fujian Academy of Agricultural Sciences, Fuzhou 350003, China

Correspondence should be addressed to Xinjian Lin; xinjianlin@vip.tom.com

Received 18 March 2016; Accepted 3 July 2016

Academic Editor: Thangavel Lakshmipriya

Catalases are widely used in many scientific areas. A catalase gene (*Kat*) from *Geobacillus* sp. CHB1 encoding a monofunctional catalase was cloned and recombinant expressed in *Escherichia coli* (*E. coli*), which was the first time to clone and express this type of catalase of *genus Geobacillus* strains as far as we know. This *Kat* gene was 1,467 bp in length and encoded a catalase with 488 amino acid residuals, which is only 81% similar to the previously studied *Bacillus* sp. catalase in terms of amino acid sequence. Recombinant catalase was highly soluble in *E. coli* and made up 30% of the total *E. coli* protein. Fermentation broth of the recombinant *E. coli* showed a high catalase activity level up to 35,831 U/mL which was only lower than recombinant *Bacillus* sp. WSHDZ-01 among the reported catalase production strains. The purified recombinant catalase had a specific activity of 40,526 U/mg and K_m of 51.1 mM. The optimal reaction temperature of this recombinant enzyme was 60°C to 70°C, and it exhibited high activity over a wide range of reaction temperatures, ranging from 10°C to 90°C. The enzyme retained 94.7% of its residual activity after incubation at 60°C for 1 hour. High yield and excellent thermophilic properties are valuable features for this catalase in industrial applications.

1. Introduction

Catalases (EC1.11.1.6) are a class of enzymes that specifically catalyze the decomposition of H_2O_2 to H_2O and O_2 [1]. H_2O_2 has been applied to sterilization and bleaching processes in the medical, food, textile, and paper-making industries [2, 3]. Residual H_2O_2 in products or by-products is harmful to human health and environment. Thus, the removal of residual H_2O_2 is necessary in textile production processes, food health, pollution prevention, and other fields [2]. Catalase is an ideal choice for removing H_2O_2 due to its efficiency and lack of secondary pollution compared with chemical decomposition methods [4].

Catalase can be divided into four classes: monofunctional heme catalases, catalase-peroxidases, non-heme catalases, and minor catalases [5]. Catalases are widely present in animals, plants, fungi, most aerobic bacteria, and some anaerobic bacteria [5]. Commercial catalase produced by animals liver, plant tissues, and microbial fermentation is mainly mesophilic catalase, but many industrial applications need thermostable catalase; for example, textile bleaching temperature is always up to 60°C [6], so thermophilic catalase is more comparable on that condition. There have been some thermophilic catalases reported [7–10], but they were either catalase-peroxidase or Mn-dependent catalase. Thermophilic monofunctional heme catalases are rarely reported as we know.

High yielding strains are also necessary for enzyme production in fermentation processes. Recombinant expression is a practical method to increase the yield of a target gene. Currently, *Pichia pastoris* [11], *Hansenula polymorpha* [12], *Lactococcus lactis* [13], *Bacillus subtilis* (*B. subtilis*) [14, 15], and *Escherichia coli* (*E. coli*) [9] are used as host cells to produce recombinant catalase, but those recombinant catalases were mainly mesophilic, successfully recombinant expression precedents of thermophilic catalases which were few. The advantages of *E. coli* systems, such as their convenience, high yields, and ease of purification promote their wide application in genetic engineering. But many thermophilic enzymes cannot be overproduced in active forms in mesophilic host [8].

For example, though *Thermus thermophilus* catalase could solubly be expressed in *E. coli*, the recombinant catalase was absolutely inactive [8]; recombinant *E. coli* with *Bacillus stearothermophilus* catalase-peroxidase gene also showed a comparatively lower catalase level (1055.3 U/mL) [16]. So high soluble expression with an active form in *E. coli* is important for thermophilic catalase.

Previously, we screened thermophilic bacteria strains isolated from different high-temperature compost samples and *Geobacillus* sp. CHB1 was found to be a high catalase production strain. So, in this work, we cloned a novel *Kat* gene encoding a monofunctional catalase from thermophiles *Geobacillus* sp. CHB1 and recombinant expressed this gene in *E. coli* in a highly soluble form. The recombinant catalase was also purified and characterized.

2. Materials and Methods

2.1. Materials, Bacterial Strains, Plasmids, and Medium. *E. coli* BL21 (DE3) was cultured in our laboratory, and the expression vector pEASY-E2 was purchased from Beijing TransGen Biotech. The *Geobacillus* sp. CHB1 was isolated in Fuzhou, China. LB medium (10 g/L tryptone, 5 g/L yeast extract, 10 g/L NaCl, pH 7.0) was used in culturing *E. coli* BL21 (DE3). Auto-induction medium ZYM-5052 [17] was used for inducing the expression of recombinant catalase. The medium for culturing the *Geobacillus* sp. CHB1 consisted of soya peptone 0.9%, yeast extract 0.5%, NaCl 0.1%, K_2HPO_4 0.1%, and KH_2PO_4 0.075%, at pH 7.2.

2.2. Expression Vector Construction. *Geobacillus* sp. CHB1 was incubated at 60°C for 18 h at 180 r/min; then the genome was extracted according to the method of Zhou et al. [18]. The *Kat* gene was amplified using primers CatalaseF: (5′-GCAGATACAAAAAAGCTCACAAC-3′) and CatalaseR: (5′-TGCGTTTGTAATCACATCGTCCG-3′). Polymerase chain reaction (PCR) was performed with ExTaq DNA polymerase (TaKaRa, Dalian, China) under the following conditions: 95°C initial denaturation for 5 min, followed by 32 cycles of 40 s at 94°C, 40 s at 55°C, and 1 min 30 s at 72°C. The PCR product was purified using a PCR purification kit (Omega Bio-Tek, Inc., USA) and sequenced by Sangon Biotech Co., Ltd. (Shanghai, China).

Homology search of gene and amino acid sequence was carried out at BLAST server (http://blast.ncbi.nlm.nih.gov). Program blastp was used to analyze homology of the amino acid sequences; nonredundant protein sequences (Nr) database and Swiss Prot database were both used for blastp program. Sequences with high similarity in Swiss Prot database were selected to construct phylogenetic tree and do multiple alignment. MEGA 4.0.2 was used to construct the phylogenetic tree. Multiple alignment of the amino acid sequences was carried out using DNAMAN V6.0.3.99.

The purified fragment was ligated with pEASY-E2 using the described protocol of the kit. The ligated product was transformed into the competent *E. coli* cell strain Trans-T1 (TransGen Biotech, Beijing, China). A positive clone was selected using the T7 promoter primer (5′-TAATACGACTCACTATAGGG-3′) and CatalaseR (5′-TGCGTTTGTAATCACATCGTCCG-3′) and then cultured with LB medium containing 100 μg/mL of ampicillin. The recombinant vector pEASY-E2-*Kat* was extracted using a Plasmid Mini Kit (Omega Bio-Tek, Inc., USA) and then transformed into competent *E. coli* BL21 (DE3) cells. A positive clone for BL21/pEASY-E2-*Kat* was selected using PCR as described above.

2.3. Inducing Expression and Purification of Recombinant Catalase. Positive clones were cultured in 5 mL of LB medium containing 100 μg/mL of ampicillin at 37°C at 220 rpm for 12 h. Next, 1 mL of the above culture was inoculated into 50 mL of ZYM-5052 medium and was cultured at 30°C and 220 rpm for 16 h to induce the expression of the enzyme. To confirm expression, 8 mL of the induced culture was centrifuged at 10,000 ×g for 2 min and then suspended with 3 mL PBS (50 mM, pH 7.0). The suspended culture was subjected to ultrasonication at 400 W until clear. Then, 200 μL of ultrasonicated sample was centrifuged at 12,000 ×g for 5 min at 4°C, and the supernatant was transferred to a new centrifuge tube. The supernatant and sediment sample were both subjected to 12% SDS-PAGE to detect the expression of the recombinant enzyme; a sample containing an empty vector was used as a blank control. Electrophoresis parameters were set as follows: 30 V for 30 min, followed by 80 V until the end. The coomassie brilliant blue R250 protocol [23] was used to dye the gel.

2.4. Recombinant Strain Enzyme Production Curve. First, 1 mL of seed liquid was inoculated into shake flasks containing 50 mL of ZYM-5052 medium, and the flasks were placed in shaking tables at 220 rpm and 30°C. Every 4 h, samples were collected and analyzed for catalytic activity. The samples were ultrasonicated before activity measurement collection. Enzyme production curves were then obtained.

2.5. Purification of Recombinant Catalase. First, 100 mL of the induced recombinant *E. coli* was centrifuged at 10,000 ×g for 5 min and washed once with Buffer A (50 mM NaH_2PO_4, 300 mM NaCl, pH 8.0). After centrifugation, the recombinant *E. coli* pellet was resuspended with 3 mL of Buffer A. The resuspended sample was ultrasonicated until clear. The ultrasonicated sample was centrifuged, and the supernatant was subjected to a Nickel-iminodiacetic acid (Ni-IDA) column. Then, 10 volumes of Buffer A (50 mM NaH_2PO_4, 300 mM NaCl, pH 8.0) were used to wash proteins that were nonspecifically bound to the column. Then, 10 volumes of Buffer B (50 mM NaH_2PO_4, 300 mM NaCl, 20 mM imidazole, pH 8.0) were used to remove other proteins. Finally, 5 volumes of Buffer C (50 mM NaH_2PO_4, 300 mM NaCl, 100 mM imidazole, pH 8.0) and 5 volumes of Buffer D (50 mM NaH_2PO_4, 300 mM NaCl, 500 mM imidazole, pH 8.0) were applied to elute the recombinant catalase. The purity of catalase was confirmed by SDS-PAGE. The purified catalase was placed into a dialysis bag and dialyzed against Buffer A to remove the high concentrations of imidazole. Buffer A was replaced every several hours until the imidazole was removed. The quantity

of purified catalase was assayed using the Bradford method [24].

2.6. Recombinant Catalase Characteristics. A catalase activity assay was performed according to the method described by Beers Jr. and Sizer [25]. Purified recombinant catalase was diluted several times with PBS (20 mM, pH 7.0) to a suitable concentration, and 2.7 mL of 30 mM H_2O_2 (diluted with 20 mM PBS, pH 7.0) was then immediately added to 300 μL of diluted enzyme. The absorbance changes at 240 nm were measured every 5 s for 1 min. 1 U of activity was defined as the amount of enzyme to decompose 1 μmol of H_2O_2 per min. Each measurement was performed at least three times.

To assess the optimal reaction temperature, 30 mM H_2O_2 was preincubated at different temperatures from 10°C to 90°C (in 10°C increment), and then activities at different temperatures were measured with above preincubated H_2O_2.

To assess enzyme thermostability, diluted enzyme was incubated at 40, 50, 60, 70, 80, and 90°C for 30 min and 1 hour. After the incubation time, the heated enzyme was immediately transferred onto ice. Residual activities were measured with method described above.

The optimum pH was assayed with 30 mM H_2O_2 prepared in the following 50 mM buffers: sodium citrate 50 mM (pH 4–6), sodium phosphate 50 mM (pH 6–8), and glycine-NaOH 50 mM (pH 9–11). Activities at different pH values were measured as above in least three replicates.

Kinetic parameters were assayed by calculating the activity of the enzyme under different concentrations of H_2O_2 ranging from 2.5 to 25 mM in 20 mM PBS (pH 7.0) at 30°C. K_m was obtained by double-reciprocal plots according to Lineweaver and Burk [26].

3. Results and Discussion

3.1. Kat Sequence. The PCR product (Figure 1) and sequencing results showed that the total length of the *Kat* gene was 1,467 bp, which encoded a protein with 488 amino acids. Nucleotide sequence was submitted to GenBank, and GenBank accession number KP202252 was assigned. blastp was run in the nonredundant protein sequences of NCBI database for homologs of the amino acid sequence. The amino sequence had higher similarity with the catalase sequences of other *Geobacillus* spp.; however, all of these highly similar *Kat* genes were submitted in the form of sequenced genomes, and none had been previously cloned or expressed. Among all studied catalase sequences obtained from Swiss Prot database, this catalase was most similar to that of a *Bacillus* sp. [27], and its identity was 80%. Phylogenetic tree (Figure 2) based on the amino acid sequences similarity showed this catalase shared closest phylogenetic relationship with catalase of *Bacillus subtilis* and *Lactobacillus sakei* in Swiss Prot database. Multiple alignment of the amino acid sequence showed this catalase has seven typically conserved amino acid residuals for heme binding (Figure 3). All of the reported thermostable catalases [28, 29] from *Geobacillus stearothermophilus* were different from this catalase herein because they belonged to the second group of catalase family (catalase-peroxidase) and were encoded by *Per* gene, but catalase in this paper belonged to the first group (monofunctional heme catalase) which was encoded by gene *Kat* [5]. Therefore, to our knowledge this study was the first to clone and express this type of *Geobacillus* spp. *Kat* gene.

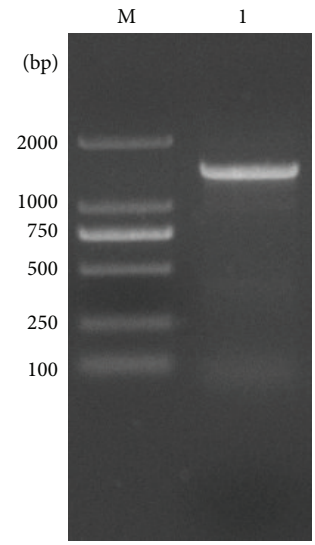

Figure 1: PCR product showing a 1,452-length band that corresponds to *Kat* from a *Geobacillus* sp. CHB1. Lanes: M, DNA marker; Lane 1, PCR product.

3.2. Construction of Recombinant Expression Vector pEASY-E2-Kat. A positive clone was selected, and its sequence was confirmed by sequencing. The expression vector pEASY-E2-*Kat* (Figure 4) was transformed into BL21 (DE3) cells. Then, SDS-PAGE was applied to confirm whether the catalase was expressed and to determine the molecular weight of the enzyme. A band was observed between 60 and 70 kDa, and the recombinant catalase was highly soluble (make up to 30% of the total *E coli* protein) with a low inclusion body content (Figure 5). The theoretical molecular weight of the recombinant enzyme herein, calculated using its amino sequence, was 56 kDa, including the 6×His tag, which conflicted with the molecular weight of 65 kDa observed via SDS-PAGE. Some studies [30] have found that the 6×His tag might result in a recombinant protein with a greater molecular weight; however, the reason for this phenomenon remains unclear. The specific activity of the purified catalase was 40,526 U/mg under optimal conditions (60°C, pH 7.0).

3.3. Production Curve for Recombinant Catalase. Production curves for the recombinant catalase were constructed at 30°C. When cultured at 30°C for 20 h, the total activity of the fermentation broth reached a maximum level of 35,831 U/mL assayed under optimal conditions (Figure 6). This level was much higher than many catalase production strains and only lower than recombinant *Bacillus* sp. WSHDZ-01 (Table 1) as we know. High production ensured further application of this catalase.

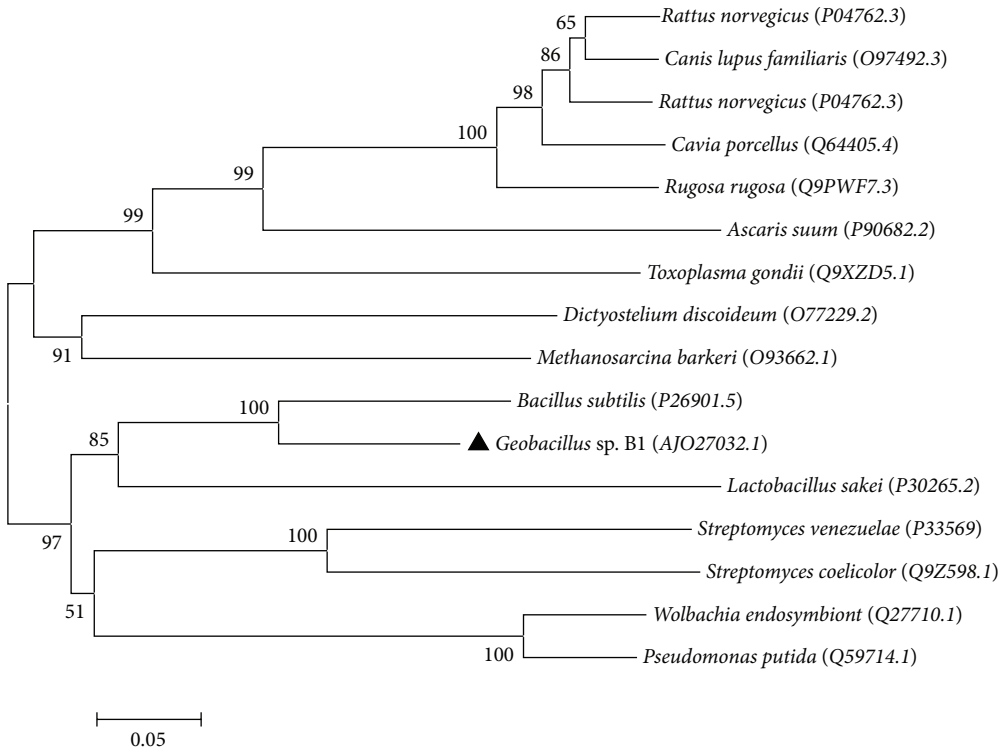

Figure 2: Phylogenetic tree of CHB1 catalase amino acid showing the relationship with other strains on catalase amino acid sequence. Protein sequences were selected by running blastp program with CHB1 catalase sequence in Swiss Prot database; accession numbers in brackets were the corresponding accession numbers of the strains in Swiss Prot database. Phylogenetic tree was constructed with MEGA 4.0.2 with the method Neighbor-Joining. Test of inferred phylogeny was Bootstrap for 1000 replications.

Table 1: Catalase production levels of recombinant *E. coli* BL21 and other strains.

Strains	Activity (U/mL)	Reference
Recombinant *E. coli* BL21 (DE3)	35,831	This study
Recombinant Bacillus sp. WSHDZ-01	39,117	[15]
Bacillus sp. WSHDZ-01	28,990	[19]
Exiguobacterium oxidotolerans T-2-2T	22,000	[20]
Serratia marcescens SYBC08	20,353	[21]
Rhizobium radiobacter strain 2-1	17,035	[22]
M. luteus	6920	[22]

3.4. Purified Recombinant Catalase Characteristics

3.4.1. Effect of Temperature and pH on This Catalase. Temperature is a major factor in the application of many enzymes. The activity and stability of our purified catalase at different temperatures were assayed. The catalase in this study showed a high activity over a wide range of temperatures, from 10°C to 90°C (Figure 7(a)), and showed maximum activity at 60°C to 70°C. The temperature range was wider and optimal temperature was higher than many reported catalases, such as *Serratia marcescens* SYBC08 at temperatures ranging from 0°C to 70°C with optimal temperature of 20°C [31]; *Psychrobacter piscatorii* T-3 from 10°C to 60°C with optimal temperature of 45°C [32]; and *Bacillus altitudinis* SYBC hb4 from 20°C to 40°C with optimal temperature of 30°C [33]. This catalase was stable at temperatures ≤60°C (Figure 7(b)) and when incubated at 70°C for 1 h, the enzyme maintained >70% residual activity; however, when the incubation temperature was >80°C, the residual activity was <10% after incubation for 1 h. Although this enzyme was inactive at ≥80°C, it still maintained high activity when added to reaction systems at 80°C and 90°C. Thermophilic catalase isolated from thermophilic *Thermoascus aurantiacus* [34] can retain 100% residual activity after incubation at 60°C for 1 h, which was similar to that of CHB1 catalase. This thermophilic property was much better than the properties of other catalases, such as those from *Psychrobacter piscatorii* (*P. piscatorii*) (65°C, 15 min, 20%) [32, 35], *Vibrio salmonicida* (60°C, 20 min, 0%) [36], *Vibrio rumoiensis* S-1T (65°C, 10 min, 0%) [37], and *Halomonas* sp. SK1 (55°C, 30 min, 0%) [38]. These properties enable the enzyme to be applied in both low and high-temperature processes in industry. The optimal pH of the enzyme was 6-7, and the enzyme retained >50% of its activity between pH 5 and 9 (Figure 8).

3.4.2. Kinetic Parameters of This Catalase. The enzyme kinetics of the recombinant catalase were assayed using

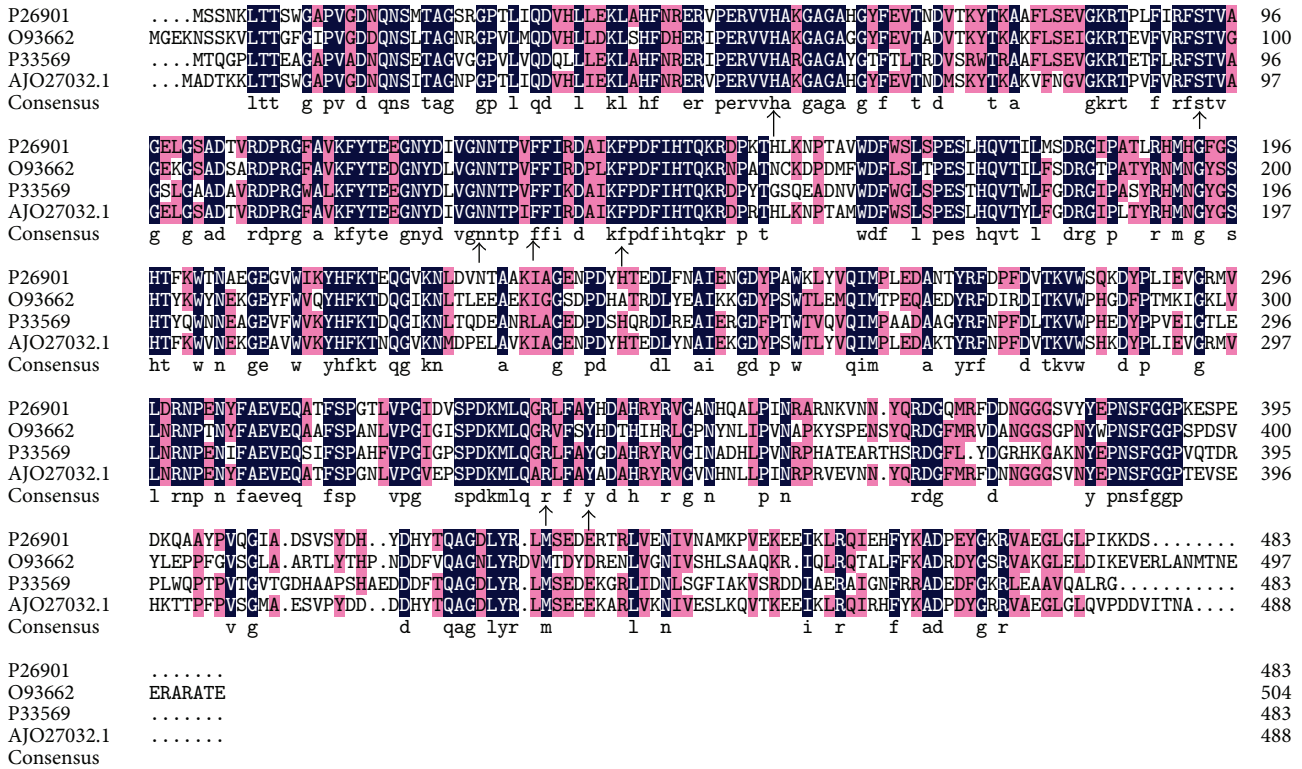

Figure 3: Multiple alignment of amino acid sequences for CHB1 catalase and catalase from Swiss Prot database. The sequences were those from *Bacillus subtilis* subsp. str. 168 (Swiss Prot number P26901), *Methanosarcina barkeri* str. Fusaro (Swiss Prot number O93662), *Streptomyces venezuelae* ATCC 10712 (Swiss Prot number P33569), and *Geobacillus* sp. CHB1 (GenBank number AJO27032.1). Identical amino acid residuals were shaded in black and conserved residuals were shaded in gray. Arrows showed the conserved residuals of home binding pocket of this kind of catalase.

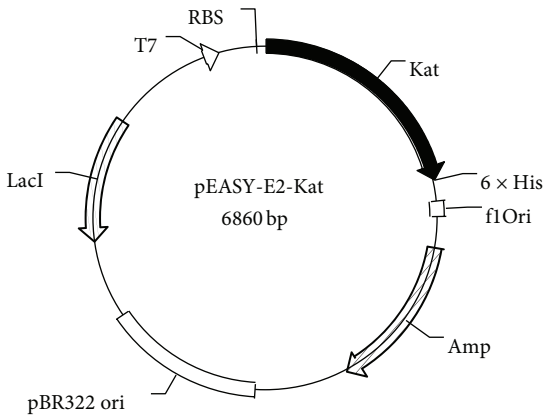

Figure 4: Recombinant expression construction of vector pEASY-E2-*kat*. A schematic diagram of recombinant expression vector pEASY-E2-*kat*. The *kat* gene encoding catalase was inserted into an expression vector with upstream RBS and T7 promoters and downstream 6×His.

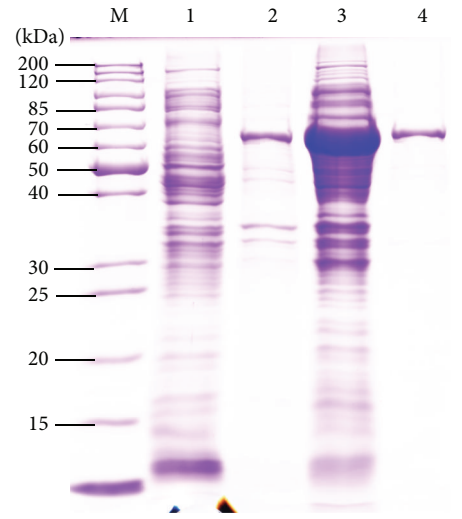

Figure 5: SDS-PAGE analyses of recombinant catalase expression and the purified enzyme. Lanes: M, protein marker; Lane 1, total bacterial protein of BL21 (DE3) cells with empty vector pEASY-E2; Lane 2, insoluble bacterial proteins of BL21 (DE3) with vector pEASY-E2-*kat* after induced expression; Lane 3, soluble bacterial proteins of BL21 (DE3) with vector pEASY-E2-*kat* after induced expression; Lane 4, SDS-PAGE analysis of purified catalase using a Ni-IDA column.

different H_2O_2 concentrations as substrates; a Lineweaver–Burk plot was used to calculate K_m, 51.1 mM, and V_{max}, 151.5 mol/min·mg (Figure 9), which is similar to previously

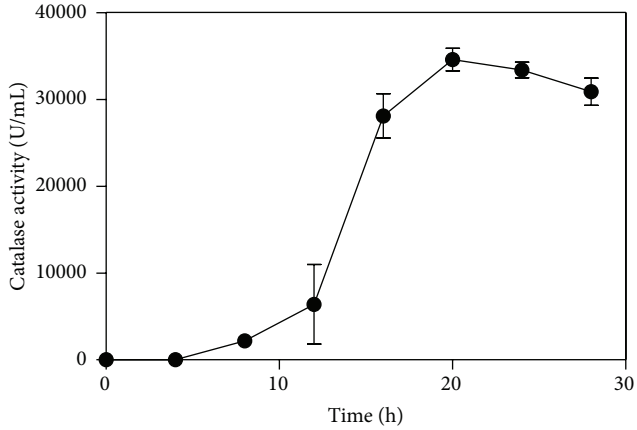

Figure 6: Catalase production curve of the recombinant *E. coli* BL21 (DE3).

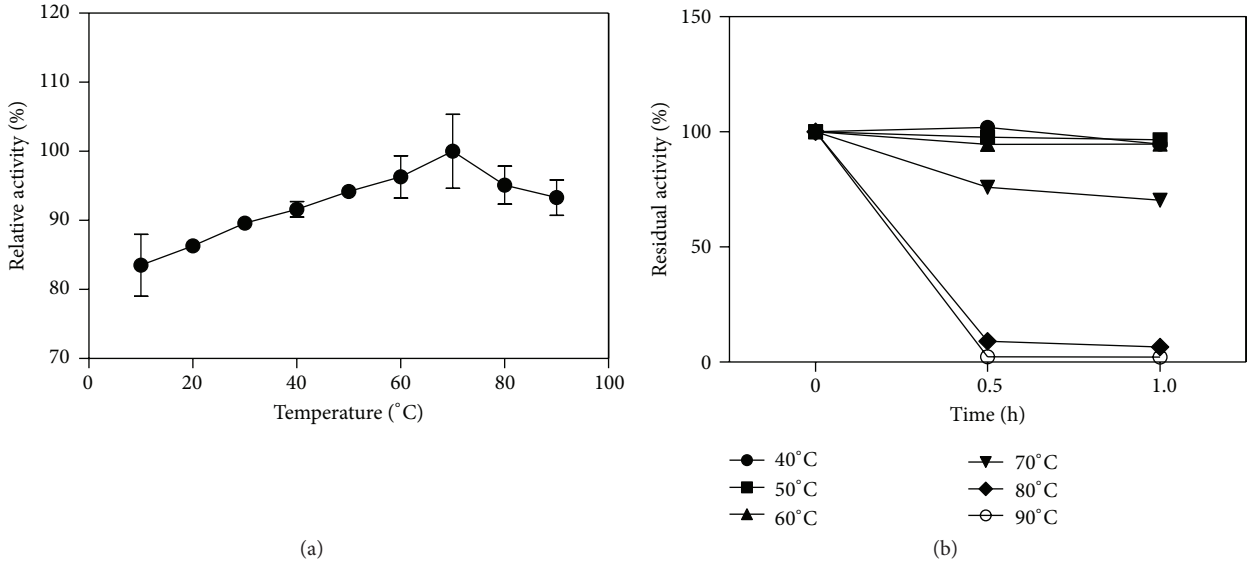

Figure 7: Effect of temperature on recombinant catalase activity. (a) Relative activity of the enzyme at 10, 20, 30, 40, 50, 60, 70, 80, and 90°C; (b) temperature stability of the enzyme. Residual activity of the recombinant enzyme by incubation at 40, 50, 60, 70, 80, and 90°C for 0.5 and 1 h.

reported values (52.5 mM [23] and 40.1 mM [2]). Many other catalases from *P. piscatorii* T-3, *Micrococcus luteus*, *Bacteroides fragilis*, *Helicobacter pylori*, *Serratia marcescens,* and *Xanthomonas campestris* have higher K_m values compared to the purified catalase [39]. The relatively low K_m indicates that the enzyme has a high affinity for H_2O_2 and that the enzyme is stable under high H_2O_2 concentrations. K_m is an important characteristic of enzymes and is vital for the assessment of their potential applications.

4. Conclusions

In this paper, we cloned, expressed, purified, and characterized a *Kat* gene of thermophilic bacteria *Geobacillus* sp. CHB1 for the first time. The recombinant enzyme could maintain its stability and showed a high activity over a wide range of temperatures from 10°C to 90°C. Specific activity of the purified recombinant catalase was 40,526 U/mg of protein, and recombinant *E. coli* BL21 strain reached a high level of catalase production to 35,831 U/mL. This enzyme's wide range of reaction temperatures, good thermostability, and high production may be suitable for the textile, paper-making, and other industries.

Competing Interests

The authors declare no conflict of interests.

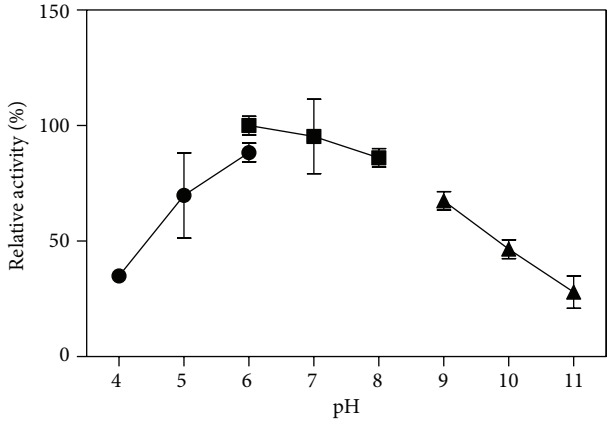

Figure 8: Optimal pH of the recombinant catalase. The buffers used for each pH region were 50 mM sodium citrate (pH 4–6), 50 mM sodium phosphate (pH 6–8), and 50 mM glycine-NaOH (pH 9–11). Each pH was assayed at least three times.

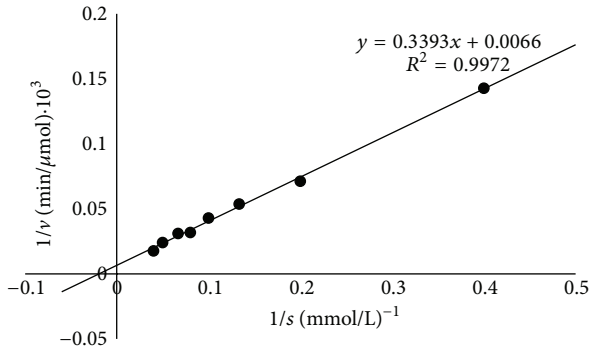

Figure 9: A Lineweaver–Burk plot of the recombinant catalase. Enzyme activity was assayed in 50 mM phosphate buffer (pH 7.0) and at 30°C.

Acknowledgments

This work was supported by the Argoscientific Research in the Public Interest (201303094-05) and Fujian Finance [2013] no. 1464.

References

[1] H.-S. Ko, H. Fujiwara, Y. Yokoyama et al., "Inducible production of alcohol oxidase and catalase in a pectin medium by *Thermoascus aurantiacus* IFO 31693," *Journal of Bioscience and Bioengineering*, vol. 99, no. 3, pp. 290–292, 2005.

[2] H.-W. Zeng, Y.-J. Cai, X.-R. Liao, S.-L. Qian, F. Zhang, and D.-B. Zhang, "Optimization of catalase production and purification and characterization of a novel cold-adapted Cat-2 from mesophilic bacterium *Serratia marcescens* SYBC-01," *Annals of Microbiology*, vol. 60, no. 4, pp. 701–708, 2010.

[3] H. D. Rowe, "Biotechnology in the textile/clothing industry—a review," *Journal of Consumer Studies & Home Economics*, vol. 23, no. 1, pp. 53–61, 1999.

[4] X. Fu, W. Wang, J. Hao, X. Zhu, and M. Sun, "Purification and characterization of catalase from marine bacterium *Acinetobacter* sp. YS0810," *BioMed Research International*, vol. 2014, Article ID 409626, 7 pages, 2014.

[5] B. S. Sooch, B. S. Kauldhar, and M. Puri, "Recent insights into microbial catalases: isolation, production and purification," *Biotechnology Advances*, vol. 32, no. 8, pp. 1429–1447, 2014.

[6] M. Spiro and W. P. Griffith, "The mechanism of hydrogen peroxide bleaching," *Textile Chemist and Colorist*, vol. 29, no. 11, pp. 12–13, 1997.

[7] M. Kagawa, N. Murakoshi, Y. Nishikawa et al., "Purification and cloning of a thermostable manganese catalase from a thermophilic bacterium," *Archives of Biochemistry and Biophysics*, vol. 362, no. 2, pp. 346–355, 1999.

[8] A. Hidalgo, L. Betancor, R. Moreno et al., "*Thermus thermophilus* as a cell factory for the production of a thermophilic Mn-dependent catalase which fails to be synthesized in an active form in *Escherichia coli*," *Applied and Environmental Microbiology*, vol. 70, no. 7, pp. 3839–3844, 2004.

[9] S. Ebara and Y. Shigemori, "Alkali-tolerant high-activity catalase from a thermophilic bacterium and its overexpression in *Escherichia coli*," *Protein Expression and Purification*, vol. 57, no. 2, pp. 255–260, 2008.

[10] M. Gudelj, G. O. Fruhwirth, A. Paar et al., "A catalase-peroxidase from a newly isolated thermoalkaliphilic *Bacillus* sp. with potential for the treatment of textile bleaching effluents," *Extremophiles*, vol. 5, no. 6, pp. 423–429, 2001.

[11] X.-L. Shi, M.-Q. Feng, J. Shi, Z.-H. Shi, J. Zhong, and P. Zhou, "High-level expression and purification of recombinant human catalase in *Pichia pastoris*," *Protein Expression and Purification*, vol. 54, no. 1, pp. 24–29, 2007.

[12] G. Gellissen, M. Piontek, U. Dahlems et al., "Recombinant *Hansenula polymorpha* as a biocatalyst: coexpression of the spinach glycolate oxidase (GO) and the *S. cerevisiae* catalase T (CTT1) gene," *Applied Microbiology and Biotechnology*, vol. 46, no. 1, pp. 46–54, 1996.

[13] T. Rochat, A. Miyoshi, J. J. Gratadoux et al., "High-level resistance to oxidative stress in *Lactococcus lactis* conferred by *Bacillus subtilis* catalase KatE," *Microbiology*, vol. 151, no. 9, pp. 3011–3018, 2005.

[14] X. Shi, M. Feng, Y. Zhao, X. Guo, and P. Zhou, "Overexpression, purification and characterization of a recombinant secretary catalase from *Bacillus subtilis*," *Biotechnology Letters*, vol. 30, no. 1, pp. 181–186, 2008.

[15] S. Xu, Y. Guo, G. Du, J. Zhou, and J. Chen, "Self-cloning significantly enhances the production of catalase in *Bacillus subtilis* WSHDZ-01," *Applied Biochemistry and Biotechnology*, vol. 173, no. 8, pp. 2152–2162, 2014.

[16] H. Luo, Y. Zhou, Y. H. Chang, L. Xiong, and L. Z. Liu, "Rapid gene cloning, overexpression and characterization of a thermophilic catalase in *E. coli*," *Advanced Materials Research*, vol. 365, pp. 367–374, 2012.

[17] F. W. Studier, "Protein production by auto-induction in high density shaking cultures," *Protein Expression and Purification*, vol. 41, no. 1, pp. 207–234, 2005.

[18] J. Zhou, M. A. Bruns, and J. M. Tiedje, "DNA recovery from soils of diverse composition," *Applied and Environmental Microbiology*, vol. 62, no. 2, pp. 316–322, 1996.

[19] Y. Deng, Z. Hua, Z. Zhao, D. Yao, G. Du, and J. Chen, "Effect of nitrogen sources on catalase production by *Bacillus subtilis* WSHDZ-01," *Chinese Journal of Applied and Environmental Biology*, vol. 14, no. 4, pp. 544–547, 2008.

[20] Y. Hanaoka and I. Yumoto, "Manipulation of culture conditions for extensive extracellular catalase production by *Exiguobacterium oxidotolerans* T-2-2T," *Annals of Microbiology*, vol. 65, pp. 1183–1187, 2014.

[21] H.-W. Zeng, Y.-J. Cai, X.-R. Liao et al., "*Serratia marcescens* SYBC08 catalase isolated from sludge containing hydrogen peroxide shows increased catalase production by regulation of carbon metabolism," *Engineering in Life Sciences*, vol. 11, no. 1, pp. 37–43, 2011.

[22] M. Nakayama, T. Nakajima-Kambe, H. Katayama, K. Higuchi, Y. Kawasaki, and R. Fuji, "High catalase production by *Rhizobium radiobacter* strain 2-1," *Journal of Bioscience and Bioengineering*, vol. 106, no. 6, pp. 554–558, 2008.

[23] V. Neuhoff, N. Arold, D. Taube, and W. Ehrhardt, "Improved staining of proteins in polyacrylamide gels including isoelectric focusing gels with clear background at nanogram sensitivity using Coomassie Brilliant Blue G-250 and R-250," *Electrophoresis*, vol. 9, no. 6, pp. 255–262, 1988.

[24] M. M. Bradford, "A rapid and sensitive method for the quantitation of microgram quantities of protein utilizing the principle of protein-dye binding," *Analytical Biochemistry*, vol. 72, no. 1-2, pp. 248–254, 1976.

[25] R. F. Beers Jr. and I. W. Sizer, "A spectrophotometric method for measuring the breakdown of hydrogen peroxide by catalase," *The Journal of Biological Chemistry*, vol. 195, no. 1, pp. 133–140, 1952.

[26] H. Lineweaver and D. Burk, "The determination of enzyme dissociation constants," *Journal of the American Chemical Society*, vol. 56, no. 3, pp. 658–666, 1934.

[27] D. K. Bol and R. E. Yasbin, "The isolation, cloning and identification of a vegetative catalase gene from *Bacillus subtilis*," *Gene*, vol. 109, no. 1, pp. 31–37, 1991.

[28] F. Wang, Z. Wang, W. Shao, J. Liu, C. Xu, and J. Zhuge, "Purification and properties of thermostable catalase in engineered *E. coli*," *Acta microbiologica Sinica*, vol. 42, no. 3, pp. 348–353, 2002.

[29] S. Loprasert, S. Negoro, and H. Okada, "Cloning, nucleotide sequence, and expression in *Escherichia coli* of the *Bacillus stearothermophilus* peroxidase gene (perA)," *Journal of Bacteriology*, vol. 171, no. 9, pp. 4871–4875, 1989.

[30] Y. Zhong, X.-H. Zhang, J. Chen et al., "Overexpression, purification, characterization, and pathogenicity of *Vibrio harveyi* hemolysin VHH," *Infection and Immunity*, vol. 74, no. 10, pp. 6001–6005, 2006.

[31] H.-W. Zeng, Y.-J. Cai, X.-R. Liao, F. Zhang, and D.-B. Zhang, "Production, characterization, cloning and sequence analysis of a monofunctional catalase from *Serratia marcescens* SYBC08," *Journal of Basic Microbiology*, vol. 51, no. 2, pp. 205–214, 2011.

[32] H. Kimoto, K. Yoshimune, H. Matsuyma, and I. Yumoto, "Characterization of catalase from psychrotolerant *Psychrobacter piscatorii* T-3 exhibiting high catalase activity," *International Journal of Molecular Sciences*, vol. 13, no. 2, pp. 1733–1746, 2012.

[33] Y. Zhang, X. Li, R. Xi, Z. Guan, Y. Cai, and X. Liao, "Characterization of an acid-stable catalase KatB isolated from *Bacillus altitudinis* SYBC hb4," *Annals of Microbiology*, vol. 66, no. 1, pp. 131–141, 2016.

[34] H. Wang, Y. Tokusige, H. Shinoyama, T. Fujii, and T. Urakami, "Purification and characterization of a thermostable catalase from culture broth of *Thermoascus aurantiacus*," *Journal of Fermentation and Bioengineering*, vol. 85, no. 2, pp. 169–173, 1998.

[35] W. Wang, M. Sun, W. Liu, and B. Zhang, "Purification and characterization of a psychrophilic catalase from Antarctic *Bacillus*," *Canadian Journal of Microbiology*, vol. 54, no. 10, pp. 823–828, 2008.

[36] M. S. Lorentzen, E. Moe, H. M. Jouve, and N. P. Willassen, "Cold adapted features of *Vibrio salmonicida* catalase: characterisation and comparison to the mesophilic counterpart from *Proteus mirabilis*," *Extremophiles*, vol. 10, no. 5, pp. 427–440, 2006.

[37] I. Yumoto, D. Ichihashi, H. Iwata et al., "Purification and characterization of a catalase from the facultatively psychrophilic bacterium *Vibrio rumoiensis* S-1T exhibiting high catalase activity," *Journal of Bacteriology*, vol. 182, no. 7, pp. 1903–1909, 2000.

[38] K. Phucharoen, K. Hoshino, Y. Takenaka, and T. Shinozawa, "Purification, characterization, and gene sequencing of a catalase from an alkali- and halo-tolerant bacterium, *Halomonas* sp. SK1," *Bioscience, Biotechnology and Biochemistry*, vol. 66, no. 5, pp. 955–962, 2002.

[39] J. Switala and P. C. Loewen, "Diversity of properties among catalases," *Archives of Biochemistry and Biophysics*, vol. 401, no. 2, pp. 145–154, 2002.

Hindawi Publishing Corporation
BioMed Research International
Volume 2016, Article ID 4652876, 5 pages
http://dx.doi.org/10.1155/2016/4652876

Research Article

Laboratory Prototype of Bioreactor for Oxidation of Toxic D-Lactate Using Yeast Cells Overproducing D-Lactate Cytochrome *c* Oxidoreductase

Maria Karkovska, Oleh Smutok, and Mykhailo Gonchar

Department of Analytical Biotechnology, Institute of Cell Biology, Drahomanov Street 14/16, Lviv 79005, Ukraine

Correspondence should be addressed to Oleh Smutok; smutok@cellbiol.lviv.ua

Received 25 April 2016; Accepted 7 June 2016

Academic Editor: Subash C. B. Gopinath

D-lactate is a natural component of many fermented foods like yogurts, sour milk, cheeses, and pickles vegetable products. D-lactate in high concentrations is toxic for children and people with short bowel syndrome and provokes encephalopathy. These facts convincingly demonstrate a need for effective tools for the D-lactate removal from some food products. The main idea of investigation is focused on application of recombinant thermotolerant methylotrophic yeast *Hansenula polymorpha* "tr6," overproducing D-lactate: cytochrome *c* oxidoreductase (EC 1.1.2.4, D-lactate cytochrome *c* oxidoreductase, D-lactate dehydrogenase (cytochrome), DLDH). In addition to 6-fold overexpression of DLDH under a strong constitutive promoter (*prAOX*), the strain of *H. polymorpha* "tr6" (*gcr1 catX*/Δ*cyb2*, *prAOX_DLDH*) is characterized by impairment in glucose repression of AOX promoter, devoid of catalase and L-lactate-cytochrome *c* oxidoreductase activities. Overexpression of DLDH coupling with the deletion of L-lactate-cytochrome *c* oxidoreductase activity opens possibility for usage of the strain as a base for construction of bioreactor for removing D-lactate from fermented products due to oxidation to nontoxic pyruvate. A laboratory prototype of column-type bioreactor for removing a toxic D-lactate from model solution based on permeabilized cells of the *H. polymorpha* "tr6" and alginate gel was constructed and efficiency of this process was tested.

1. Introduction

D-lactate is a natural component of many fermented foods like yogurts [1, 2], sour milk [3], cheeses [4], and pickles vegetable products [5].

D-lactate can be metabolized slowly in the human body in comparison with L-lactate isomer and can cause metabolic disorders if ingested in excess. Therefore, the World Health Organization (WHO) recommends a limited daily consumption of D-lactate up to 100 mg·kg^{-1} bodyweight. Moreover, some countries, for example, Germany, have decided to minimize the D-lactate content of fermented dairy products [6]. The high concentration of D-lactate is toxic for children [7] and people with short bowel syndrome [8–10]. Also D-lactate toxicity depends on physiological state of renal excretion. Hingorani et al. demonstrated that, in healthy men continuously infused with a D-lactate solution, excretion rates ranged between 61 and 100% [11]. In 1993, there was reported a case of chronic D-lactate encephalopathy occurring in a patient with short bowel syndrome and end-stage renal disease [12].

Originally, it was believed that, due to the lack of enzyme D-lactate dehydrogenase in humans, they are not able to metabolize D-lactate to pyruvate. However, in the past two decades there is an abundance of literature suggesting the presence of a D-lactate metabolizing enzyme D-2-hydroxy acid dehydrogenase (D-2-HDH) that is mainly found in the liver and kidney [10, 13]. This enzyme is inhibited by low-pH states, which assumes importance in the relative overproduction of D-lactate in certain clinical situations. D-lactic acidosis or D-lactate encephalopathy is a rare condition that occurs primarily in individuals who have a history of short bowel syndrome (SBS).

The predominant organ system affected by D-lactic acidosis is the central nervous system (CNS). Presenting symptoms

may include slurred speech, ataxia, altered mental status, psychosis, or even coma [8, 9, 14, 15].

The aim of the current work is construction of an effective laboratory prototype of bioreactor for removing D-lactate from fermented products based on the use of yeast cells overproducing D-lactate oxidoreductase. The D-lactate oxidoreductase (cytochrome *c*-dependent dehydrogenase, DLDH, EC1.1.2.4) is a FAD- and Zn^{2+}-containing membrane-associated protein found in yeast and bacteria. The enzyme catalyzes D-lactate oxidation to pyruvate coupled with ferricytochrome *c* reduction to ferrocytochrome *c*. It is characterized as a mitochondrial protein with a molecular weight of 63 kDa for DLDH from *Kluyveromyces lactis* and 64 kDa for DLDH from *Saccharomyces cerevisiae*, respectively [16, 17]. DLDH is highly selective to D-lactate; however, D,L-α-hydroxybutyric acid can be used as an alternative electron donor. The enzyme is not selective with respect to electron acceptors and can reduce, in addition to its native acceptor (cytochrome *c*), different low molecular artificial redox mediators (ferricyanide, dichlorphenol indophenols, etc.).

We propose using recombinant DLDH-overproducing strain *H. polymorpha* "tr6" (*gcr1 catX*/Δ*cyb2*, *prAOX_DLDH*) as a base for construction of laboratory prototype of bioreactor for removing a toxic D-lactate from fermented products. The column-type bioreactor includes alginate gel formations with incorporated permeabilized yeast cells.

2. Material and Methods

2.1. Materials. Sodium D-lactate, sodium alginate, and phenylmethylsulfonyl fluoride (PMSF) were purchased from Sigma-Aldrich Corp. (Deisenhofen, Germany) and cetyltrimethylammonium bromide (CTAB) was purchased from Chemapol Sp. (Bratislava, Slovakia). *D*(+)-glucose monohydrate was purchased from J. T. Baker (Deventer, Netherlands). $(NH_4)_2SO_4$, Na_2HPO_4, KH_2PO_4, $MgSO_4$, and $CaCl_2$ were obtained from Merck (Darmstadt, Germany). All chemicals and reagents were of analytical grade and all solutions were prepared using deionized water. D-lactate standard solution and appropriate dilutions were prepared in 100 mM phosphate buffer (PB), pH 7.8.

2.2. Cultivation and Permeabilization of Yeast Cells. Recombinant DLDH-overproducing strain *H. polymorpha* "tr6" (*gcr1 catX*/Δ*cyb2*, *prAOX_DLDH*) is characterized by 6-fold overexpression of DLDH, impaired in glucose repression, devoid of catalase and specific L-lactate-cytochrome *c* oxidoreductase activities, which was constructed by us earlier [18].

Cultivation of the *H. polymorpha* "tr6" was performed in flasks on a shaker (200 rpm) at 28°C until the middle of the stationary growth phase (~52 h) in a medium containing ($g \cdot L^{-1}$): $(NH_4)_2SO_4$, 3.5; KH_2PO_4, 1.0; and $MgSO_4 \times 7H_2O$, 0.5, supplemented with 0.75% yeast extract. A mixture of glucose (10 $g \cdot L^{-1}$) and D-lactate (2 $g \cdot L^{-1}$) was used as a carbon and energy source and (1 $g \cdot L^{-1}$) methanol as an inductor for *AOX* promoter. After washing, the cells were suspended in 50 mM PB, pH 7.8, containing 1 mM PMSF.

Before experiments, the freshly prepared yeast cells were resuspended to 30 $mg \cdot mL^{-1}$ in 50 mM PB, pH 7.8, and stored in refrigerator.

The procedure of the cells permeabilization was as follows: the same volume of permeabilizing reagent (0.85 mM CTAB) was added to the cell suspension (30 $mg \cdot mL^{-1}$ in 50 mM PB, pH 7.8). The resulting solution was treated at 30°C in a water bath for 15 min under mixing every 3-4 min. The permeabilized cells were washed by centrifugation (6000 ×g, 5 min) in 10 mM PB, pH 7.8. The precipitated permeabilized cells were resuspended to 30 $mg \cdot mL^{-1}$ in the same buffer solution and stored at +4°C. A half-life of the permeabilized yeast cells was about three weeks of storage at such conditions.

2.3. Assay of DLDH Activity in Permeabilized Cells. One unit (1 U) of the *DLDH* activity is defined as that amount of the enzyme which forms 1 μmol hexacyanoferrate(II) per minute under standard conditions of the assay (20°C, 30 mM PB, and pH 7.8). Activity was estimated by spectrophotometric monitoring of hexacyanoferrate(III) reduction at $\lambda = 420$ nm [19]. During this process, optical density of the analyzed solution becomes lower. Assay mixture consisted of 30 mM PB, pH 7.8; 16 mM sodium D-lactate; 0.83 mM $K_3Fe(CN)_6$; and 20 μL of diluted permeabilized cell suspension (30 $mg \cdot mL^{-1}$).

The specific activity of DLDH was calculated by the following formula:

$$\mathrm{SA} = \frac{\Delta E/\mathrm{min} \cdot V \cdot n}{E\mathrm{mM} \cdot C\mathrm{cells} \cdot V\mathrm{cells}}, \quad (1)$$

where $\Delta E/\mathrm{min}$ is change of optical density at $\lambda = 420$ nm per min; V is total volume of the assay solution, mL; n is dilution of the enzyme before assay; EmM is millimolar extinction of hexacyanoferrate(III), 1.04 $mM^{-1} \cdot cm^{-1}$; Vcells is volume of the added permeabilized cell suspension, mL; and Ccells is permeabilized cell concentration, $mg \cdot mL^{-1}$.

Specific DLDH activity in the cells was calculated by the following formula, considering difference between specific DLDH activity (+D-lactate) and nonspecific ferrireductase activity (without D-lactate): $A = A_{+\text{D-lact}} - A_{-\text{D-lact}}$.

3. Results and Discussion

The possibility of usage of DLDH-producer as a perspective tool for D-lactate removing from fermented products was investigated. For analysis of D-lactate utilization ability of the recombinant thermotolerant methylotrophic yeast *Hansenula polymorpha* "tr6" (*gcr1 catX*/Δ*cyb2*, *prAOX_DLDH*) constructed by us earlier, overproducing DLDH was chosen. The *H. polymorpha* DLDH-producer was constructed in two steps. First, the gene *CYB2* was deleted on the background of the C-105 (*gcr1*, *catX*) strain of *H. polymorpha* impaired in glucose repression and devoid of catalase activity to avoid specific L-lactate-cytochrome *c* oxidoreductase activity. Second, the homologous gene *DLD1* coding for DLDH was overexpressed under the control of the strong *H. polymorpha* alcohol oxidase promoter in the frame of a plasmid for multicopy integration in the Δ*cyb2* strain. The selected recombinant strain possesses 6-fold increased DLDH activity as

Table 1: The residual D-lactate concentration by Buchner method in the samples selected using two types of the *H. polymorpha* "tr6" cells analyzed.

Time of incubation, min	D-lactate, mM (permeabilized cells)	D-lactate, mM (intact cells)
0	20.0 ± 0.00	20.0 ± 0.00
10	19.3 ± 0.15	19.87 ± 0.14
20	15.5 ± 0.2	18.5 ± 0.18
30	11.9 ± 0.23	15.51 ± 0.25
40	11.98 ± 0.28	14.48 ± 0.29
50	12.5 ± 0.30	14.5 ± 0.22

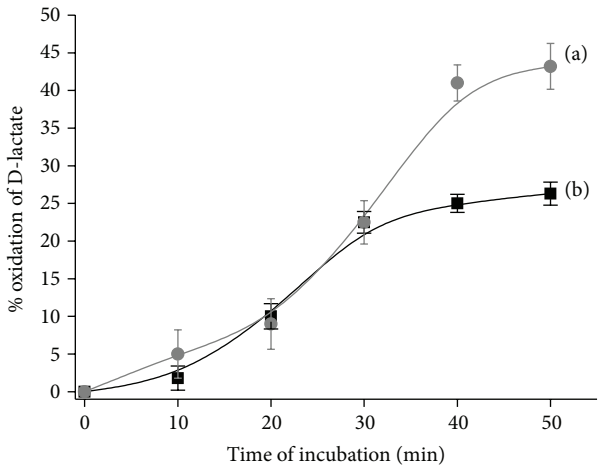

Figure 1: The profile of D-lactate oxidation using recombinant *H. polymorpha* "tr6" cells: (a) permeabilized and (b) living cells. Conditions: 10 mM PB, pH 7.8, 30°C, and shaking (200 rpm) at 30°C; the initial concentration of D-lactate was 20 mM.

compared to the initial strain [18]. Two types of yeast cells (intact and permeabilized) were tested. The experiment was carried out as follows: to 50 mL of 10 mM PB, pH 7.8, we added D-lactate (with a final concentration 20 mM) and 0.1 g of the intact yeast cells with specific enzymatic activity 12.6 U·mg^{-1}. An incubation of the same amount of permeabilized cells of the *H. polymorpha* "tr6" (with DLDH activity of 11.7 U·mg^{-1}) in the same mixture was performed in parallel. The amount of the added yeast cells of two types was calculated related to the specific DLDH activity. The obtained cell mixture was incubated about one hour at a shaker (200 rev.·min^{-1}) at 30°C. Every 10 minutes, 2 mL of the mixture was taken, centrifugated (6000 ×g, r = 8 cm, 2 min) and the eluates were frozen at −20°C. The residual D-lactate in the frozen samples was analyzed chemically by Buchner method [20] after completing the experiment (Table 1).

The profile of D-lactate utilization using recombinant *H. polymorpha* "tr6" cells is represented in Figure 1.

As shown in Figure 1, effectiveness of D-lactate oxidation (during 40-minute incubation) was calculated as 28% for intact yeast cells (activity of DLDH, 12.6 U·mg^{-1}), whereas for the permeabilized cells (with activity of DLDH, 11.2 U·mg^{-1})

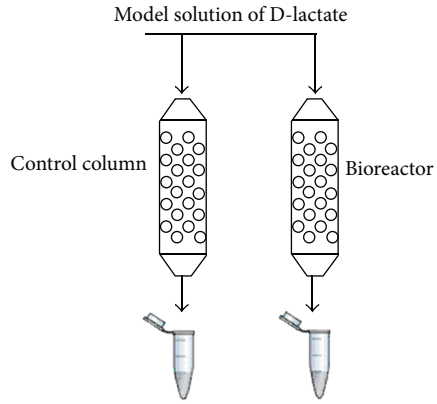

Figure 2: Principal scheme of bioreactor prototype based on permeabilized recombinant yeast cells for removing D-lactate from aqueous solution. The control column contains alginate gel without the cells.

it was about 41%. The average productivity of the process (for 30 min incubation) was about 9.0 mmol·L^{-1}·h^{-1}. It was shown that the permeabilized yeast cells are 1.5-fold more effective agent for removal of D-lactate in comparison with intact living cells. Probably this effect could be explained by higher permeability of permeabilized cells to substrate. Thus, for construction of cell-based bioreactor for D-lactate oxidation, permeabilized yeast cells of *H. polymorpha* "tr6" are more effective.

A column-type bioreactor based on permeabilized yeast cells of *H. polymorpha* "tr6" incorporated in alginate gel was constructed. The immobilization of the yeast cells in calcium alginate gel was performed as follows: 2 mL suspension of permeabilized *H. polymorpha* "tr6" cells (60 mg·mL^{-1}) was mixed with 2 mL of 4% (w/v) sodium alginate. The obtained mixture was put to medical syringe and dropped through a needle into solution of $CaCl_2$ (40 mg·mL^{-1}). The formed alginate beads (diameter around 3 mm) with incorporated permeabilized yeast cells were placed to columns 1 × 10 cm (4 mL gel). As a control, "bare" alginate gel without the cells (Figure 2) was used.

The packed columns were washed by 3 mL of PB, pH 7.8, prior to the experiment beginning. As a model solution, 20 mM of D-lactate in 50 mM PB, pH 7.8, containing 1 mM $CaCl_2$ was used.

For optimisation of flow rate for high efficiency of D-lactate oxidation, the model solution was simultaneously passed through both columns with different speed: 50 mL·min^{-1} and 10 mL·min^{-1}. Due to difference in flow rate through the alginate gel the first column with a speed 50 mL·min^{-1} was marked as a "bioreactor 1" and the other one (flow rate 10 mL·min^{-1}) was marked as "bioreactor 2," respectively. Every 15 min, a small amount (0.2 mL) of mixture flowing through the columns was collected and frozen at −20°C. After finishing the experiment, a residual D-lactate in the frozen samples was analyzed by Buhner chemical method of lactate assay (Figure 3).

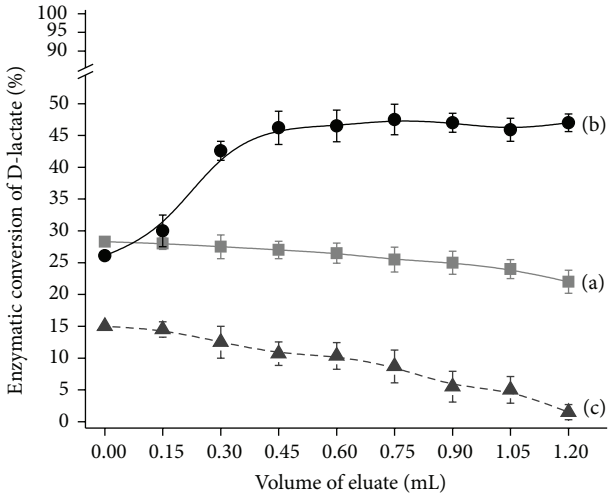

Figure 3: Optimisation of flow rate for enzymatic D-lactate conversion using a column bioreactor, (a) flow rate 50 mL·min^{-1} and (b) flow rate 10 mL·min^{-1}, and (c) control column, flow rate 10 mL·min^{-1}. Conditions: enzymatic activity of DLDH in permeabilized cells was 80 U·mL^{-1}, and the initial D-lactate concentration was 20 mM in the presence of 1 mM $CaCl_2$.

As was shown in Figure 3, both columns are able to remove D-lactate from the model solution. However, the effectiveness of this process was significantly different and depended on the flow rate through the columns. Thus, in the case of "bioreactor 1" enzymatic conversion of 2 mL 20 mM D-lactate was ranged between 15 and 28%. "Bioreactor 2" showed a twofold higher efficiency of D-lactate oxidation at the same volume of model solution (45–53%). The control alginate column was used to analyze the possibility of nonenzymatic conversion of D-lactate. As was clearly shown in Figure 3, nonenzymatic conversion of D-lactate in control reactor did not occur and the observed decrease in D-lactate concentration (about 14%) was caused by a partial dilution of sample as a result of washing the column by buffer.

The obtained results clearly confirmed the possibility of using permeabilized cells, immobilized in alginate gels, of recombinant DLDH-overproducing strain of *H. polymorpha* "tr6" as a catalyst for bioreactor able to remove D-lactate from fermented food products. It was shown that efficiency of enzymatic conversion of D-lactate for bioreactor prototype tightly depends on the flow rate through the column.

The usage of the developed cell-based prototype for removing toxic D-lactate from fermented products is in progress.

4. Conclusions

A laboratory prototype of column-type bioreactor for D-lactate removing from model solution based on permeabilized yeast cells of the *H. polymorpha* "tr6" and alginate gel has been constructed and efficiency of this process has been demonstrated. The optimal concentration of the permeabilized cells (with DLDH activity of 11.2 U·mg^{-1}) was estimated as 30 mg per 1 mL of 4% alginate. It was shown that efficiency of enzymatic oxidation of D-lactate by the bioreactor prototype tightly depends on flow rate through the column. The laboratory cell-based bioreactor would be useful in food technology for removing toxic D-lactate.

Competing Interests

The authors declare that there is no conflict of interests regarding the publication of this paper.

Acknowledgments

This research was supported in part by NAS of Ukraine in the frame of the Scientific-Technical Program "Sensor systems for medical, ecological and industrial-technological needs: metrological assurance and research exploitation," as well as by NATO Project SfP 984173.

References

[1] M. de Vrese, B. Koppenhoefer, and C. A. Barth, "D-lactic acid metabolism after an oral load of dl-lactate," *Clinical Nutrition*, vol. 9, no. 1, pp. 23–28, 1990.

[2] C. S. K. Mishra and P. Champagne, Eds., *Biotechnology Applications*, I. K. International Publishing House, New Delhi, India, 2009.

[3] C. Scheele, *The Collected Papers of Carl WilhelmScheele*, G. Bell, London, UK, 1931.

[4] Megazyme, "D-lactate acid (D-lactate) and L-lactate acid (L-lactate) assay procedures," 2007, https://secure.megazyme.com/D-Lactic-Acid-Assay-Kit.

[5] D. L. Zhang, Z. W. Jiang, J. Jiang, B. Cao, and J. S. Li, "D-lactic acidosis secondary to short bowel syndrome," *Postgraduate Medical Journal*, vol. 79, no. 928, pp. 110–112, 2003.

[6] A. Zourari, J. P. Accolas, and M. J. Desmazeaud, "Metabolism and biochemical characteristics of yogurt bacteria. A review," *Le Lait*, vol. 72, no. 1, pp. 1–34, 1992.

[7] L. Stolberg, R. Rolfe, N. Gitlin et al., "D-Lactic acidosis due to abnormal gut flora. Diagnosis and treatment of two cases," *The New England Journal of Medicine*, vol. 306, no. 22, pp. 1344–1348, 1982.

[8] M. Hudson, R. Pocknee, and N. A. G. Mowat, "D-Lactic acidosis in short bowel syndrome—an examination of possible mechanisms," *Quarterly Journal of Medicine*, vol. 74, no. 274, pp. 157–163, 1990.

[9] A. S. Day and G. D. Abbott, "D-lactic acidosis in short bowel syndrome," *The New Zealand Medical Journal*, vol. 112, no. 1092, pp. 277–278, 1999.

[10] N. Gurukripa Kowlgi and L. Chhabra, "D-lactic acidosis: an underrecognized complication of short bowel syndrome," *Gastroenterology Research and Practice*, vol. 2015, Article ID 476215, 8 pages, 2015.

[11] A. D. Hingorani, I. C. Macdougall, M. Browne, R. W. H. Walker, and C. R. V. Tomson, "Successful treatment of acute D-lactate encephalopathy by haemodialysis," *Nephrology Dialysis Transplantation*, vol. 8, no. 11, pp. 1283–1285, 1993.

[12] J. R. Thurn, G. L. Pierpont, C. W. Ludvigsen, and J. H. Eckfeldt, "D-lactate encephalopathy," *The American Journal of Medicine*, vol. 79, no. 6, pp. 717–721, 1985.

[13] H. Hove and P. B. Mortensen, "Colonic lactate metabolism and D-lactic acidosis," *Digestive Diseases and Sciences*, vol. 40, no. 2, pp. 320–330, 1995.

[14] B. E. Coronado, S. M. Opal, and D. C. Yoburn, "Antibiotic-induced D-lactic acidosis," *Annals of Internal Medicine*, vol. 122, no. 11, pp. 839–842, 1995.

[15] S. C. Kadakia, "D-lactic acidosis in a patient with jejunoileal bypass," *Journal of Clinical Gastroenterology*, vol. 20, no. 2, pp. 154–156, 1995.

[16] T. Lodi and I. Ferrero, "Isolation of the DLD gene of *Saccharomyces cerevisiae* encoding the mitochondrial enzyme D-lactate ferricytochrome c oxidoreductase," *Molecular and General Genetics*, vol. 238, no. 3, pp. 315–324, 1993.

[17] T. Lodi, D. O'Connor, P. Goffrini, and I. Ferrero, "Carbon catabolite repression in *Kluyveromyces lactis*: isolation and characterization of the *KINLD* gene encoding the mitochondrial enzyme D-lactate ferricytochrome *c* oxidoreductase," *Molecular and General Genetics*, vol. 244, no. 6, pp. 622–629, 1994.

[18] O. V. Smutok, K. V. Dmytruk, M. I. Karkovska, W. Schuhmann, M. V. Gonchar, and A. A. Sibirny, "D-lactate-selective amperometric biosensor based on the cell debris of the recombinant yeast *Hansenula polymorpha*," *Talanta*, vol. 125, pp. 227–232, 2014.

[19] C. A. Appleby and R. K. Morton, "Lactic dehydrogenase and cytochrome b_2 of baker's yeast; purification and crystallization," *The Biochemical journal*, vol. 71, no. 3, pp. 492–499, 1959.

[20] E. Buchner and K. Schottenhammer, "Die Einwirkung von Diazo-essigester auf Mesitylen," *Berichte der Deutschen Chemischen Gesellschaft (A and B Series)*, vol. 53, no. 6, pp. 865–873, 1920.

Hindawi Publishing Corporation
BioMed Research International
Volume 2016, Article ID 3265895, 9 pages
http://dx.doi.org/10.1155/2016/3265895

Research Article

Improved Production of *Aspergillus usamii* endo-β-1,4-Xylanase in *Pichia pastoris* via Combined Strategies

Jianrong Wang, Yangyuan Li, and Danni Liu

Guangdong VTR Bio-Tech Co., Ltd., Zhuhai, Guangdong 519060, China

Correspondence should be addressed to Jianrong Wang; believe1234@126.com

Received 11 November 2015; Accepted 24 January 2016

Academic Editor: Bidur P. Chaulagain

A series of strategies were applied to improve expression level of recombinant endo-β-1,4-xylanase from *Aspergillus usamii* (*A. usamii*) in *Pichia pastoris* (*P. pastoris*). Firstly, the endo-β-1,4-xylanase (*xynB*) gene from *A. usamii* was optimized for *P. pastoris* and expressed in *P. pastoris*. The maximum xylanase activity of optimized (*xynB-opt*) gene was 33500 U/mL after methanol induction for 144 h in 50 L bioreactor, which was 59% higher than that by wild-type (*xynB*) gene. To further increase the expression of *xynB-opt*, the *Vitreoscilla hemoglobin* (*VHb*) gene was transformed to the recombinant strain containing *xynB-opt*. The results showed that recombinant strain harboring the *xynB-opt* and *VHb* (named X33/*xynB-opt-VHb*) displayed higher biomass, cell viability, and xylanase activity. The maximum xylanase activity of X33/*xynB-opt-VHb* in 50 L bioreactor was 45225 U/mL, which was 35% and 115% higher than that by optimized (*xynB-opt*) gene and wild-type (*xynB*) gene. Finally, the induction temperature of X33/*xynB-opt-VHb* was optimized in 50 L bioreactor. The maximum xylanase activity of X33/*xynB-opt-VHb* reached 58792 U/mL when the induction temperature was 22°C. The results presented here will greatly contribute to improving the production of recombinant proteins in *P. pastoris*.

1. Introduction

Xylan, the major hemicellulose component in plant cell wall and the most abundant renewable hemicellulose, is a heterogeneous polysaccharide consisting of a β-1,4-linked D-xylose backbone [1]. Xylan occupies one-third of the overall plant carbohydrate and is the second most prevalent biomass after cellulose in nature [2]. Xylanase (EC 3.2.1.8) can hydrolyze xylan into xylooligosaccharides and D-xylose. Xylanases have generated considerable research interest and are becoming a major group of industrial enzymes. Xylanases have wide commercial applications in industrial processes, such as the paper and pulp industry, the foodstuff industry, the feed industry, and the energy industry [3, 4]. In recent years, increasing numbers of xylanases have been identified and characterized from various microorganisms, such as bacteria and fungi [5]. Among microbial sources, the filamentous fungi *Aspergillus* are especially interesting as they secrete these enzymes into the medium and their xylanase activities are higher than those produced by other microorganisms [6–8]. In previous studies, an endo-β-1,4-xylanase with high specific activity and good enzymatic properties was isolated from *A. usamii*. Furthermore, the gene encoding endo-β-1,4-xylanase from *A. usamii* was cloned and expressed in *P. pastoris* [9, 10]. However, the low expression level does not allow the recombinant xylanase to be applied practically and economically in industry. For commercial exploitation of the recombinant *A. usamii* endo-β-1,4-xylanase, it is essential to achieve high yield of the protein.

P. pastoris is now widely used for heterologous production of recombinant proteins. As a single-celled microorganism, *P. pastoris* has been proved as a highly successful system for variety of recombinant proteins. There are many advantages in this expression system such as high level expression, efficient extracellular protein secretion, proper protein folding, posttranslational modifications, and the potential to high cell density fermentation [11, 12]. Due to the wide use of this system, many strategies have been developed to

further improve expression level of heterologous protein in *P. pastoris*, including codon optimization, intracellular coexpression of *Vitreoscilla hemoglobin* (VHb), high heterologous gene copy number, altering the secretion signal peptide in expression vector, high efficient transcriptional promoters, and cultivation optimization [13–15]. However, there is little report about integrating these optimization methods as a whole to optimize gene expression.

In order to improve production of *A. usamii* endo-β-1,4-xylanase in *P. pastoris*, the *xynB* from *A. usamii* was firstly expressed in *P. pastoris*. To further improve the production of recombinant *A. usamii* endo-β-1,4-xylanase, we combined codon optimization, intracellular coexpression of VHb, and optimization of induction temperature as a whole to optimize *xynB* expression in *P. pastoris*. To our knowledge, this is the first report to improve *A. usamii* endo-β-1,4-xylanase production in *P. pastoris* by integrating these three optimization methods. The results presented here will greatly contribute to improving the production of recombinant proteins in *P. pastoris* and offer a greater value in various industrial applications.

2. Materials and Methods

2.1. Strains, Plasmids, Reagents, and Media. The *P. pastoris* strain X33 and the expression vector (pPIC3.5K and pPICZαA) were purchased from Invitrogen (Carlsbad, CA, USA). The *E. coli* strain Top 10 is routinely conserved in our laboratory. Restriction enzymes, T4-DNA ligase, and Pfu DNA polymerase were purchased from Sangon Biotech (Shanghai, China). All other chemicals used were analytical grade reagents unless otherwise stated. Yeast extract peptone dextrose (YPD) medium, buffered glycerol complex (BMGY) medium, and buffered methanol complex (BMMY) medium were prepared according to the manual of Pichia Expression Kit (Version F, Invitrogen). Fermentation Basal Salts Medium (BSM) and PTM1 Trace Salts used for fermentation were prepared according to the Pichia Fermentation Process Guidelines (Invitrogen).

2.2. Codon Optimization and Screening of High Xylanase Activity Clones

2.2.1. Codon Optimization and Synthesis of the Gene. The codon usage of *xynB* gene (GenBank DQ302412) from *A. usamii* and *VHb* gene (GenBank AY278220) was analysed using Graphical Codon Usage Analyser (http://gcua.schoedl.de/) and they were optimized by replacing the codons predicted to be less frequently used in *P. pastoris* with the frequently used ones (https://www.dna20.com/). The optimized genes (*xynB-opt* and *VHb*) were synthesized by Sangon (Shanghai, China).

2.2.2. Vector Construction, Transformation, and Screening of High Xylanase Activity Clones. The synthetic gene encoding the mature region of xylanase without the predicted signal sequence was digested by EcoRI and NotI and then ligated into pPICZαA to form pPICZαA-*xynB-opt*. The native xylanase gene (*xynB*) was cloned from *A. usamii* by reverse transcription PCR and then inserted into plasmid pMD20-T to form pMD20-T-*xynB*. The pMD20-T-*xynB* was digested by EcoRI and NotI and then ligated into pPICZαA, resulting in the recombinant plasmid pPICZαA-*xynB*. The synthetic *VHb* gene was digested by EcoRI and NotI and then ligated into pPIC3.5K to form pPIC3.5K-*VHb*. The recombinant plasmids were checked by DNA sequencing.

P. pastoris X33 was transformed with 10 μg of PmeI-linearized pPICZαA-*xynB-opt* and pPICZαA-*xynB* vector by electrotransformation, according to Invitrogen's recommendations. Transformants were plated on YPDS plates (10 g/L yeast extract, 20 g/L peptone, 20 g/L dextrose, 20 g/L agar, and 1 M sorbitol) containing 100 μg/mL Zeocin to isolate resistant clones. The method for screening transformants was the same as our previous described method except the microplates [16]. In this study, transformants were picked and cultured in 24-deep-well microplates containing 1.2 mL/well BMGY medium at 30°C for 24 h. After this, the cells were harvested by centrifugation, resuspended, and cultured in 1 mL/well BMMY medium. After 24 h, plates were subjected to centrifugation again and supernatants were used in subsequent activity assays. The clones showing higher activities were checked by shaking flask fermentation.

2.2.3. Expression of xynB-opt and xynB in P. pastoris Shake-Flask Cultures. Thirty clones which had higher enzyme activity were selected for shake-flask cultures. The seeds were inoculated in 10 mL of BMGY medium in a 100 mL shake flask and incubated at 30°C until the culture reached OD_{600} = 2.0–6.0. The cells were harvested by centrifugation and resuspended in 50 mL of BMMY medium and incubated at 30°C. The methanol induction temperature was set at 30°C, and 0.7% (v/v) methanol was fed at 24 h intervals for 5 days. The activities of the xylanase were checked at 24, 48, 72, 96, and 120 h. The colony with the highest activity was selected as the host for the transformation of the pPIC3.5K-*VHb* and pPIC3.5K vectors.

2.3. Intracellular Coexpression of VHb

2.3.1. Construction of Recombinant Strains Containing VHb and xynB-opt. A clone named X33/*xynB-opt* (the recombinant strain containing *xynB-opt*) exhibiting the maximum xylanase activity under shake-flask cultures was chosen as the host for the transformation of the pPIC3.5K-*VHb* and pPIC3.5K vectors. The plasmids pPIC3.5K-*VHb* and pPIC3.5K were both linearized by SacI and transformed into X33/*xynB-opt* to form X33/*xynB-opt-VHb* and X33/*xynB-opt-p*. The X33/*xynB-opt-p* was used as control during the experiments. The transformants were plated on YPDG plates (10 g/L yeast extract, 20 g/L peptone, 20 g/L dextrose, 20 g/L agar, and 1 M sorbitol) containing 4 mg/mL G418 to isolate resistant clones.

2.3.2. Expression of Recombinant Strains in P. pastoris Shake-Flask Cultures. The G418-resistant clones were cultivated in shaking flask. The cultivation conditions and medium

composition were the same as described above. The clone exhibiting higher enzyme activity in shaking flask was selected for further experiments.

2.4. High Cell Density Fermentation. The transformed strains (X33/*xynB*, X33/*xynB-opt*, X33/*xynB-opt-p,* and X33/*xynB-opt-VHb*) showing the highest xylanase activity in shake-flask culture were cultivated in high cell density fermentor. High cell density fermentation was carried out in 50 L bioreactor (Baoxing Co., Shanghai, China). The cultivation conditions and medium composition were the same as the previous described method [17]. The enzyme activity of the supernatant and dry cell weight (DCW) were monitored throughout the cultivation.

2.5. Optimization of the Induction Temperature. To investigate the effects of temperature on the production of xylanase of recombinant strain X33/*xynB-opt-VHb*, the induction temperature was optimized in a 50 L bioreactor. During the methanol fed-phase, the temperature was designed in the range of 30°C to 22°C.

2.6. Assay of Xylanase Activity, Protein Determination, Cell Viability, Oxygen Uptake, and Dry Cell Weight. Xylanase activity was assayed according to the method described by previous study and with some modification [18]. All enzyme assays, unless otherwise stated, were carried out at 50°C for 30 min in 100 mM acetic acid-sodium acetic acid buffer (pH 5.0). 2 mL basic reaction mixture (containing 1 mL of 1.0% (w/v) oat spelt xylan and 1 mL of a suitably diluted enzyme solution) was incubated at 50°C for 30 min and reducing sugar (xylose) was measured by the dinitrosalicylic acid (DNS) according to the standard method and xylose was used as a standard. One unit of xylanase activity was defined as the amount of enzyme that produced 1 μM reducing sugar from substrate solution per minute under the assay conditions. The protein content was determined according to the Bradford method using BSA as standard. The measurement of cell viability was performed by methylene blue dye exclusion technique as described by the previous study [19]. The oxygen uptake (OUR) was determined according to the previous studies [20, 21]. Cell density was expressed as grams of dry cell weigh (DCW) per liter of broth and was obtained by centrifuging 10 mL samples in a preweighted centrifuge tube at 8000 g for 10 min and washing twice with deionized water, then allowing the pellet to dry at 100°C to constant weight.

3. Results and Discussion

3.1. Improved Production of A. usamii Xylanase in P. pastoris by Codon Optimization. As an easy and simple system, *P. pastoris* is now widely used for heterologous production of recombinant proteins [22]. Due to the discrepancy of codon usage between the host and their original strains, researchers have used codon optimization to increase the expression of heterologous gene. Codon optimization by using frequently used codons in the host is an efficient strategy to improve the expression level of heterologous gene. Generally, this is accomplished by replacing all codons with preferred codons, eliminating AT-rich stretches, and adjusting the G+C content [8, 23]. Analysis of the DNA sequence of *VHb* and native *xynB* using Graphical Codon Usage Analyser revealed that some amino acid residues were encoded by codons that are rarely used in *P. pastoris*. These codons TCG (Ser), CCG (Pro), GGC (Gly), AGC (Ser), and GCG (Ala) shared less than 15% of usage percentage, which may result in a much lower expression level of *xynB* in *P. pastoris* (Tables 1 and 2). To solve this problem, we took a strategy of rewriting the native *xynB* and *VHb* according to *P. pastoris* preferred codon usage. G+C content affects the secondary structure of mRNA and then affects the expression level of heterologous gene. In this study, the G+C content of *VHb* was increased from 42 to 51% and the native *xynB* was reduced from 57.6 to 55.1%, which is in the appropriate range for *Picha* system. Totally, there were 105 and 57 amino acids optimized in native *xynB* and *VHb*, respectively (Tables 1 and 2). As shown in Figures 1 and 2, the optimized gene (*xynB-opt* and *VHb-opt*) shared 83% and 86% of nucleotide sequence identity with that of the native gene (*xynB* and *VHb*).

The recombinant plasmids pPICZαA-*xynB-opt* and pPICZαA-*xynB* were transformed into *P. pastoris* X33 and hundreds of transformants were obtained on YPDZ plates. The positive clones were cultured in 24-deep-well microplates and further screened by xylanase activity assay. Two clones (one carrying *xynB-opt* named X33/*xynB-opt* and the other carrying *xynB* named X33/*xynB*) showing the higher activity were chosen for shake-flask cultures. The recombinant strains X33/*xynB-opt* and X33/*xynB* were cultivated in shaking flask. After 120 h of cultivation under inducing conditions, the xylanase activities of X33/*xynB-opt* and X33/*xynB* were 920 U/mL and 520 U/mL, respectively. The total protein content of X33/*xynB-opt* and X33/*xynB* were 0.25 mg/mL and 0.15 mg/mL, respectively. The recombinant strain X33/*xynB-opt* was chosen as the host for the transformation of the pPIC3.5K-*VHb* and pPIC3.5K vectors.

3.2. Intracellular Coexpression of VHb. Oxygen supply is one of the most critical parameters for cell growth and heterologous protein expression in recombinant *P. pastoris*. VHb is a suitable oxygen uptake improving protein for expression in *P. pastoris* due to its high oxygen trapping and releasing ability, enabling it to satisfy extremely high oxygen demand during fermentations [24]. In this study, in order to enhance oxygen uptake and improve the production of recombinant xylanase, we attempted to coexpress the *VHb* with *xynB-opt* in *P. pastoris*. The recombinant plasmids pPIC3.5K-*VHb* and pPIC3.5K were linearized and transformed into recombinant strain X33/*xynB-opt* to form recombinant strains VHb^+ (X33/*xynB-opt* containing *VHb*) and VHb^- (X33/*xynB-opt* containing pPIC3.5K). Transformants were plated on YPDG plates. Then the G418-resistant clones were cultured in shaking flasks. The VHb^+ (named X33/*xynB-opt-VHb*) showed higher cell density and xylanase activity than VHb^- (named X33/*xynB-opt-p*). The cell density of X33/*xynB-opt-VHb* was approximately 2.5 g/L higher than X33/*xynB-opt-p*. Moreover, the xylanase activity of X33/*xynB-opt-VHb* was

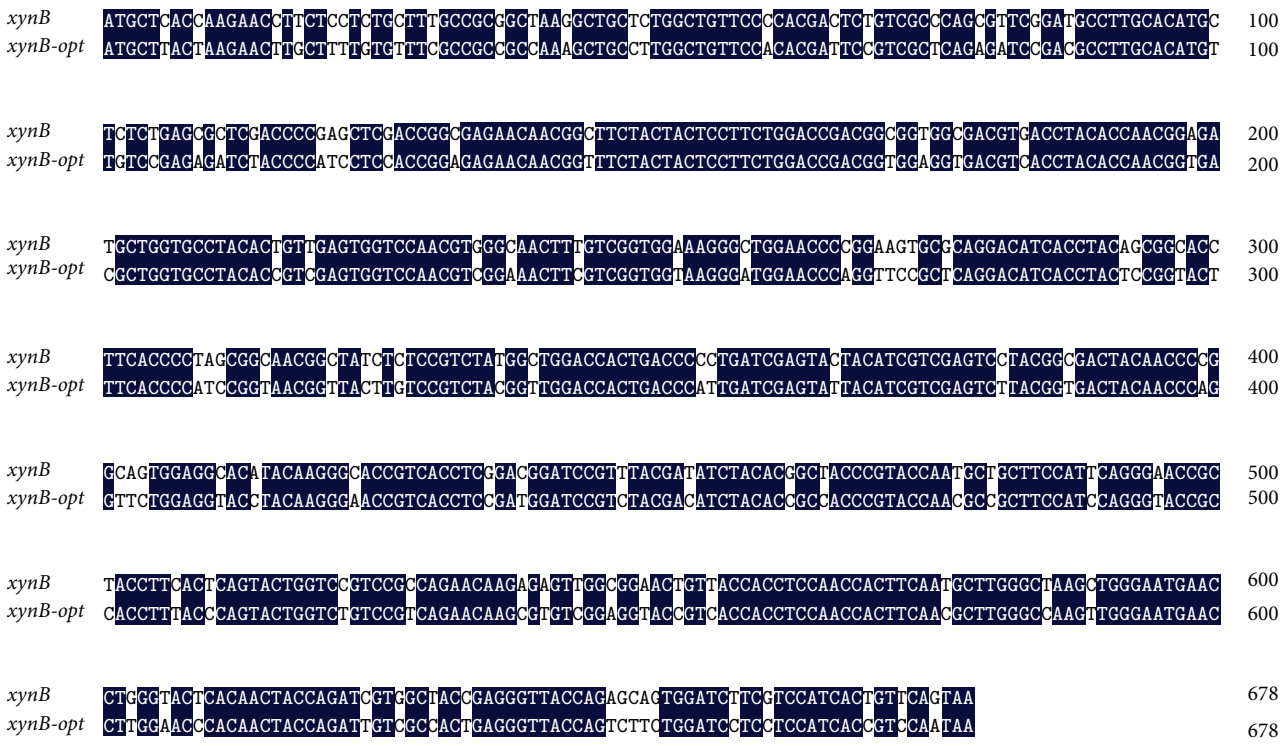

Figure 1: Sequence comparison between the original (*xynB*) and the optimized (*xynB-opt*) genes. Identical residues are marked in black background.

Figure 2: Sequence comparison between the original (*VHb*) and the optimized (*VHb-opt*) genes. Identical residues are marked in black background.

1300 U/mL, which was 31% and 60% more than that of X33/*xynB-opt-p* and X33/*xynB*.

3.3. High Cell Density Fermentation. In order to obtain a large amount of active protein, the recombinant strains X33/*xynB-opt*, X33/*xynB*, X33/*xynB-opt-p,* and X33/*xynB-opt-VHb* were cultivated in 50 L fermentor. As shown in Figure 3, the maximum xylanase activity and total protein concentration produced by X33/*xynB-opt* reached 33500 U/mL and 3.8 g/L, respectively. Compared with X33/*xynB*, the maximum xylanase activity and total protein concentration were increased by 60% and 80%, respectively. In this study, the fermentation conditions and DCW of X33/*xynB-opt* and X33/*xynB* were almost the same during the high cell density fermentation (data not shown). These results showed that the improved production of recombinant xylanase in *P. pastoris* was reached by codon optimization. Codon optimization is an effective method to improve the expression level of

Table 1: Comparison of the codon usage for native (*xynB*) and synthetic (*xynB-opt*) targeted genes at *Pichia pastoris* for expression.

AA	Codon	Host fraction	*xynB*	*xynB-opt*
Gly	GGG	0.10	0	0
	GGA	0.32	9	11
	GGT	0.44	5	18
	GGC	0.14	15	0
Glu	GAG	0.43	6	6
	GAA	0.57	0	0
Asp	GAT	0.58	3	2
	GAC	0.42	7	8
Val	GTG	0.19	3	0
	GTA	0.15	0	0
	GTT	0.42	6	1
	GTC	0.23	6	14
Ala	GCG	0.06	2	0
	GCA	0.23	0	0
	GCT	0.45	12	7
	GCC	0.26	4	11
Arg	AGG	0.16	0	0
	AGA	0.48	1	2
	CGG	0.05	0	0
	CGA	0.10	0	0
	CGT	0.16	2	3
	CGC	0.05	2	0
Lys	AAG	0.53	6	5
	AAA	0.47	0	1
Ser	AGT	0.15	3	0
	AGC	0.09	4	0
	TCG	0.09	5	0
	TCA	0.19	0	0
	TCT	0.29	3	6
	TCC	0.20	9	18
Stop	TAA	0.53	1	1
Asn	AAT	0.49	2	0
	AAC	0.51	13	15
Met	ATG	1.00	3	3
Ile	ATA	0.19	0	0
	ATT	0.50	1	1
	ATC	0.30	6	6
Thr	ACG	0.11	1	0
	ACA	0.24	1	0
	ACT	0.40	4	4
	ACC	0.25	19	23
Trp	TGG	1.00	6	6
Cys	TGT	0.65	0	1
	TGC	0.35	1	0
Tyr	TAT	0.46	2	1
	TAC	0.55	15	16
Leu	TTG	0.33	1	8
	TTA	0.16	0	0
	CTG	0.16	4	0
	CTA	0.11	0	0
	CTT	0.16	1	3
	CTC	0.08	5	0
Phe	TTT	0.54	2	1
	TTC	0.46	5	6
Gln	CAG	0.39	8	7
	CAA	0.61	0	1
His	CAT	0.57	0	0
	CAC	0.43	4	4
Pro	CCC	0.15	4	0
	CCG	0.09	1	0
	CCA	0.41	0	6
	CCT	0.35	1	0

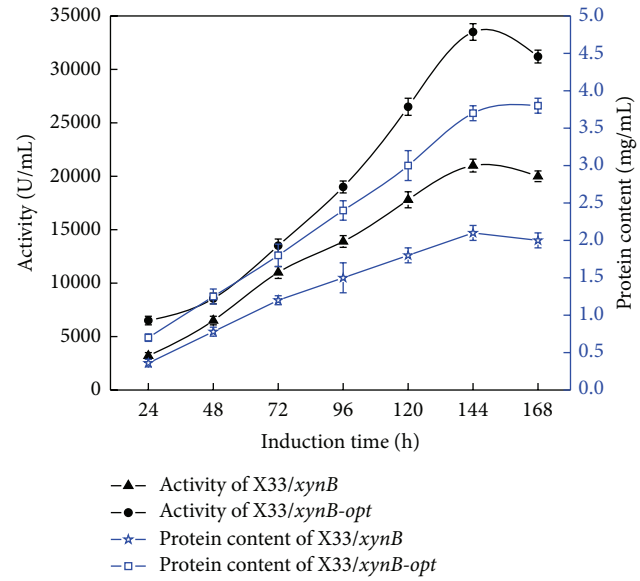

Figure 3: Xylanase activity and total protein content of X33/*xynB-opt* and X33/*xynB* during fed batch fermentation in 50 L bioreactor.

heterologous gene in *P. pastoris*. In our previous study, the α-amylase gene from *Bacillus licheniformis* was codon optimization according to the codon usage of *P. pastoris* and the optimized gene was expressed at a significantly higher level than the wild-type gene [17]. Through codon optimization the glucanase gene from *Fibrobacter succinogenes* resulted in a 2.34-fold increase of target protein production [25].

The growth and xylanase activity profile of X33/*xynB-opt-p* and X33/*xynB-opt-VHb* in 50 L bioreactor were shown in Figure 4. The DCW and xylanase activity of X33/*xynB-opt-VHb* were higher than those of X33/*xynB-opt-p* during the methanol induction phase. The highest xylanase activity of X33/*xynB-opt-VHb* was 45225 U/mL which was about 1.35-fold higher than that of X33/*xynB-opt-p*. The higher xylanase activity and DCW of X33/*xynB-opt-VHb* were probably caused by coexpression of VHb. The function of VHb is usually considered to be the enhancement of respiration, cell viability, and energy metabolism by facilitating oxygen uptake. As shown in Figure 5(a), SOUR of both strains was almost the same before methanol induction. After induction, SOUR of X33/*xynB-opt-VHb* increased higher than

Table 2: Comparison of the codon usage for native (*VHb*) and synthetic (*VHb-opt*) targeted genes at *Pichia pastoris* for expression.

AA	Codon	Host fraction	*VHb*	*VHb-opt*
Gly	GGG	0.10	0	0
	GGA	0.32	1	0
	GGT	0.44	7	8
	GGC	0.14	0	0
Glu	GAG	0.43	7	1
	GAA	0.57	2	8
Asp	GAT	0.58	2	8
	GAC	0.42	6	0
Val	GTG	0.19	0	0
	GTA	0.15	0	0
	GTT	0.42	4	10
	GTC	0.23	10	4
Ala	GCG	0.06	0	0
	GCA	0.23	0	0
	GCT	0.45	17	23
	GCC	0.26	6	0
Arg	AGG	0.16	0	0
	AGA	0.48	1	2
	CGG	0.05	0	0
	CGA	0.10	0	0
	CGT	0.16	1	0
	CGC	0.05	0	0
Lys	AAG	0.53	9	10
	AAA	0.47	1	0
Ser	AGT	0.15	0	0
	AGC	0.09	0	0
	TCG	0.09	0	0
	TCA	0.19	0	0
	TCT	0.29	0	1
	TCC	0.20	1	0
Stop	TAA	0.53	1	1
Asn	AAT	0.49	0	0
	AAC	0.51	4	4
Met	ATG	1.00	3	3
Ile	ATA	0.19	0	0
	ATT	0.50	5	5
	ATC	0.30	7	7
Thr	ACG	0.11	0	0
	ACA	0.24	0	0
	ACT	0.40	1	8
	ACC	0.25	7	0
Trp	TGG	1.00	1	1
Cys	TGT	0.65	1	1
	TGC	0.35	0	0
Tyr	TAT	0.46	0	0
	TAC	0.55	4	4
Leu	TTG	0.33	14	14
	TTA	0.16	0	0
	CTG	0.16	0	0
	CTA	0.11	0	0
	CTT	0.16	0	0
	CTC	0.08	0	0
Phe	TTT	0.54	0	2
	TTC	0.46	4	2
Gln	CAG	0.39	6	2
	CAA	0.61	3	7
His	CAT	0.57	1	4
	CAC	0.43	3	0
Pro	CCC	0.15	0	0
	CCG	0.09	0	0
	CCA	0.41	6	7
	CCT	0.35	1	0

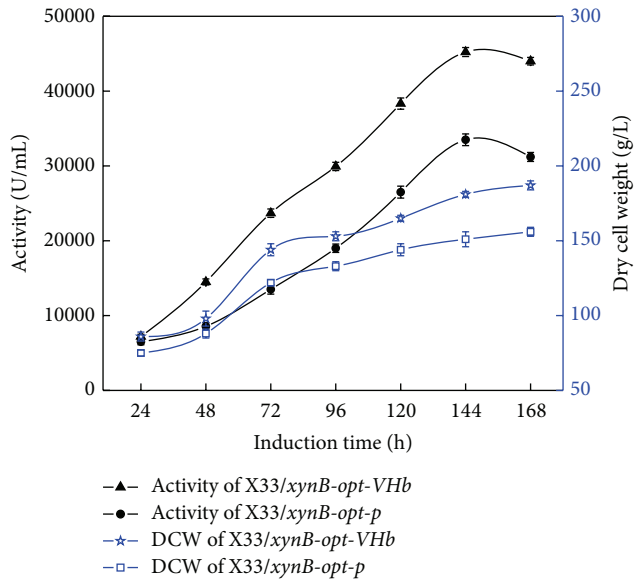

Figure 4: Xylanase activity and DCW of X33/*xynB-opt-p* and X33/*xynB-opt-VHb* during fed batch fermentation in 50 L bioreactor.

X33/*xynB-opt-p* during the whole induction phase, which was probably caused by VHb expression improving oxygen utilization and respiratory efficiency. The VHb-expressing strain with higher oxygen demand was similar to previous studies [26]. Furthermore, we also compared the cell viabilities of X33/*xynB-opt-p* and X33/*xynB-opt-VHb*. The cell viabilities of X33/*xynB-opt-p* and X33/*xynB-opt-VHb* at the end of 144 h of cultivation were 75% and 60%, respectively (Figure 5(b)). This indicates that VHb expression resulted in an increase in cell viability. In this study, coexpression of VHb increased SOUR and then improved cell viability and DCW of X33/*xynB-opt-VHb*. Our results indicated that coexpression of VHb is also an effective method to improve the production of heterologous protein in *P. pastoris*.

3.4. Optimization of the Induction Temperature. Temperature is a key factor for optimization of heterologous proteins expressed in *P. pastoris*. In order to evaluate the effects of cultivation temperature on cell growth, cell viability, and xylanase production, X33/*xynB-opt-VHb* was grown in BSM (pH 5.0) at 22, 25, 28, and 30°C (Figure 6). As shown in

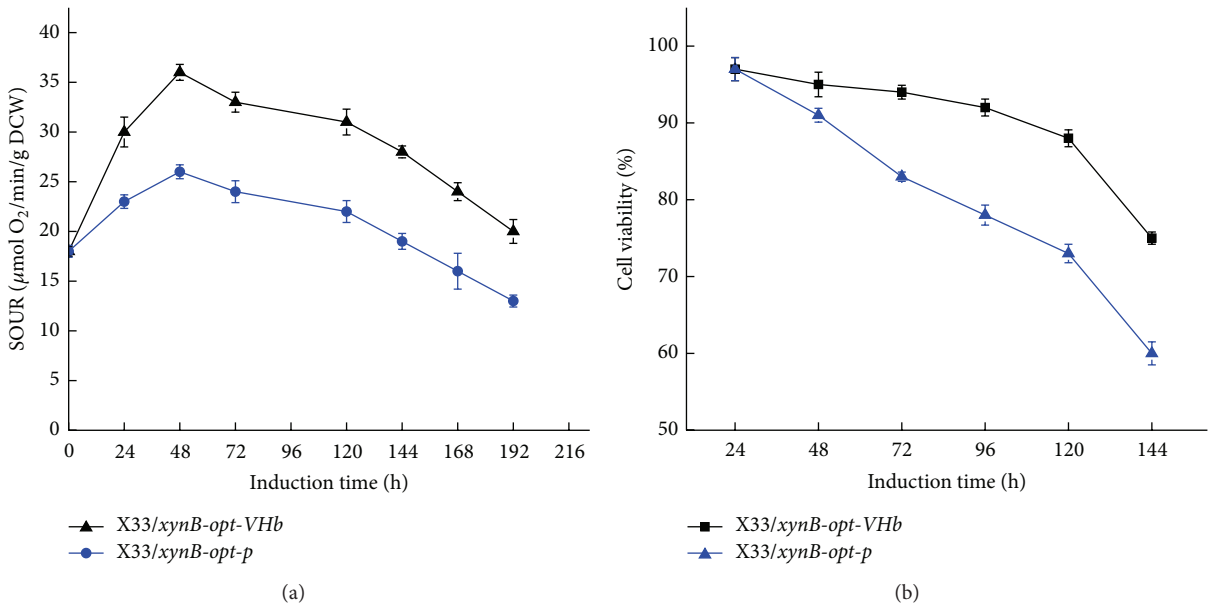

FIGURE 5: Comparison of specific oxygen uptake (a) and cell viability (b) profile between X33/*xynB-opt-p* and X33/*xynB-opt-VHb* during fed batch fermentation in 50 L bioreactor.

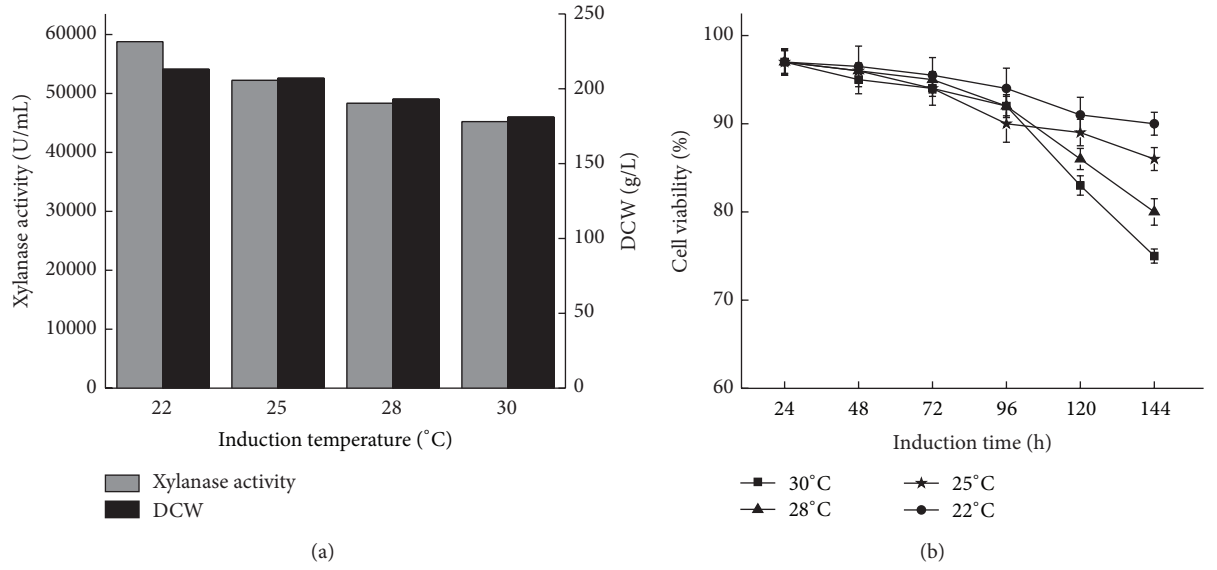

FIGURE 6: Xylanase activity and DCW of X33/*xynB-opt-VHb* during fed batch fermentation in 50 L bioreactor under different induction temperature (a). Cell viability profile of X33/*xynB-opt-VHb* during fed batch fermentation in 50 L bioreactor under different induction temperature (b).

Figure 6(a), xylanase activities at lower induction temperature were higher than that at higher induction temperature. The maximum xylanase activity of 58792 U/mL with a cell density of 213 g DCW was obtained after 144 h of culture at 22°C, which was 1.29-fold and 1.17-fold higher than that at 30°C. Until now, several *Aspergillus* endo-β-1,4-xylanases have also been successfully expressed in *P. pastoris*. The *Aspergillus sulphureus* and *Aspergillus niger* endo-β-1,4-xylanases were functionally expressed and secreted in the *P. pastoris*, the enzyme activity of which reached 105 and 20424 U/mL [8, 27], which were lower than the expression level of *A. usamii* endo-β-1,4-xylanase in this study. However, these values are not fully comparable since different cultivation conditions and activity assays with different substrates and conditions have been used. Meanwhile, the cell viabilities of X33/*xynB-opt-VHb* under different temperature were also determined. The cell viability remained below 80% under the temperature at 30°C and 28°C and above 90% in the cultivation with a temperature of 22°C (Figure 6(b)). These results indicated that lower induction temperature could

facilitate production of recombinant xylanase. According to the findings by other researchers, lowering induction temperature can reduce cell death and increase cell viability and then improved the production of heterologous proteins in *P. pastoris* [28]. Furthermore, lowering induction temperature can enlarge VHb effect on cell performance of *P. pastoris* and then obtain a higher final cell density and viability in comparison with higher temperature [24].

4. Conclusions

In this study, we combined codon optimization, intracellular coexpression of VHb, and optimization of induction temperature as a whole to improve the expression level of recombinant *A. usamii* endo-β-1,4-xylanase in *P. pastoris*. To our knowledge, this is the first report to combine these methods as a whole to improve the production of *A. usamii* endo-β-1,4-xylanase in *P. pastoris*. Our results indicated that combined codon optimization, intracellular coexpression of VHb, and optimization of induction temperature are an effective method to improve the production of heterologous protein in *P. pastoris*. Furthermore, our results presented here will greatly contribute to improving the production of recombinant proteins in *P. pastoris* and offer a greater value in various industrial applications.

Competing Interests

The authors declare no conflict of interests.

Authors' Contributions

Danni Liu made substantial contributions to the design of the experiments and the draft the paper. Jianrong Wang and Yangyuan Li carried out this research, interpreted the data, and drafted the paper. Jianrong Wang and Yangyuan Li contributed equally to this work.

Acknowledgments

This work was supported by the National High-Technology Project of China (no. 2014AA093514) and the Key Science and Technology Program of Zhuhai (no. 2012D0201990042).

References

[1] Q. K. Beg, M. Kapoor, L. Mahajan, and G. S. Hoondal, "Microbial xylanases and their industrial applications: a review," *Applied Microbiology and Biotechnology*, vol. 56, no. 3-4, pp. 326–338, 2001.

[2] M. L. T. M. Polizeli, A. C. S. Rizzatti, R. Monti, H. F. Terenzi, J. A. Jorge, and D. S. Amorim, "Xylanases from fungi: properties and industrial applications," *Applied Microbiology and Biotechnology*, vol. 67, no. 5, pp. 577–591, 2005.

[3] A. C. E. Gregory, A. P. O'Connell, and G. P. Bolwell, "Xylans," *Biotechnology and Genetic Engineering Reviews*, vol. 15, no. 1, pp. 439–456, 1998.

[4] R. A. Prade, "Xylanases: from biology to biotechnology," *Biotechnology and Genetic Engineering Reviews*, vol. 13, pp. 101–131, 1996.

[5] S. Subramaniyan and P. Prema, "Biotechnology of microbial xylanases: enzymology, molecular biology, and application," *Critical Reviews in Biotechnology*, vol. 22, no. 1, pp. 33–64, 2002.

[6] Y. Takahashi, H. Kawabata, and S. Murakami, "Analysis of functional xylanases in xylan degradation by *Aspergillus niger* E-1 and characterization of the GH family 10 xylanase XynVII," *SpringerPlus*, vol. 2, article 447, 2013.

[7] A. Hmida-Sayari, S. Taktek, F. Elgharbi, and S. Bejar, "Biochemical characterization, cloning and molecular modeling of a detergent and organic solvent-stable family 11 xylanase from the newly isolated *Aspergillus niger* US368 strain," *Process Biochemistry*, vol. 47, no. 12, pp. 1839–1847, 2012.

[8] Y. Li, B. Zhang, X. Chen, Y. Chen, and Y. Cao, "Improvement of *Aspergillus sulphureus* endo-β-1,4-xylanase expression in *Pichia pastoris* by codon optimization and analysis of the enzymic characterization," *Applied Biochemistry and Biotechnology*, vol. 160, no. 5, pp. 1321–1331, 2010.

[9] C. Zhou, J. Bai, S. Deng et al., "Cloning of a xylanase gene from *Aspergillus usamii* and its expression in *Escherichia coli*," *Bioresource Technology*, vol. 99, no. 4, pp. 831–838, 2008.

[10] H.-M. Zhang, J.-Q. Wang, M.-C. Wu, S.-J. Gao, J.-F. Li, and Y.-J. Yang, "Optimized expression, purification and characterization of a family 11 xylanase (AuXyn11A) from *Aspergillus usamii* E001 in *Pichia pastoris*," *Journal of the Science of Food and Agriculture*, vol. 94, no. 4, pp. 699–706, 2014.

[11] J. R. Wang, Y. Y. Li, S. D. Xu, P. Li, J. S. Liu, and D. N. Liu, "High-level expression of pro-form lipase from *Rhizopus oryzae* in *Pichia pastoris* and its purification and characterization," *International Journal of Molecular Sciences*, vol. 15, no. 1, pp. 203–217, 2014.

[12] D. Teng, Y. Fan, Y.-L. Yang, Z.-G. Tian, J. Luo, and J.-H. Wang, "Codon optimization of *Bacillus licheniformis* β-1,3-1,4-glucanase gene and its expression in *Pichia pastoris*," *Applied Microbiology and Biotechnology*, vol. 74, no. 5, pp. 1074–1083, 2007.

[13] R. Ramón, P. Ferrer, and F. Valero, "Sorbitol co-feeding reduces metabolic burden caused by the overexpression of a *Rhizopus oryzae* lipase in *Pichia pastoris*," *Journal of Biotechnology*, vol. 130, no. 1, pp. 39–46, 2007.

[14] X. Li, Z. Liu, G. Wang, D. Pan, L. Jiao, and Y. Yan, "Overexpression of *Candida rugosa* lipase Lip1 via combined strategies in *Pichia pastoris*," *Enzyme and Microbial Technology*, vol. 82, pp. 115–124, 2016.

[15] M. R. Yu, S. Wen, and T. W. Tan, "Enhancing production of *Yarrowia lipolytica* lipase Lip2 in *Pichia pastoris*," *Engineering in Life Sciences*, vol. 10, no. 5, pp. 458–464, 2010.

[16] J. Wang, Y. Li, and D. Liu, "Gene cloning, high-level expression, and characterization of an alkaline and thermostable lipase from *Trichosporon coremiiforme* V3," *Journal of Microbiology and Biotechnology*, vol. 25, no. 6, pp. 845–855, 2015.

[17] J. R. Wang, Y. Y. Li, D. N. Liu et al., "Codon optimization significantly improves the expression level of α-amylase gene from *Bacillus licheniformis* in *Pichia pastoris*," *BioMed Research International*, vol. 2015, Article ID 248680, 9 pages, 2015.

[18] H. Y. Cai, P. J. Shi, Y. G. Bai et al., "A novel thermoacidophilic family 10 xylanase from *Penicillium pinophilum* C1," *Process Biochemistry*, vol. 46, no. 12, pp. 2341–2346, 2011.

[19] X. Wang, Y. Sun, X. Shen et al., "Intracellular expression of *Vitreoscilla hemoglobin* improves production of *Yarrowia*

lipolytica lipase LIP2 in a recombinant *Pichia pastoris*," *Enzyme and Microbial Technology*, vol. 50, no. 1, pp. 22–28, 2012.

[20] M. Urgun-Demirtas, K. R. Pagilla, and B. Stark, "Enhanced kinetics of genetically engineered *Burkholderia cepacia*: role of vgb in the hypoxic cometabolism of 2-CBA," *Biotechnology and Bioengineering*, vol. 87, no. 1, pp. 110–118, 2004.

[21] J.-M. Wu and W.-C. Fu, "Intracellular co-expression of *Vitreoscilla hemoglobin* enhances cell performance and β-galactosidase production in *Pichia pastoris*," *Journal of Bioscience and Bioengineering*, vol. 113, no. 3, pp. 332–337, 2012.

[22] A.-S. Xiong, Q.-H. Yao, R.-H. Peng et al., "High level expression of a synthetic gene encoding *Peniophora lycii* phytase in methylotrophic yeast *Pichia pastoris*," *Applied Microbiology and Biotechnology*, vol. 72, no. 5, pp. 1039–1047, 2006.

[23] J. K. Yang and L. Y. Liu, "Codon optimization through a two-step gene synthesis leads to a high-level expression of *Aspergillus niger* lip2 gene in *Pichia pastoris*," *Journal of Molecular Catalysis B: Enzymatic*, vol. 63, no. 3-4, pp. 164–169, 2010.

[24] J.-M. Wu, S.-Y. Wang, and W.-C. Fu, "Lower temperature cultures enlarge the effects of *Vitreoscilla hemoglobin* expression on recombinant pichia pastoris," *International Journal of Molecular Sciences*, vol. 13, no. 10, pp. 13212–13226, 2012.

[25] H. Huang, P. Yang, H. Luo et al., "High-level expression of a truncated 1,3-1,4-β-D-glucanase from *Fibrobacter succinogenes* in *Pichia pastoris* by optimization of codons and fermentation," *Applied Microbiology and Biotechnology*, vol. 78, no. 1, pp. 95–103, 2008.

[26] R. Mora-Lugo, M. Madrigal, V. Yelemane, and M. Fernandez-Lahore, "Improved biomass and protein production in solid-state cultures of an *Aspergillus sojae* strain harboring the *Vitreoscilla hemoglobin*," *Applied Microbiology and Biotechnology*, vol. 99, no. 22, pp. 9699–9708, 2015.

[27] F. Li, S. Yang, L. Zhao, Q. Li, and J. Pei, "Synonymous condon usage bias and overexpression of a synthetic xynB gene from *Aspergillus Niger* NL-1 in *Pichia pastoris*," *BioResources*, vol. 7, no. 2, pp. 2330–2343, 2012.

[28] Y. Wang, Z. Wang, Q. Xu et al., "Lowering induction temperature for enhanced production of polygalacturonate lyase in recombinant *Pichia pastoris*," *Process Biochemistry*, vol. 44, no. 9, pp. 949–954, 2009.